Nene Phosphate in Sediment Investigation - Environment Agency Project REF:30258

Water Framework Directive   Report OR/13/031

BRITISH GEOLOGICAL SURVEY

Water Framework Directive

Nene Phosphate in Sediment Investigation - Environment Agency Project REF:30258

A.M. Tye, M.D. Hurst, A.K.A.P. Barkwith

Contributor/editor

A.M. Tye

Keyworth, Nottingham   British Geological Survey
2013

BRITISH GEOLOGICAL SURVEY

The full range of our publications is available from BGS shops at Nottingham, Edinburgh, London and Cardiff (Welsh publications only) see contact details below or shop online at www.geologyshop.com

The London Information Office also maintains a reference collection of BGS publications, including maps, for consultation.

We publish an annual catalogue of our maps and other publications; this catalogue is available online or from any of the BGS shops.

The British Geological Survey carries out the geological survey of Great Britain and Northern Ireland (the latter as an agency service for the government of Northern Ireland), and of the surrounding continental shelf, as well as basic research projects. It also undertakes programmes of technical aid in geology in developing countries.

The British Geological Survey is a component body of the Natural Environment Research Council.

British Geological Survey offices

BGS Central Enquiries Desk

Tel 0115 936 3143   Fax 0115 936 3276
email enquiries@bgs.ac.uk

Environmental Science Centre, Keyworth, Nottingham NG12 5GG

Tel 0115 936 3241   Fax 0115 936 3488
email sales@bgs.ac.uk

Murchison House, West Mains Road, Edinburgh EH9 3LA

Tel 0131 667 1000   Fax 0131 668 2683
email scotsales@bgs.ac.uk

Natural History Museum, Cromwell Road, London SW7 5BD

Tel 020 7589 4090   Fax 020 7584 8270
Tel 020 7942 5344/45   email bgslondon@bgs.ac.uk

Columbus House, Greenmeadow Springs, Tongwynlais, Cardiff CF15 7NE

Tel 029 2052 1962   Fax 029 2052 1963

Maclean Building, Crowmarsh Gifford, Wallingford OX10 8BB

Tel 01491 838800   Fax 01491 692345

Geological Survey of Northern Ireland, Colby House, Stranmillis Court, Belfast BT9 5BF

Tel 028 9038 8462   Fax 028 9038 8461

www.bgs.ac.uk/gsni/

Parent Body

Natural Environment Research Council, Polaris House, North Star Avenue, Swindon SN2 1EU

Tel 01793 411500   Fax 01793 411501
www.nerc.ac.uk

Website www.bgs.ac.uk
Shop online at www.geologyshop.com

Environment Agency Office
Goldhay Way,
Orton Goldhay,
Peterborough,
PE2 5ZR
www.environment-agency.gov.uk

Foreword

This report is the published product of a study by the British Geological Survey (BGS) for the UK Environment Agency, project number 30258.

Acknowledgements

A number of BGS staff contributed greatly towards this project. Barry Rawlins helped write the tender proposal and reviewed the report. Murray Lark and Ben Marchant wrote the statistical code to fit the isotherm and kinetic data respectively as well as providing general statistical advice. Alex Bradley drew the maps. Mick Strutt was invaluable for undertaking the field work, its preparation and looking after all the boat maintenance and driving. Rob Price was our Environment Agency Project Manager and client, providing requirement specification, local knowledge, water body access, health and safety and as well as contributing to the sample collection.

Contents

FIGURES

PLATES

TABLES

List of abbreviations and definitions

Within this report a number of abbreviations and different species of phosphorus are measured. Their definitions and abbreviations are given below:

Total P (TP) is used to define the total concentration of phosphorus in the sediment measured. This is undertaken by dissolving the sediment in strong acid and expressing the result as a concentration (mg kg $^{-1}$) on a dry weight basis. This measurement will include both Olsen Extractable Phosphate as well as that Phosphorus locked away or occluded within the mineral and oxide structures.

Phosphate (PO$_4$-P) is the generic term used for the phosphate ions which in its simplest form is ortho-phosphoric acid (H$_3$PO$_4$).

Olsen Extractable PO$_4$-P (OEP) is a measure of the PO$_4$-P in the sediment that is considered to be in a bio-available form and which could be readily utilised by water plants and microbial communities. OEP is expressed as a concentration (mg kg $^{-1}$) on a dry weight basis and is extracted in a 0.5M NaHCO$_3$ solution whereby the carbonate ions in the extracting solution exchange with the phosphate ions held on any mineral and organic matter surfaces. The measurement is expressed as P, therefore multiplying by 3 will give an approximate value for phosphate (PO$_4^-$).

Soluble Reactive Phosphate (SRP) is the soluble reactive P found in river waters after filtering through a 0.45μm filter. Multiplying the value given by three will give an approximate result as phosphate (PO$_4^-$).

Water Framework Directive (WFD) is the EU legislation aimed at improving the quality and biodiversity of surface waters.

Water Body describes a defined length of the River Nene which is managed and monitored with a view to achieve and sustain good ecological status (GES).

Executive Summary

This report details the results of research the British Geological Survey has undertaken for the UK Environment Agency on sediment and phosphorus dynamics in the main six Water Framework Directive (WFD) water bodies of the River Nene in eastern England. The sampled water bodies started in the head waters of the Nene near Daventry (water body 1) and continued to the Dog in Doublet lock to the east of Peterborough (water body 6). The project comprised of three parts. These were (i) sampling and laboratory analysis (ii) landscape evolution modelling and catchment erosion assessments to provide first order estimates of sediment inputs and transport in the River Nene and (iii) combining these results to determine sediment TP (TP) and sediment Olsen extractable phosphate (OEP) budgets for the river. Results showed that there appeared to be geological/soil parent material controls on the concentrations of TP in the sediments of the River Nene, with water bodies 1-3 containing less TP than water bodies 4-6. Analysis of OEP showed that sediments contained high concentrations (up to 100 mg kg^{-1} OEP) that could be utilised by macrophytes and also potentially desorb to the river water. Calculation of the Effective Phosphorus Concentrations (EPC$_0$) in each of the water bodies suggested that sediments were currently most likely to act as a sink for soluble reactive phosphorus (SRP) in the river water, rather than as a source. However this is likely to remain dependent on how river water SRP concentrations vary in the long-term and how EPC$_0$ concentrations vary with ongoing deposition and erosion of sediment. Calculations of sorption of SRP within the active zone of the river bed (the 10 cm of water above the sediment surface and the top 5 cm of sediment) suggests that up to 10 % of the SRP in this water layer could be sorbed by the sediment as the river travels over a distance of 1 km.

Catchment erosion rates, river inputs and transport through the six water bodies were examined using the Caesar Desc Platform (CDP) landscape evolution model and compared to reported literature values. The CPD model gave first order estimations of natural baseline catchment erosion of ~0.5 t km^2 yr^{-1}. However, human impacts on erosion such as land drainage are not included within this estimate. Therefore, literature erosion rates were identified, with the most robust catchment erosion rate being ~6.6 t km^2 yr^{-1}. Using output variables calculated from the CPD model we applied these to this value to give a range of likely erosion and transport for each of the six water bodies based on typical annual precipitation rates. It was calculated that between 1000 and 10000 tonnes sediment would pass through the end of water body 6 (Dog in Doublet) each year. Water body 5 had the greatest quantity of sediment leaving it whilst greatest sediment deposition occurred in water body 6. Sediment associated TP and OEP transport and deposition corresponds to these sediment movements as well as their respective concentrations in the sediment. It was calculated that between 4 and 42 T of TP and 0.074 and 0.69 T of OEP attached to sediment passes through the exit of water body 6 each year, either as suspended sediment or bedload.

Water samples were analysed and a strong correlation found between SRP and Boron, suggesting that SRP in the river waters at the time of sampling had a strong sewage treatment works (STW) signature. With EPC$_0$ results suggesting that river sediments are currently active sorbents of SRP, the presence of sediment is likely acting to decrease the SRP in the river water. Thus, the greatest management task to improve water quality with respect to the concentration of SRP is preventing the sediment becoming a source of SRP if the river water concentration falls below the EPC$_0$ concentration. This may represent a balance between de-silting (although this would involve removing a SRP sink), the harvesting of macrophytes to remove P in the biomass and a continued decrease in P inputs from Sewage Treatment Works in addition to Catchment Sensitive farming approaches to reduce diffuse P inputs.

1 Introduction

The introduction of the Water Framework Directive (Directive EC 2000/60/EC) aims to prevent further deterioration, and to improve the quality of inland surface waters. One of its major aims is to promote 'good ecological status (GES)' with respect to biodiversity in rivers (Johnes et al. 2007). Phosphate (PO_4-P) is the major nutrient in rivers that is typically in shortest supply, and therefore has the greatest potential to limit river productivity (Mainstone & Parr, 2002). Thus, excessive phosphate concentration in river waters is one of the most common reasons why GES is often not achieved (Withers & Haygarth, 2007; Johnes et al. 2007). Major inputs of phosphate in river waters are from point sources such as sewage treatment plants (Jarvie et al. 2006; Neal et al. 2010) or diffuse sources such as agricultural land where phosphate enters the river primarily attached to soil particles (Bilotta et al. 2010; Quinton et al. 2010). The most common pathways for agriculturally derived diffuse phosphorus contamination is either via soil erosion (Haygarth et al. 2006; Quinton et al. 2010) or through under field land drainage systems (Reid et al. 2012; Bilotta et al. 2008). Detrimental outcomes for rivers include (i) eutrophication leading to a loss in aquatic biodiversity, (ii) sediment deposition leading to enhanced plant growth and further siltation of the channel and (iii) potential future desorption of phosphate from the sediment to the water body (Jarvie et al. 2005; McDowell et al. 2001; McDowell et al., 2003).

This report details work commissioned by the Environment Agency to examine sediment and Phosphorus dynamics in the six main WFD water bodies of the River Nene, which flows through Northamptonshire, Lincolnshire and Cambridgeshire, and out into the North Sea via the Wash. The Nene has a largely agricultural catchment, and its low relief, slow drainage and wide catchment give it a tendency to silt up. Large scale siltation of the river has been recorded and in 1930 the River Nene Catchment Board started to undertake extensive dredging (Meadows, 2007). Within these water bodies, SRP concentrations are often greater than the limits suggested for Good Ecological Status (0.12 mg L^{-1} is considered by the EA as the high concentration) to be achieved. It is considered that a significant potential source of dissolved P in the River Nene is that stored in the river channel sediment. Therefore the Environment Agency wishes to investigate the extent that P associated with this sediment can contribute towards greater SRP concentrations in the River Nene as well as the volume of sediment deposits in the river channel. Sediment deposition and phosphate concentrations are intimately linked in determining ecological status as well as the wider functioning of the river in providing a range of 'ecosystem services'. These include the role sediment and phosphate play in (i) maintaining navigability of the river to Northampton, (ii) the role phosphate plays in river bank macrophyte growth which can cause further siltation problems, (iii) the reduction of river channel capacity for flood alleviation and (iv) the reduction in amenity services such as angling and navigation. Results from this study will help inform future approaches and management with respect to both the effect phosphate has on GES, but also sediment management such as the desilting programme.

The study consists of three parts, these being (i) a sediment sampling program and laboratory analysis of the sediments for the six non-tidal part of the River Nene, (ii) a landscape modelling component that will produce first order estimates of sediment dynamics in the catchment and river channel and (iii) where we bring parts (i) and (ii) together to provide assessments of phosphate movement through the water bodies of the River Nene.

The objectives of each work package are given below:

Work Package 1: Sediment Sampling and laboratory analysis

The objectives of work package 1 were

- To derive first order estimates of sediment volumes in the six water bodies of the non-tidal river Nene
- To determine mean concentrations of TP (TP) and Olsen extractable P (OEP) in the sediment of six water bodies along the River Nene
- To determine the concentration of TP and OEP with depth from cores of sediment collected from six water bodies of the River Nene
- To determine the Effective Phosphate Concentration (EPC$_0$) for sediment samples from each of the six water bodies to assess whether sediments are a potential source or sink of phosphate
- To determine the kinetics of phosphate sorption or desorption for each of the water bodies

Work Package 2: Sediment dynamics computer modelling

The objectives of work package 2 were to produce first order estimates of erosion and deposition within the Nene river channel for the six water bodies using a landscape evolution model that will

- Estimate the amount of sediment entering the River Nene
- Determine the movement of sediment between the six water bodies of the River Nene as suspended sediment and bed load
- Compare model estimates with literature values of sediment movement in the River Nene

Work package 3: Combining sediment movement and phosphorus dynamics

The outputs from work package 1 and 2 will be used to answer the fundamental questions as set out in the project specification. For each of the 6 water bodies (and for the total length of the six water bodies) we use our analyses and modelling to estimate

- the mass of TP in the sediment
- the mass of OEP bound in the sediment
- the volume of suspended and bed load sediment passing each water body
- the potential mass of OEP released to the water column each year
- maps showing the erosion and deposition along with estimated depth of sediment along the main channel

2 Material & Methods

2.1 THE RIVER NENE CATCHMENT

The river Nene is the UK's 10th longest river and rises close to the village of Badby near Daventry, flowing in a north-easterly direction out to the Wash via the town of Northampton and City of Peterborough (Figure 1). It is 161 km long and has a catchment area of 2,270 km^2. The catchment for the upper six water bodies of interest in this study has an area of 1,590 km^2. The river is navigable from the sea as far as Northampton where it connects with the Grand Union Canal. The floodplain is relatively wide (from a few hundred meters to a couple of km) and the channel frequently bifurcates and rejoins (Williams & Fawthrop, 1988; Meadows, 2007). A major characteristic of the catchment is that the river generally has very slow flow. The river course falls from ~160 m AOD at source to ~6 m AOD at Peterborough. The majority of this fall occurs in the first 9.5 km, with the channel lying at 80 m AOD at Weedon (Meadows, 2007). In

the first section the river drops 1m in 270m and by the time it reaches Northampton it drops 1 m every 1500-2000 m and then by Thrapston it drops 1 m in every 3000 m (Meadows, 2007).

Figure 1: Map of the sampling locations in each of the six water bodies of the River Nene referred to in this study. The symbols for each water body are colour coded to represent the 'Ecological status' for that water body (Green = good; Orange = moderate; Red = poor).
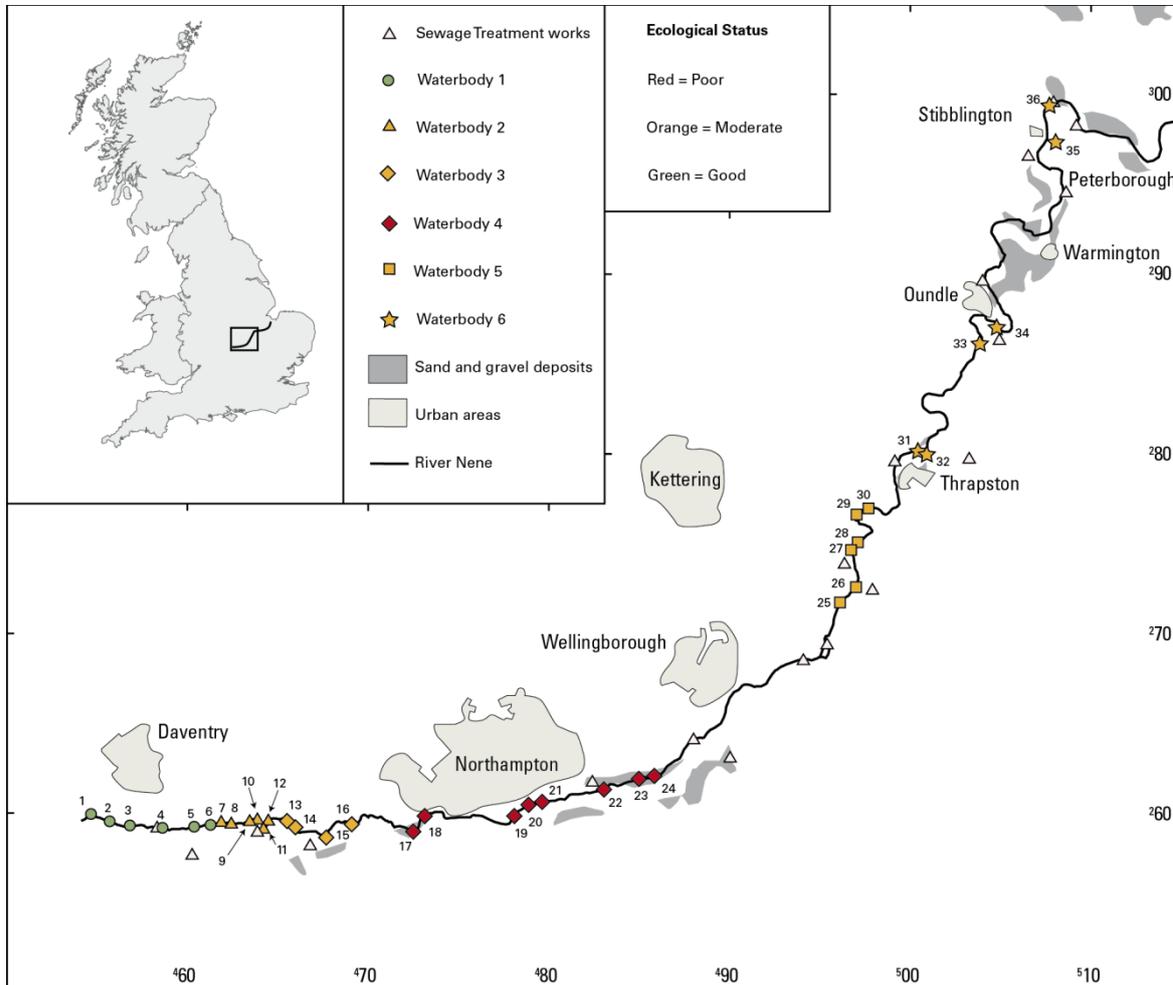
2.2   BEDROCK GEOLOGY

The bedrock geology of the River Nene catchment comprises rocks of the Lias group, oolites and the Kellaways and Oxford clay formations (Fig 2). The Lias group rocks that the Nene flows over includes in order, the Charnmouth Mudstone Formation, the Dyrham Formation (interbedded siltstones and mudstones) and predominantly the Whitby Mudstone formation. Descriptions of the lithologies are from Cox et al. (1999)

Charnmouth Mudstone formation: Dark grey laminated shale, and dark to pale grey and bluish grey mudstones; occasional concretionary and tabular beds of argillaceous limestone; abundant argillaceous limestone, phosphatic or sideritic nodules in some areas; organic-rich 'paper shales' are found at some levels. Silty and fine sandy beds are particularly found in the upper part.

Dyrham Formation: Pale to dark grey and greenish grey, silty and sandy mudstone, with interbeds of silt or very fine sand (in some cases muddy or silty), weathering to a brown or yellow colour. There are impersistent beds or ferruginous limestone (some ooidal) and sandstone which may be very fine or laminated. There are occasional large argillaceous, silty or sandy limestone nodules.

3

Whitby Mudstone formation: Medium and dark grey fossiliferous mudstone and siltstone, laminated and bituminous in part, with thin siltstone or silty mudstone beds and rare fine-grained calcareous sandstone beds. Dense, smooth argillaceous limestone nodules are very common at some horizons and phosphatic nodules are found at some levels. Nodular and fossiliferous limestones occur at the base in some areas.

Figure 2 Bedrock geology map of the main six water bodies of the River Nene based on the BGS 625k scale geological map
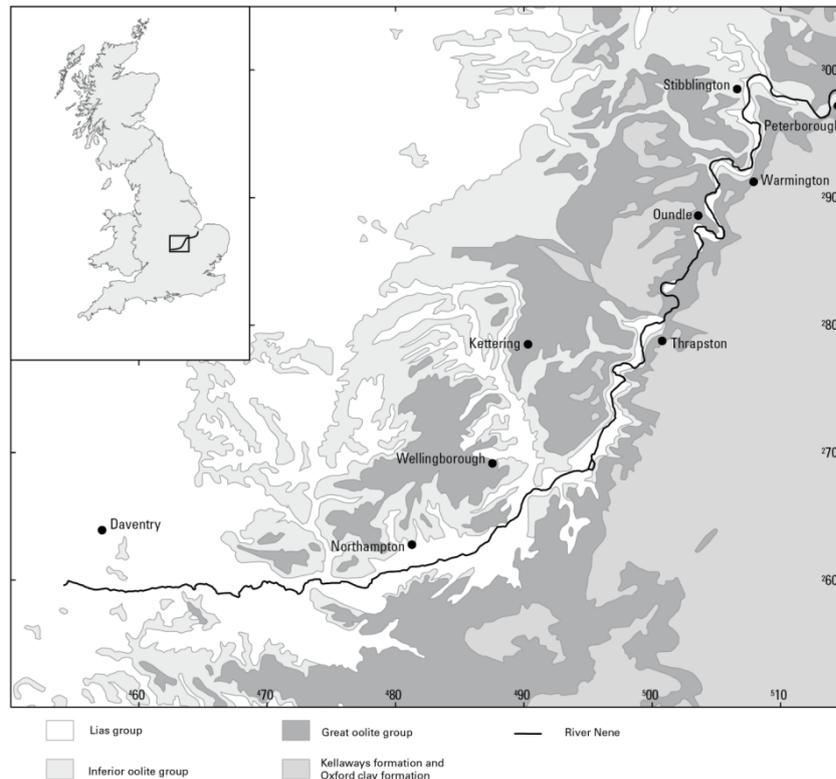
2.3   SUPERFICIAL GEOLOGY

The Nene Catchment was beyond the ice limits of the Devensian stadial but some glacial outwash is found in the catchment. These glaciogenic sediments are underlain by sands and gravels (Milton Sand) that represent earlier trunk rivers (Brown *et al*., 1994). Significant extraction of this sand and gravel has occurred along some reaches of the river, leaving a range of adjacent wetland environments. Major sand and gravel deposits are marked on Fig. 1. On the modern floodplains alluvial soils and deposits are found.

2.4   SAMPLING STRATEGY & SITE SELECTION

The body of the river Nene sampled was from the source waters at Badby down to Stibbington, west of Peterborough. This section of the River Nene is non-tidal and is divided into six water bodies by the Environment Agency. The sampling strategy was designed to obtain robust estimates of sediment TP and OEP concentrations in each of the six water bodies with a reasonable estimate of variability, whilst keeping the overall analytical cost within the budget provided by the Environment Agency. Therefore, five cores were collected from each water body which were to be homogenised prior to analysis of TP and OEP, whilst a sixth core (Core$_D$) was extracted from each water body to allow analysis of TP and OEP variation with depth. This core was divided into 5 segments, with the top section always being 0-5 cm depth from the sediment surface. This is a standard depth on which phosphate dynamics analysis is undertaken (Jarvie et al. 2005). This 0-5 cm section was used to calculate 'Effective phosphorous

concentrations (EPC$_0$)' (Section 3.9) and the rate of adsorption and desorption (Section 3.10) of phosphate. This was undertaken in conjunction with data collected from chemical analysis of a water sample for SRP taken in the water column above the sediment core. This water sample was filtered immediately after collection through a 0.45µm syringe filter and kept in the dark until analysis, within 5 days of collection (Jarvie et al. 2002).

Figure 1 shows the location of the cores extracted from the six water bodies. Site selection was initially based on a desk survey of the six water bodies. Consideration was given to under water infrastructure through line searches. For water bodies 1 & 2 and several samples of water body 3, the cores were collected by wading in the river. For water bodies 4, 5 and 6 a boat was used to enable sampling. Sampling positions were partially determined for these cores by the available boat launch sites and travelling distance upstream and downstream.

2.5   COLLECTION OF SEDIMENTS

2.5.1   Overview

Sampling was delayed from the original planned date (October/November 2012) because of the very wet autumn/winter of 2012/13. Consequently the EA placed high stream alerts on the river which prevented sampling. High stream alerts were briefly lifted in the first week of January 2013, allowing water bodies 1 & 2 to be sampled. Further rain meant that high stream alerts were next cancelled on the 14-02-13 allowing boat work to begin shortly after. The subsequent sampling of the sediments therefore needs to be put into the context of unusually long periods of flooding and high stream flows experienced during the autumn and winter period of 2012 -2013.

2.5.2   Sediment collection

Where possible, cores were taken by pushing a length of polycarbonate tube (diameter = 58mm internal diameter) into the sediment. Core retention was through the use of a core catcher, designed by BGS workshops, at the base of the tube. However, in the upper two water bodies there was little sediment so grab samples of the pebble and sand lag were taken. The total depth of sediment at each location was examined by probing at each site. This data was used to estimate the total quantities of TP and OEP within each water body. At the site in each water body where Core$_D$ was extracted, additional measurements were taken. These included (i) the width of river, (ii) the speed of water movement, and (iii) the depth of water. These measurements were required in the calculation of SRP desorption and adsorption fluxes to/from the sediment.

Plate 1: Sampling sediment in water body 3

2.6   LABORATORY MATERIAL & METHODS

2.6.1   Sample Preparation

Five core samples taken from each water body were air-dried before being sieved to < 2 mm. The mass of air-dry sediment from each of these cores in each water body was measured to estimate the average bulk density of the sediment in the cores (g cm^{-3}). Core$_D$ from each water body was cut into 5 sections, the top 0-5cm being wet-sieved < 2 mm for isotherm and kinetic analysis. After isotherm and kinetic analysis was completed the remainder of this sample was air-dried for other analyses. The other four sections were air dried immediately before being sieved to < 2 mm.

2.6.2   Sediment Bulk Density

The bulk density of sediment is required to estimate the mass of sediment from the volume of < 2mm sediment. This will allow calculation of TP and OEP in the sediment of each water body. Bulk Density (D_b) is calculated as

$$Db\ (g\ cm^{-3}) = \frac{M_d - M_s}{V - V_s} \qquad\qquad \textbf{Equation 1}$$

Where M_d = the total mass of oven dry soil, V = total volume, M_s = mass of stones and V_s = volume of stones.

2.6.3   Particle Size Analysis

Particle size distribution (PSD) of sediment samples (0.01 to 2000 μm) was determined using a Beckman Coulter LS13 320 laser diffraction particle size analyser. Prior to analysis organic matter was removed using H_2O_2.

2.6.4   Loss on Ignition – organic matter content

Estimates of organic matter in the samples from the sediment cores were obtained by igniting 1g samples at 475°C for 4 hours. The difference in mass before and after ignition provides an estimate of the organic matter content.

2.6.5   TP measurements in sediments

TP analysis was undertaken on subsamples of the dried sediment (~30g) which were ground in an agate mill to <150μm. Milled samples were digested by accurately weighing 0.25g of soil into a Savillex™ vial and adding HF, HNO_3 and $HClO_4$ concentrated and analytical grade acids, with a subsequent stepped heating program up to 170°C overnight, the purpose being the digestion of silicate and oxide phases. The dry residue was re-constituted after warming with MQ water, HNO_3 and H_2O_2, to 25 mL of 5 % v/v HNO_3 and stored in HDPE bottles. Reference materials (NIST SRM2710, SRM2711, GSS-6, BGS102 and BCR-2), duplicated samples and blanks were all prepared in a similar manner to check accuracy of the analytical and digestion method. In addition to the quantification of TP, a range of elements associated with P mineralogy and phosphate sorption were measured including Al, Fe, Mn and Ca by ICP-MS in the BGS UKAS and MCERTS accredited laboratory.

2.6.6   OEP measurements in sediments

OEP concentrations were determined using the Olsen P method (Olsen et al., 1954) on the air-dry homogenised samples from each of the cores. Olsen P is 0.5M $NaHCO_3$ adjusted to pH 8.5. Samples were shaken in a 1:20 sediment : solution ratio for 30 minutes before centrifuging at 2500 rpm for 15 minutes. Analysis was carried out in triplicate and the results expressed on a dry weight basis.

2.6.7   Calculation of Effective Phosphorus concentration

The potential relationship between sorbed and solution SRP was examined with isotherms using sediment from the top 5 cm of $Core_D$ from each water body. The isotherm was based on the Freundlich model (equation 2) which was fitted using the least squares method. The Freundlich model takes the form

$$\Delta N_a = K_f C_i^n \hspace{4cm} \textbf{Equation 2}$$

Where ΔN_a = change in adsorbed P (μmol g^{-1}), K_f is the Freundlich constant, C_i is the concentration of SRP in solution and n is a constant. Using the fitted isotherms the Equilibrium Phosphorus Concentrations (EPC_0) was calculated for each sample (see House et al., 1995; Jarvie et al., 2005). When considering the dynamics of the interactions of SRP with river sediment, it is important to have knowledge of whether the sediment has the potential to act as a source or a sink. The EPC_0 represents the equilibrium concentration of SRP in solution (i.e. when there is no net sorption or desorption over a 24 hour period). Thus, when SRP concentrations in the overlying water are greater than EPC_0, the sediment has the potential to sorb SRP from the water column and act as a sink. By contrast when SRP concentrations are less than the EPC_0, the sediment has the potential to release SRP to the water column and act as a source. EPC_0 analysis was undertaken on wet sediment (0-5cm) within seven days of sampling to minimize sample deterioration as suggested by Jarvie et al. (2005). The methodology for the isotherms was similar to that applied by Palmer-Felgate et al. (2011). A measured mass of sediment was placed in 6 bottles with 200 ml of a synthetic water composition roughly matching the major element chemistry of the River Nene (2 mmol $CaCl_2$). The bottles were spiked with different concentrations of KH_2PO_4, and placed in an orbital shaker in the dark at 10°C for 24

hours. Samples were then centrifuged and their SRP concentration determined (Murphy and Riley, 1962). In addition, the linear portion of the isotherms was used to derive K_d values (L kg^{-1}) (Jarvie et al., 2005).

2.6.8   Calculation of rate constants for SRPsorption / desorption from sediments

To calculate the rate of release or sorption of SRP from/to sediments, the kinetic methodology described by Jarvie *et al.* (2005) was used. For SRP release experiments (where EPC$_0$ > dissolved SRP), a measured mass of wet sediment (equivalent to 0.5 g dry sediment) was placed in polypropylene bottles with 200 ml of CaCl$_2$ solution, pre-chilled to 10 °C, with no additions of KH$_2$PO$_4$. For SRP uptake experiments (where SRP > EPC$_0$), the synthetic river solution in each bottle was spiked with KH$_2$PO$_4$ to an appropriate SRP concentration (greater than the EPC$_0$ and close to the measured SRP concentration in the water column at the time of sediment sampling). Bottles were then placed in an orbital incubator in the dark and shaken at 150 rpm at 10˚C and aliquots removed after specific time intervals (5 mins, 15 mins, 30 mins, 1 h, 3 h, 6 h, 15 h, 24 h), then centrifuged and analysed for their SRP concentrations. The sorption/desorption rates of SRP (House and Warwick, 1999; Jarvie et al. 2005) to or from the sediments were calculated based on the equation:

$$R = K_r(C_t - C_0)^n \hspace{4cm} \textbf{Equation 3}$$

R is the change in amount of orthophosphate sorbed (µmol g^{-1} h^{-1}), C_t is the orthophosphate concentration (µmol l^{-1}) in the overlying water, C_0 is the orthophosphate concentration in the overlying water after 24 h (µmol l^{-1}), K_r is a rate constant (µmol^{1-n} l^n g^{-1} h^{-1}) and n is a power term. The Nelder-Mead algorithm as implemented in Matlab (Lagarias et al., 1998) was used to determine the parameter values by minimizing the squared difference between the observed concentrations and those predicted by the rate curve. Using the calculated values the quantity of orthophosphate released from the sediment or removed from solution at any time, d_t, is obtained from equation 4 below.

$$dM = K_r(C_t - EPC_0)^n Sdt \hspace{3cm} \textbf{Equation 4}$$

Where M is the amount of orthophosphate sorbed (mmol), C_t is the concentration in solution at any time (t), EPC$_0$ is the equilibrium P concentration and S is the estimated mass of fine (<2 mm) sediment (g) in the reach of the river.

The fine bed-sediment mass S (g) within each waterbody was taken from calculation of sediment volumes obtained by probing and the mean bulk density of the sediment determined from the analyses of the cores. The flux of orthophosphate to/from the bed sediment is then calculated by integrating Eq. (2) over the residence time (T_{res}) of river water within the length of the river reach:

$$T_{res} = (D_{cs}W_{Cs}L_{riv})/Q \hspace{3cm} \textbf{Equation 5}$$

where D_{cs} is the mean cross-sectional depth of the reach, the length of the river reach (L_{riv}), and Q is the mean annual discharge of the reach and W_{Cs}.is the average width of the cross section. Bed sediment orthophosphate fluxes to the boundary layer of the river channel are expressed as g

P T_{res}^{-1}. The annual flux of orthophosphate to/from the bed sediment into the boundary layer can then be estimated by multiplying the flux for this residence time by the number of residence time periods in a calendar year. However, this ignores seasonal effects.

2.6.9   Molybdenum Blue method for analysis of orthophosphate (PO$_4$-P)

Phosphate concentrations in (a) river water samples (b) Olsen P extracts, (c) isotherm analysis and (d) kinetic analysis were undertaken using the molybdenum blue method (Murphey & Riley, 1962). All samples used a calibration curve with concentrations of 0, 0.125. 0.25, 0.5, 0.75 and 1mM P in 100ml volumetric flasks; these being equivalent to ~3.7, 7.5, 15, 22.5 and 30 µg P. Calibration curves and analysis were undertaken using a Perkin Elmer Lambada 35 uv/vis spectrometer.

Figure 3: Photo showing (a) calibration and (b) Olsen P extract solutions.

A combined calibration curve from all the phosphate analysis runs is shown in Figure 4. Concentrations were converted from µM L^{-1} to µg L^{-1} to generate the relationship in equation 6 from values shown in figure 4 which relates PO$_4$-P concentrations to absorbance readings

µg L^{-1} P-PO$_4$ = 142.59 x Absorbance   **Equation 6**

This combined calibration equation was used to determine all P-PO$_4$ concentrations in solutions from absorbance readings. In addition, 'Limits of Detection (LOD)' were calculated for each of the different matrices used. These included water, 2mMol CaCl$_2$, and the 0.5M NaHCO$_3$ Olsen P extractions (Table 1). Limits of detection were calculated by making up 10 samples of each of the blank matrices, measuring the absorbance and calculating the standard deviation. The LOD was then calculated as the standard deviation multiplied by 3.

Figure 4: Calibration curve for molybdenum blue method for determining PO_4-P (μm L^{-1}). Standard deviations for each point are shown but are generally contained within the symbol.
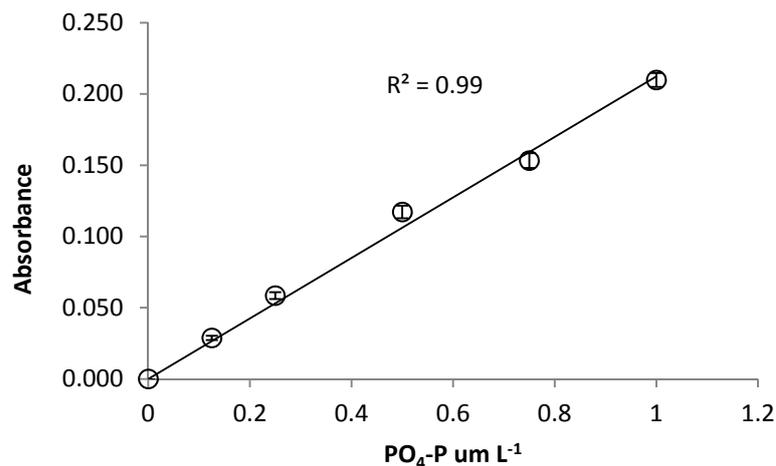
Table 1: Calculated Limits of detection for each of the matrices used in PO_4-P analysis

Sample Matrix	Mean of blank (n=10) (μg P)	Standard deviation	LOD μg P (3 x SD)
Water	0.08	0.07	0.22
2mM 20 ml	0.11	0.11	0.34
2mM 40 ml	0.22	0.07	0.22
2mM 60 ml	0.72	0.06	0.18
2mM 80 ml	0.74	0.12	0.37
Olsen P	1.61	0.16	0.59

2.7   CALCULATING SEDIMENT FLUXES USING A LANDSCAPE EVOLUTION MODEL

2.7.1   Background

The modelling phase of this project utilises a complex, distributed landscape evolution platform to derive sediment transport, erosion and deposition over the last century. During this period, the widespread heavy usage of phosphate fertiliser was introduced into the arable farming industry as a means of increasing production. Through processes of runoff and fluvial sediment deposition, phosphates sorbed to sediment during this period can accumulate in the river bed. Phosphates stored in this manner can later be remobilised and transported during a storm event. The CDP (CAESAR-DESC Platform), based on the well established CAESAR landscape evolution model, uses distributed rainfall, potential evaporation and soil properties to drive an integrated surface-subsurface hydrological model. Sediment transport in the model is dictated by the regional hydrology and terrain characteristics. Continuous monitoring of erosion and deposition allows the spatial distribution of sediments to be mapped.

2.7.2   Model Description

2.7.2.1 INTRODUCTION

This CDP was created by combining algorithms from various backgrounds to produce a modelling system from which a variety of earth system interactions can be explored. A modified version of the well established Cellular Automaton Evolutionary Slope and River (CAESAR) model (Coulthard and Van De Wiel, 2006), CAESAR-Listflood (Bates et al., 2010) is used as the platform kernel. CAESAR is quasi three-dimensional and incorporates a modular design, with great versatility in the range of simulated spatio-temporal scales to which it can be applied. CAESAR has been used to investigate a variety of sediment transport, erosional and depositional processes under differing climatic and land use pressures in river reaches and catchments around the world. Improvement of the surface hydrological representation prior to this study allowed bespoke distributed fluvial soil pathway and confined groundwater models to be added to the CAESAR model, forming the CDP. The recently updated components have previously been validated against analytical solutions and observed data, and the coupled model has been applied at a regional scale in the Eden Valley catchment, Cumbria (UK), where the role that subsurface water fluxes play in shaping catchment scale geomorphology was examined (Barkwith et al., 2012).

2.7.2.2 WATER PARTITIONING

The partitioning of rainfall between, evaporation, runoff and recharge to groundwater in the CDP is achieved using a soil water balance model (Wang et al., 2012). We implement a simple technique that represents potential groundwater recharge and runoff processes based on spatio-temporally distributed soil moisture conditions. Soil moisture is a function of; rainfall, potential evapotranspiration, soil moisture condition, topography, soil types, crop type and base flow index (BFI). The method we use represents these soil water processes responding to variable soil water storage properties (see Rushton, 2003) and vegetation growth stages (see Allen et al., 1998). When soil moisture reaches field capacity and is unable to store further additions of water, water drains freely in the saturated soil. Additional water inputs to the soil result in lateral runoff (routed by Lisflood), if a gradient exists towards adjacent locations, and if required as percolation downwards through the saturated soil (groundwater recharge). If the rainfall intensity is greater than the capacity of soil to maintain infiltration, water accumulates on the soil surface and becomes surface runoff. Water not accounted for in soil storage, evapotranspiration or uptake by vegetation is termed excess water. Excess water is divided between runoff and recharge to groundwater based on a base flow index parameter. Base flow index is an average surface to subsurface water partitioning ratio reflecting the permeable nature of the catchment in addition to other catchment characteristics. The base flow index parameter is estimated, by performing a baseflow separation on a river flow time-series, and further refined through an iterative calibration process. In general, greater runoff and reduced recharge is observed in areas with steeper slopes. Consequently, average and nodal terrain gradient are factored into the calculation of recharge and runoff.

2.7.2.3 SURFACE WATER ROUTING

Routing of surface runoff and channel flow is controlled by Lisflood (Van der Knijff et al., 2010), a two-dimensional hydrodynamic flow model. Routing is based on the one dimensional Saint-Venant equations, as modified by Bates et al (2010), where surface flow takes into account; acceleration, water surface gradient and friction properties and has enhanced stability due to increased friction forcing water flow towards zero (Liang et al., 2006). If the flow depth, as calculated using the surface partitioning component, is above a defined threshold and stability criteria are met, the flux between cells at the proceeding time-step depends on the water surface gradient between the adjacent cells, Manning's coefficient, the time-step length and the gravitational constant. For each time-step flow between neighbouring cells is computed and flow

depths updated simultaneously at all points within the model domain. A full description of Lisflood is provided by Van der Knijff et al. (2010).

2.7.2.4 GROUNDWATER FLOW

Groundwater flow is simulated using a two dimensional lattice of square cells interacting according to the von Neumann type neighbourhood in a technique similar to that utilised by Rothman (1988). Cells consist of distributed hydraulic conductivity and specific yield, and a datum referenced aquifer head that is modified through time. Aquifer head is updated at each time-step using Darcy's law to calculate water flux between cells. Transmissivity can be approximated by multiplying hydraulic conductivity by aquifer depth. The total flux for a central cell is a combination of; fluxes to neighbouring cells and additional source and sink terms. Recharge from the surface hydrological component provides the source term and baseflow to the surface acts as a sink. Total fluxes are used to update aquifer heads at each point in the domain simultaneously at each time step using a discrete mass balance equation (see Ravazanni, 2011). Two user-defined lateral boundary condition types have been implemented into the CDP code, allowing a variety of hydrological situations to be represented. Specified (Dirichlet) boundary conditions fix aquifer head at the boundary to the initial condition and a no-flow (Neumann B) condition sets flux across the boundary to zero. The base of the aquifer is defined as impermeable; however, leakage to and from the base of the modelled aquifer is included in the flux algorithm as a secondary source and sink terms. The surface boundary allows water flux to be returned to the surface component as baseflow where aquifer head is greater than terrain height.

2.7.2.5 SEDIMENT TRANSPORT

Following the derivation of flow depth at each node, fluvial erosion and deposition are calculated, where fluvial transport is determined using the Wilcock and Crowe (2003) method, to calculate mixed-size particle movement. The Wilcock and Crowe formulation (equation 7) derives the sediment flux of a grain size fraction using the fractional volume of the particular sediment size (F_i), shear velocity (u_*), ratio of sediment to water density (ρ_{ws}), gravity (g_i), and the function W_i; which allows the total transport to be calculated from a shear stress factor (Φ) derived from shear stress (τ) of the fractional grain size and τ_{ri}, a reference shear stress:

$$q_{sed} = \frac{F_i u_*^3 W_i}{(\rho_{ws}-1)g} \qquad\qquad \textbf{Equation 7}$$

$$W_i = 0.002(\Phi)^{7.5} \qquad \textbf{for } \Phi < \textbf{1.35} \qquad \textbf{Equation 8}$$

$$= 14\left(1 - \frac{0.894}{\Phi^{0.5}}\right)^{4.5} \qquad \textbf{for } \Phi \geq \textbf{1.35}$$

$$\Phi = \frac{\tau}{\tau_{ri}} \qquad\qquad \textbf{Equation 9}$$

The Wilcock and Crowe method can transport sediment within a catchment as a suspended load or a bedload (Equation 10). Both depend on the volume of sediment (q_{sed}) transported per time-step (dt), where the sediment transported from a central cell to a neighbouring cell (k) is

calculated by equating the coefficient *X* to either; slope, for bedload transport, or velocity for suspended load transport. The calculation of suspended load transport is simplified, as it assumes an equal distribution of sediment throughout the water column. Sediment deposition also differs between the two transport types, with bedload sediment deposited (and subsequently re-entrained) at every time-step and suspended sediment deposition based on fall velocities.

$$V = \frac{X_k}{\sum X} q_{sed} dt$$

Equation 10

2.7.2.6 INPUT PARAMETERS

Initialisation of the CDP requires a number of essential input items in the form of either gridded or list based ASCII files. Spatially discretised initial model inputs are entered as Cartesian grids, with header information containing cell size, domain dimensions and geo-referencing details.

Distributed daily rainfall, land use, DEM, soil type hydrology and evapotranspiration datasets are used to initialise and force the surface hydrology model. Field capacity, wilting point, maximum root depth and crop coefficient are used in conjunction with the reference evapotranspiration to calculate the PE values for different crop types. As the groundwater module is enabled for this study, the distributed hydraulic conductivity and specific yield need to be defined, initial groundwater levels need to be derived and the boundary conditions specified. A description of this process is contained in the 'Setup' section of this report. Platform sediment transport is based upon relative density of submerged sediment, grain size, flow depth and the water surface gradient. The latter two are derived from the platform hydrological model, while the distribution of grain size and density is determined through analysis of the cored sediment samples collected during the fieldwork phase of this study.

2.7.3   Output

Simulated changes to sediment volume, representing the past century, are presented for the Nene catchment and the six sub-catchment water bodies as defined by the Environment Agency in the project scope. Through analysis of the changes in volume during the simulation over the latter half of the century, and through a projection of these rates back in time, the time averaged and total twentieth century sediment flux rates and phosphate levels can be derived. Using modelled suspended sediment and bed load volumes calculated by the simulation at the exit of each water body of the Nene, the annual phosphorus and phosphate volumes released into the river can be estimated.

2.7.4   Model Application

2.7.4.1 CONCEPTUAL MODEL AND STUDY AREA

The overall Nene catchment area is approximately 2,270 km². Despite the presence of some large population centres (Northampton, Wellingborough, Kettering, Corby and Peterborough) the catchment is largely rural. Areas surrounding the Fens and to the East of Peterborough, where arable crop is produced, are intensively farmed. To the west of Peterborough, the land is farmed less intensively.

The River Nene and its tributaries, the Kislingbury Branch, the Brampton Branch and Wootton Brook, meet close to Northampton and flow across gently undulating rural country to the flat plains around Peterborough, before entering the embanked tidal reach across the Fens. Much of the Fens lies below sea level relying on pumping stations for drainage.

The underlying geology of the catchment broadly comprises mudstones to the west of Northampton, limestones between Northampton and Peterborough, and clays to the east of Peterborough. Where the underlying rock is composed of non-porous mudstones, there are higher rates of rainfall runoff, which flows directly into the surrounding watercourses. In the areas where limestone or sandstone bedrock is present, runoff may infiltrate the rock, lagging the response of rivers to rainfall and reducing peak flood flows. Excess storm water contained in the groundwater store can make these areas prone to flooding with little subsequent rainfall. In the lower fenland areas downstream of Peterborough the predominance of peat soils and the low gradients means that water moves slowly to the river channels.

For this study we are not interested in the area to the east of Peterborough, and therefore, to reduce the computational expense, this region of the catchment is discarded from the numerical modelling.

2.7.4.2 DISCRETISATION

Model boundaries and internal sub-catchment boundaries are defined in Figure 5. The groundwater and surface water catchments are bounded by the Neumann B condition, where no water can flow across the boundary. The exception to this setting is along the eastern boundary, where surface water can be discharged from the catchment in the form of a river. The Nene catchment is discretised into 200 m square grid cells, with a variable sub-daily time-step utilised for calculations of surface flow and sediment transport. The sub-daily time-step limits the amount of sediment that can be passed between cells, maintaining stability within the model during simulation. The selected grid spacing allows a viable execution time, whilst retaining enough detail to adequately represent the sediment transport system. In addition to a catchment wide assessment, the grid spacing also facilitates the sediment and water flux properties of the six sub-catchments to be assessed post-simulation.

Figure 5: Digital Elevation Model of the area used for landscape evolution modelling. The model boundaries are no flux type boundaries except for the eastern edge of the model domain. Water body outlets and catchment areas are also shown.
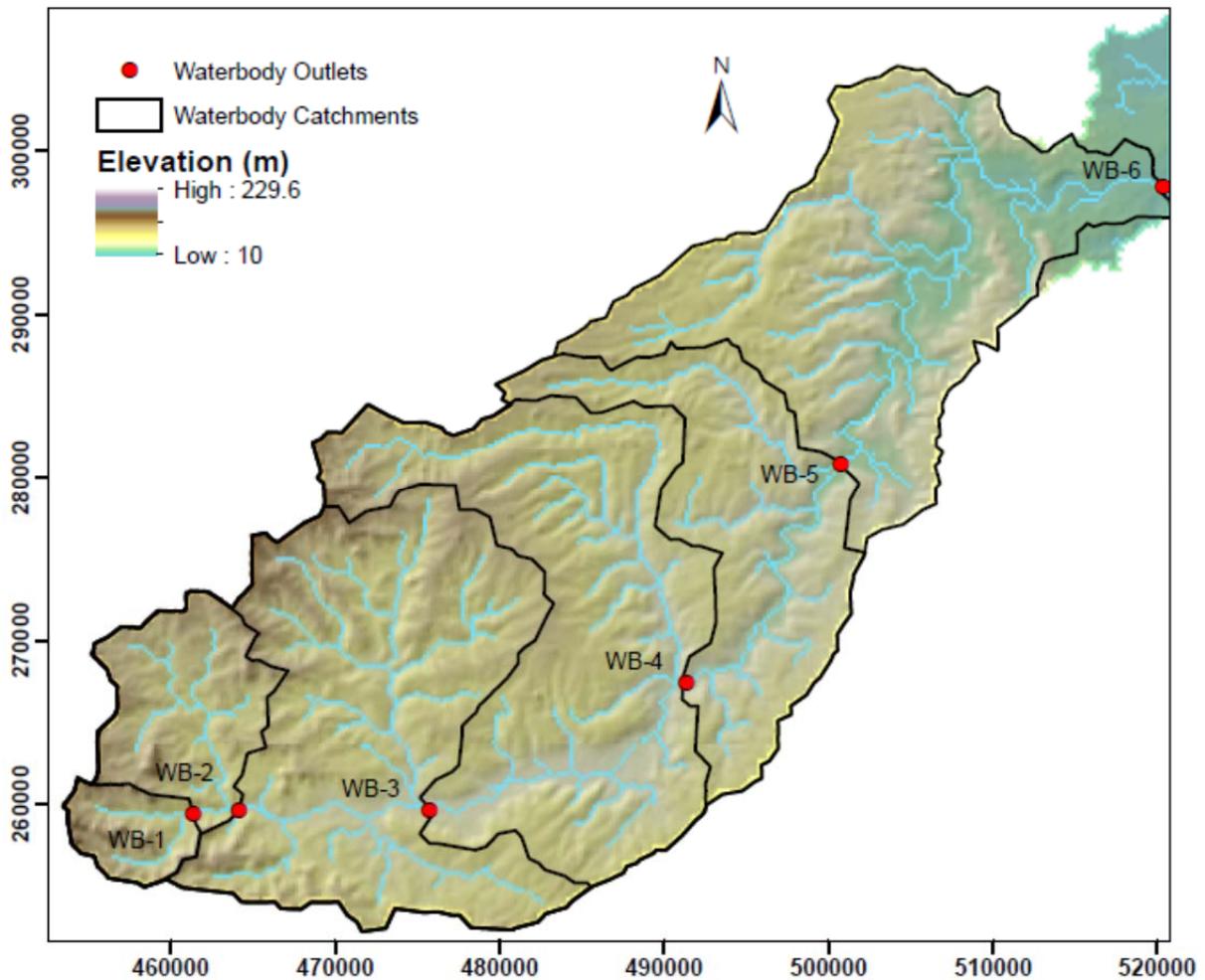
2.7.4.3 PARAMETERISATION

Distributed daily rainfall, landuse (LCM2000), DEM, the hydrology of soil types (HOST), river flow and evapotranspiration (MORECS) datasets are used to initialise and force the surface hydrology model. The HOST dataset contains 29 soil classes of similar hydrological response and the BFI value for each class. Field capacity and wilting point of each soil type, and the maximum root depth and crop coefficient (which is multiplied by the reference evapotranspiration to calculate the PE values for different crop types) for each landuse type which was gathered from the experimental data of Allen et al. (1998) and the hydrological modelling work of Griffiths et al. (2008) and Young et al. (2008). The sediment transport components of the platform utilise the same DEM as the hydrology components, but also require bedrock elevation referenced to the same datum to determine the thickness of the sediment store layer. Grain size distributions as determined by field measurement of fluvial sediment are used to initialise the model.

2.7.5   Setup

Although it would be preferable to run the model for the entire century, access to rainfall and potential evapotranspiration data for the region is limited to the forty years 1962-2001. Representation of sediment flux rates for each of the water bodies over the periods not covered

by the simulation will be projected back to 1910 and forward to 2010. The input data required by the model, and a short description of each, is contained in Table 2.

Table 2: Input datasets for the calibration, 'spin-up' and transient simulations. The 'spin-up' is the period where the model is allowed to reach a 'steady state' and accounts for initial conditions that are not correct (i.e. no water in the system and heterogeneous sediment distribution).

Input	Type	Description
Hydraulic Conductivity	Single	Value determined through calibration of groundwater levels and base flow return to river
Specific Yield	Single	Value determined through calibration of groundwater levels and base flow return to river
Potential Evapotranspiration	Distributed	1962 – 2002 at a 40km daily resolution, as determined by the Met. Office MORECS dataset
Precipitation	Distributed	1962 – 2002 at a 25 km daily resolution, as determined by CEH dataset
Landuse	Distributed	LCM2000 land cover map, as determined by CEH dataset based on satellite data
HOST	Distributed	Fixed, 1km national soil map dataset, integrating river catchment behaviour
Initial NSSS	Distributed	Determined through spin-up to steady-state value
Initial SMD	Distributed	Determined through spin-up to steady-state value
Initial Sediment Distr.	Heterogeneous	Nine grain size fractions determined by averaging field observations
Hydrological Boundary	Distributed	No-flow at all boundaries, except at the river outlet
Debris Flow Method	Single	Sand-pile method, with critical failure angle set to 30°

The percentage distribution by weight of nine grain size fractions was incorporated into the model domain (Table 3), which were determined by dry-sieving stream sediment from two core samples, taken in Water Bodies 1 and 2 respectively, and taking the mean of the two. This distribution is assumed to be fully mixed and applied throughout the catchment in the initial model setup. As the model evolves through time, sediment grain sizes are spatially redistributed across the active parts of the catchment. This distribution initially occurs as a strongly transient volumetric sediment flux that recedes as grain size distributions adjust to the local hydrological conditions. During the initial period, sediment transport fluxes will be much greater than the period that they represent. By negating sediment flux rates during this 'spin-up' period, which approaches a steady-state after approximately ten simulated years for the Nene catchment at the desired resolution, uncertainty in the modelled output is reduced.

The main simulation will comprise a forty year transient run representing 1962-2002, where sediment erosion and deposition are monitored on a 10-day basis and suspended sediment and river flows are monitored continuously.

Table 3: Catchment average initial grain size distribution as determined by field observation

Grain Size (mm)	<0.06	<0.16	<0.36	<0.55	<0.8	<1.5	<3.0	<7.0	<30.0
Percentage (%)	5.4	11.8	45.6	50.1	62.1	78.1	88.4	98.0	100.0

2.7.6   Modelling Caveats

As with all numerical modelling techniques, there are several caveats associated with the datasets utilised by the CDP. Firstly, discretisation of the grid reduces all observed sub-grid variation to a nodal average. As we are working at the catchment scale, this should have little influence on the model output. The spatial resolution of the meteorological and soil based datasets is much greater than that of the grid, reducing the accuracy of the modelling. It is currently not possible to obtain higher resolution datasets without extensive field campaigns, which are beyond the scope of this study. Again, as the resolution of these datasets is an order of magnitude less than the catchment size, they do not impart much error in the final model output. The ability of the model to represent gauged river flow record, suggests that, although improvements are possible, the use of these datasets is justified. The homogenisation of sediment distribution across the catchment during initialisation is rectified by the model during attenuation to steady state during simulation. During this process, sediment is sorted in a distributed manner across the catchment, with upper reaches consisting of coarser materials and the lower reaches having a greater percentage of fines.

2.7.7   Meteorological and gauged river flow data

The distributed average 1962-2001 precipitation (mm d^{-1}) is presented in Figure 6. Due to the interaction of orography and the atmosphere boundary layer under the prevalent wind flow direction, precipitation is up to 33% greater in the elevated sections of the catchment in comparison to the lowest sections.

The Upton (west) and Orton (east) river gauging stations are used to calibrate the model hydrology between 1970 and 1979 (Figure 7). Although the gauging stations are at opposite ends of the catchment and have a flow values at differing orders of magnitude, they exhibit the same pattern of flow fluctuation. During the 70 years of available flow data (1939-2010), the highest flows were found on the 18th May 1947, remaining well above average for over two weeks. This peak coincided with widespread flooding associated with the rapid thaw of deep snow, which had accumulated during the previous winter. These river floods were the largest floods for over 200 years (RMS, 2007) although other major floods have occurred in 1976/77 and 1998. The peak flows during the 1947 flood are more than double any subsequent observations. The effect of this level of flooding on sediment fluxes for the Nene catchment is unknown and, therefore, there is an elevated level of uncertainty associated with projecting results to beyond this date.

Figure 6: Distributed mean daily precipitation in the Nene Catchment, averaged over the period 1962-2001
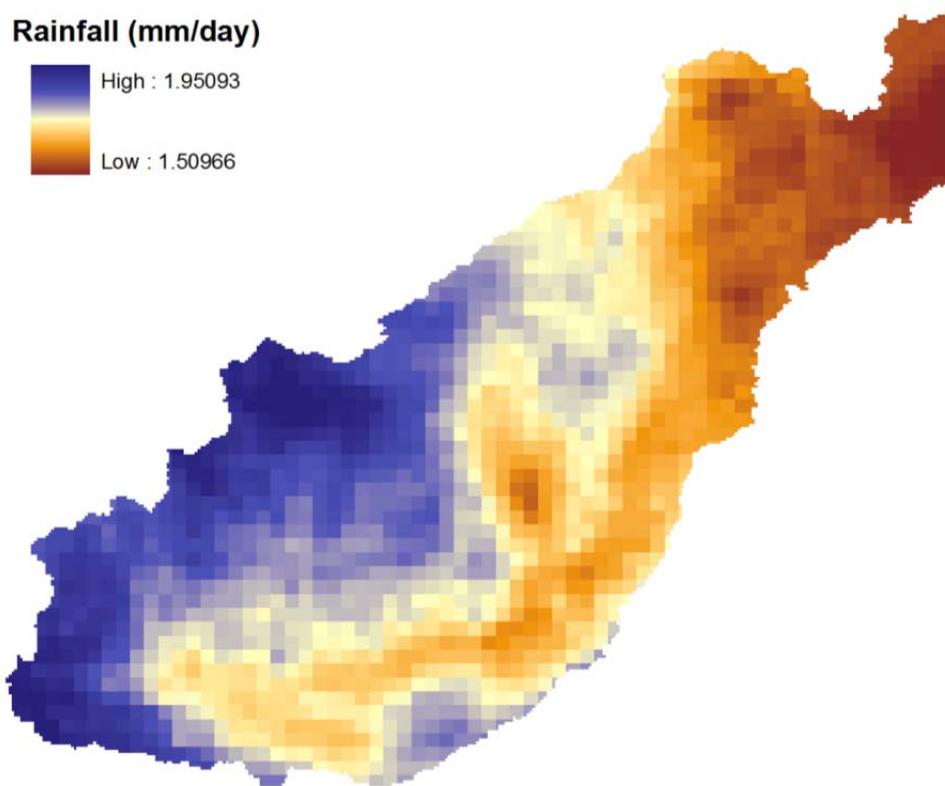
Figure 7: Gauged river flow data for the Orton (Blue) and Upton (red) stations. Note the differing flow scales on the vertical axis
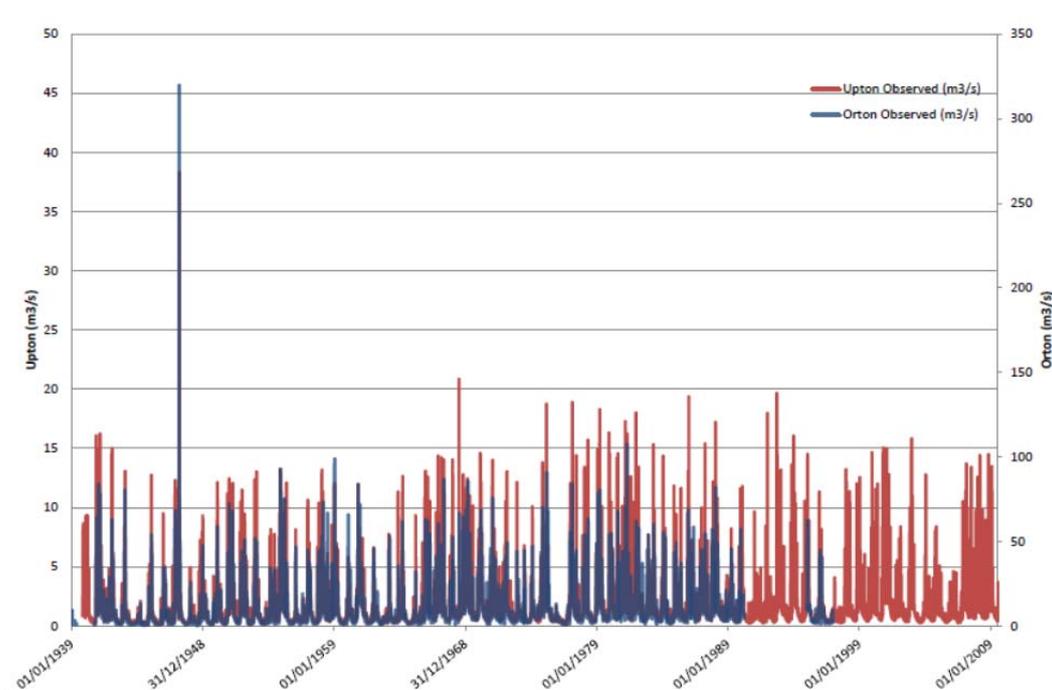
2.7.8 Calibration

For the calibration, a daily cycle of model output was specified for the calculation of groundwater level (mAOD), base flow (m^3 day^{-1}), recharge (m^3 day^{-1}) and surface water (m^3 day^{-1}). To assess the errors associated with differing water flow routes, and to simplify the process, time series of simulated groundwater and surface flow were calibrated to observed data separately. The first phase of calibration removed the simulated base flow component from surface flows. These where compared to a base flow separated flow records from the Orton and Upton gauging stations for the surface component analysis. Once an acceptable agreement was achieved, the second phase of calibration was implemented, where the base flow component was re-instated in the simulation and a comparison to the non-separated gauged river flow dataset used for analysis. The same river gauging stations were used for both phases of the calibration.

Following the first phase of calibration, there is an acceptable match between simulated and observed river flows with the base flow component removed (see Figure 8 for the comparison at the Orton gauging station). The timing of large flow discharge events shows excellent agreement; however, the representation of peak discharge values is not as good. The disparity most likely arises from the misrepresentation of true rainfall and surface frictional characteristics under the current discretisation scheme, and would be improved with input data at a higher spatial resolution. Although the peak discharges are not fully represented in the simulation, the average peak discharge value is very similar to the observed value. Following the second phase of calibration, where base flow is introduced, the match between simulated and observed river flows is in some places poor (Figure 9). The worst representation occurs during recession of the river, where groundwater recession rates are not fully representative of the system. This suggests that the parameterisation of the groundwater model is not accurate. However, the simulated peak flow values show close agreement with the observed values. For this study the latter is the most important attribute of the calibrated output, as it is during these periods where the majority of sediment is transported.

Figure 8: Base flow separated surface runoff derived from the Orton gauged river flow dataset (blue) compared to the simulated runoff (red) from 1970-1979. These datasets were used to calibrate the surface flow characteristics of the CDP.
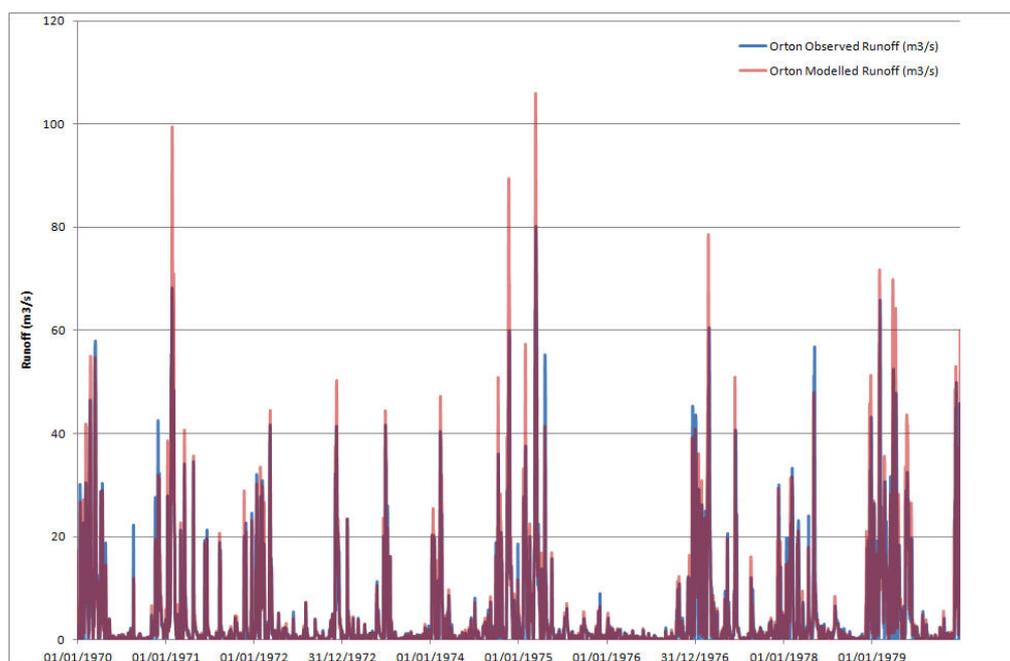
Figure 9: Surface flow (m^3 s^{-1}) from the Orton gauged river flow dataset (blue) compared to the simulated runoff (red) from 1970-1979. These datasets were used to calibrate the groundwater surface flow characteristics of the CDP.
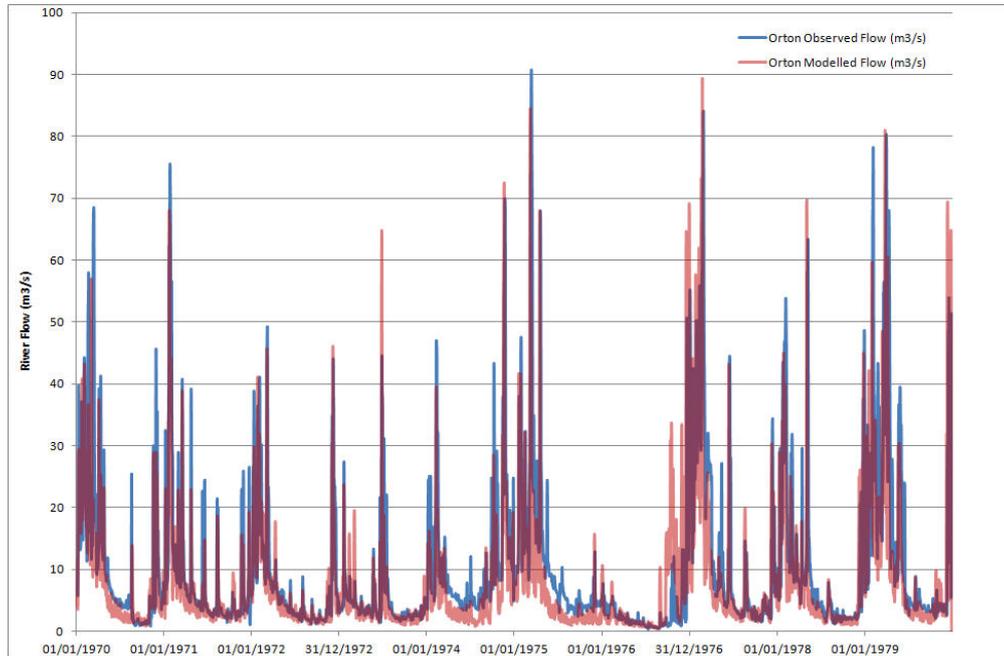
2.7.9   Simulation Projection

The projection of results forwards and backwards in time through a post-processing analysis forms an important part of this project. It is necessary as we do not have meteorological data required to drive the hydrological model available for this catchment prior to 1962 or after 2002. Therefore, based on a statistical analysis of the simulated sediment flux rates, we projected the rates forwards and backwards in time.

2.8   CALCULATIONS OF TOTAL PHOSPHORUS AND PHOSPHATE IN RIVER SEDIMENTS AND WATERS

2.8.1   Total mass of P in sediment of the six water bodies

For each of the six water bodies we calculated the mean TP content from the five cores (*VPC*):

$$V\hat{P}C = \frac{1}{n}\sum_{i=1}^{n}\mathbf{TP}_i \times \mathbf{BD}_i \qquad\qquad \textbf{Equation 11}$$

Where $\mathbf{TP}_i$ and $\mathbf{BD}_i$ are respectively, the TP concentration and bulk density of the *i*th core. The total mass or stock of P (Sed P$_{tot}$) in the sediment of each water body can then be computed by:

$$\text{Sed P}_{tot} = V\hat{P}C \times S_{vol} \qquad\qquad \textbf{Equation 12}$$

where S_{vol} is the estimate of the total volume of sediment in the channel (from work package 3). The total stock of P in the sediment of all six water bodies is the sum of the stock in each water body.

20

2.8.2   Extractable P stock in sediments of the six water bodies

The approach to estimate OEP stock in sediment will be the same as for the TP shown above, but in this case the data for OEP will be used instead of the TP concentrations in Equation 11. So, here mean volumetric OEP (*VêPC*) will be estimated using OEP P concentrations (**TeP**):

$$V\hat{e}PC = \frac{1}{n}\sum_{i=1}^{n} \mathbf{TeP}_i \times \mathbf{BD}_i \qquad\qquad \textbf{Equation 13}$$

and the total mass or stock of OEP (Sed eP$_{tot}$) in the sediment of each water body can then be computed by:

$$\mathbf{Sed\,eP_{tot}} = V\hat{e}PC \times Svol \qquad\qquad \textbf{Equation 14}$$

The total stock of OEP in the sediment of all six water bodies is the sum of the mass in each water body.

2.8.3   Estimating the annual mass of orthophosphate adsorbed/desorbed to each water body and across all water bodies.

The river system can be considered as a series of inter-connected reaches, each of which has a known mass of fine (<2 mm) sediment in the river bed which interacts with the overlying water column to sorb or release orthophosphate. The approach used is the same as that of Jarvie et al. (2005) where they assumed that the boundary layer of water that interacts with the bed sediment is 0.1 m thick, and orthophosphate is exchanged between the river bed and the volume of water within the boundary layer during the residence time of the river water within the reach. This exchange is characterised by: (i) the measured initial SRP concentration in the water column, (ii) the EPC$_0$ of the bed sediment and (iii) kinetic parameters for P-sorption, which were measured in the laboratory (Section 2.6.8). Therefore orthophosphate flux estimates to/from bed sediments can be calculated for each of the 6 water bodies and for the Nene as a whole using the outputs of mean annual river flux from the CDP model which is calibrated to data from flow gauging stations. These fluxes provide a quantitative estimate of the orthophosphate uptake/release potential of the river bed sediments to the river water. This analysis will not provide predictions of river water orthophosphate concentrations, but it will provide an assessment of the magnitude of potential release or sorption of orthophosphate to water in each water body.

3 Results and Discussion

3.1   SEDIMENT DISTRIBUTION AND DEPTH IN THE RIVER NENE

At each sampling site the sediment was probed to allow the calculation of sediment volume (Plate 2).

Plate 2: Probing of the sediment to determine depth and volume in water body 3

This probing allowed the mass of TP and PO_4-P to be calculated for each water body. Figure 10 shows generalised patterns of sediment distribution, found in each water body as determined by probing. It is not clear to what extent this is due to the high flows in the winter period of 2012/13 which may have eroded and transported much of the channel sediment. Sediment patterns were found to be highly heterogeneous with the absence of sediment deposits being very common in much of the river. Sediment was generally found where the water currents were slowest. Figure 11 reports the average depth ± 1 Standard deviation (SD) for the sediment found in each water body. Below are descriptions of the sediment characteristics for each water body.

Water body 1

Water body 1 was sampled on the 7th and 8th January. Steam flow was fast throughout the sampling period at 0.4 m s^{-1} at site 1 of this water body. Sediment consisted at most of the sampling sites as a mixture of gravel and sand (mostly gravel) although slight build ups of coarse silt were found in areas of slower flow such as site 2 where $Core_D$ was taken.

Water body 2

Water body 2 was sampled on the 9th and 10th January. Site 6 was not sampled during this initial sampling period as the stream was too deep for wading as a result of the high flow. Sediment consisted at most of the sampling sites as a mixture of gravel and sand (mostly gravel). $Core_D$ (Site 1) was taken on one of the few bends in this stretch of water.

Water body 3

Water body 3 was sampled between 20th and 21st February. Sites 1 & 2 were similar in nature to the previous water body, consisting largely of a gravel and sand lag. By site 3, there was a change in the nature of the sediment as it became deeper and more silt and clay based rather than the gravel and sand previously found. Deposition of sediment also increased and was found to be 1m + (Site 3) close to the river bank. These sediment deposits extended up to 1m from the bank with no sediment in the central channel. At sites 4-6 the depth and nature of sediment was variable and appeared to be dependent on position within the channel and the speed of the river.

Water body 4

Water body 4 was sampled on the 26th and 27th Feb. Again the depth and nature of sediment was highly variable and appeared to be dependent on position within the channel and the speed of the river. Site 1 was taken just after a sluice/lock in a position of slower water. Around the gravel pits there was very little sediment present anywhere in the main river channel due to scouring. The sample from site 2 was taken where the river widens and therefore current slows, whereas Site 3 was taken in a smaller backwater channel where 45 cm sediment was found. Again this was a result of no sediment being found in the main channel of the river at this point. Sites 4, 5, and 6 were again taken in the slower waters of the rivers found in inlets along the channel and before locks as the main river channel was heavily scoured. In particular, the river channel close to sand and gravel extractions were found to be highly scoured such as after White Mills Lock (site 6).

Water body 5

At sites 1, 2, 3 and 4 sediment was generally taken in slack waters as a result of scouring of the main channel. The sampling of site 4 was moved upstream because of the lack of sediment. In the area of the river where sites 4, 5, and 6 were originally to be sampled the sediment was generally found in slack water along the channel edges as a result of the main river channel being heavily scoured. This was especially so around the sand & gravel pits near Ringstead where the water had a depth of 2+ m no sediment was found in the channel. The majority of river banks in this section appeared to be mechanically made (e.g. from dredging) but the observation from the owner of the Willy Watts marina and supporting evidence from the Environment Agency suggested that this was a result of the high stream flows removing a lot of vegetation (and probably the sediment along with it). Where sediment was found it was in areas of slack water with plants and extended about a meter into river before dropping off sharply.

Water body 6

Water Body 6 was characterised by extensive scouring of the channel of the main river channel with sediment at all sites being found in the slack and back waters where it generally extended between 1 and 2m from the river bank edge.

Plate 3: Photos showing (a) water body 1 near Badby, (b) water body 2 near Weedon, (c) water body 3 near Kislingbury, (d) water body 4 near White Mills and (e) Denford lock, waterbody 5.

Figure 10: Generalised description of how sediment was observed in river channel of river Nene determined through probing. Dark areas represent where sediment found.

Waterbody 1:
River - 1.55m wide, 0.18m deep

Gravel and sand 15cm deep

Waterbody 2:
River =3.05m wide, 0.80m deep

Gravel and sand 15cm deep
Some silt deposits on sharp corners

Waterbody 3:
River = 11.55m wide 1.0m deep

Up to 0.6 m of silt along river banks with silt deposit extending 1-2m out into river

Main river channel scoured

Waterbody 4:
River = 24m wide, 1.80m deep

Up to 0.8m of silt along river banks with silt deposit extending 1-2m out into river

Main river channel scoured

Waterbody 5:
River = 28m wide, 1.80m deep

Between 0.5 and 1m deep of silt extending 1m -2m into river

Main river channel scoured

Waterbody 6:
River = 20.0m wide, 1.80m deep

Between 0.5 and 1m deep of silt extending 1m - 2m into river

Main river channel scoured

Figure 11: Variation in sediment depth observed in the 6 water bodies of the River Nene
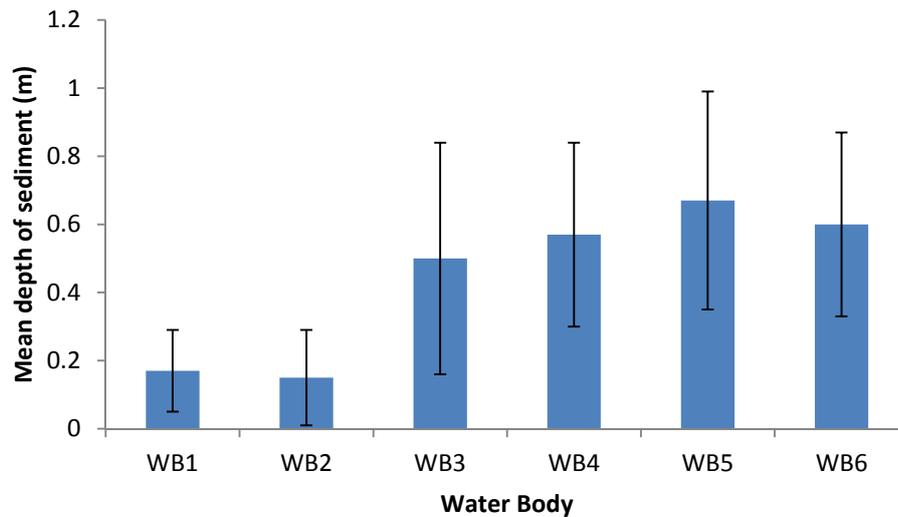
3.2   USE OF PROBING DATA IN CALCULATIONS OF P SEDIMENT VOLUME

A major objective of this research was to calculate first order estimates of the TP and extractable P in the sediments of each water body. Thus, calculation of sediment volume in each water body is required. Section 3.1 demonstrated that there was considerable heterogeneity in the distribution of sediment deposition. The justifications used in calculating first order estimates of sediment volume are given in Table 4.

Table 4: Descriptions of how sediment probing data will be used in calculation of TP and Extractable P loads of each water body

Water body Number	Description	For calculations
1	Largely gravel and sand however <2mm fraction probably only amounts to 5 cm depth in gravel lag.	Use 5cm < 2mm in calculations. Use mean measured depth of sediment and use channel width measured at Site 1.
2	Largely gravel and sand however <2mm fraction probably only amounts to 5 cm depth in gravel lag.	Use 5cm < 2mm in calculations. Use mean measured depth of sediment and use channel width measured at Site 2.
3, 4, 5, 6	Sediment largely found in slack water / plants along side channel. However, not both sides. Sediment extends out between 1 and 2m	Use sediment width of 1.5m Use mean sediment depth measured for water body. Assume distance covered by sediment is 1/32 of the distance of the two river banks.

3.3   BULK DENISTY OF SEDIMENT

Bulk density data is required to convert the estimated volume of sediment into a mass measurement that we can use to calculate TP and PO_4-P loadings. From the core measurements (an average value of 0.5 g cm^{-3} was obtained which is similar to the value used by Jarvie et al. (2005) in calculations. Bulk Density measurements for each core can be found in Appendix 1.

3.4   PARTICLE SIZE DISTRIBUTION (PSD) OF SEDIMENTS

Figure 12 shows how the percentage sand, silt and clay fractions in the 36 sediment cores change with distance downstream. Overall, there appeared to be a slight fining of particles with distance downstream but no consistent pattern is evident. The major influence on the particle sizes is likely the depositional environment (e.g. position in relation to current, density of plants that can trap sediment, etc). In addition, Fisher et al. (2004) suggest that tributaries flowing into a river will provide pulses of fresh material and energy that can affect sediment deposition. It is also apparent that the cores represent a history of deposition and would represent changes in the depositional environment with time. In addition, the local geology may play a role in determining PSD as eroding river banks will add to the load. For example, where the river is cutting through sand and gravel deposits (Fig 1) it is likely that cores taken from these areas may have a coarser particle size distribution, particularly as the sediment was found largely along the margins of the channel.

Figure 12: Changes in the sand, silt and clay particle size distributions in the 36 cores taken from the River Nene's six water bodies. Water body 1 (cores 1-6), water body 2 (Cores 7-12), water body 3 (cores 13-18), water body 4 (cores 19-24), water body 5 (cores 25-30) and water body 6 (cores 31-36).
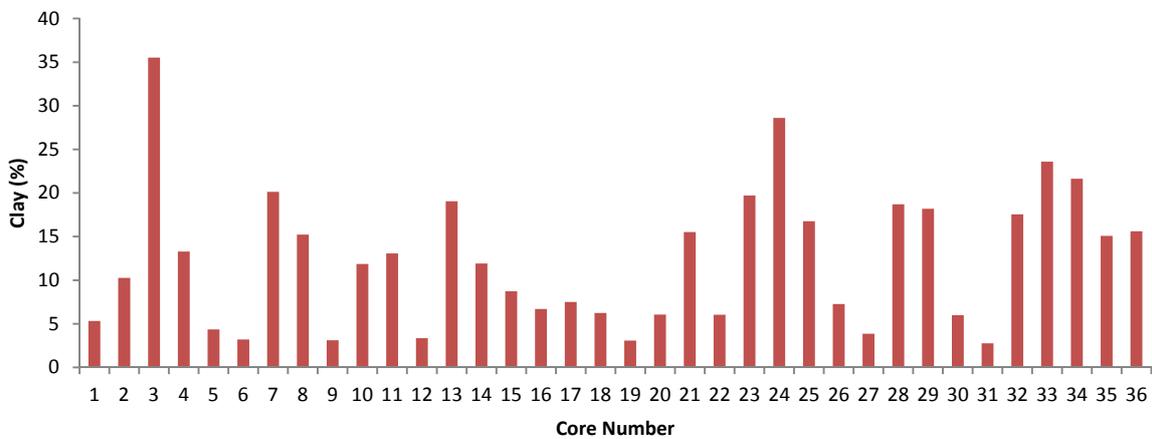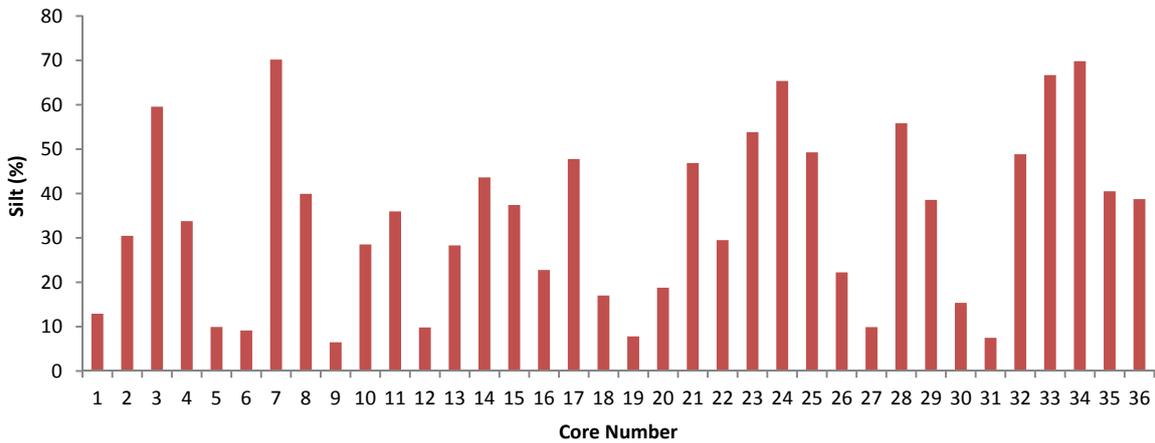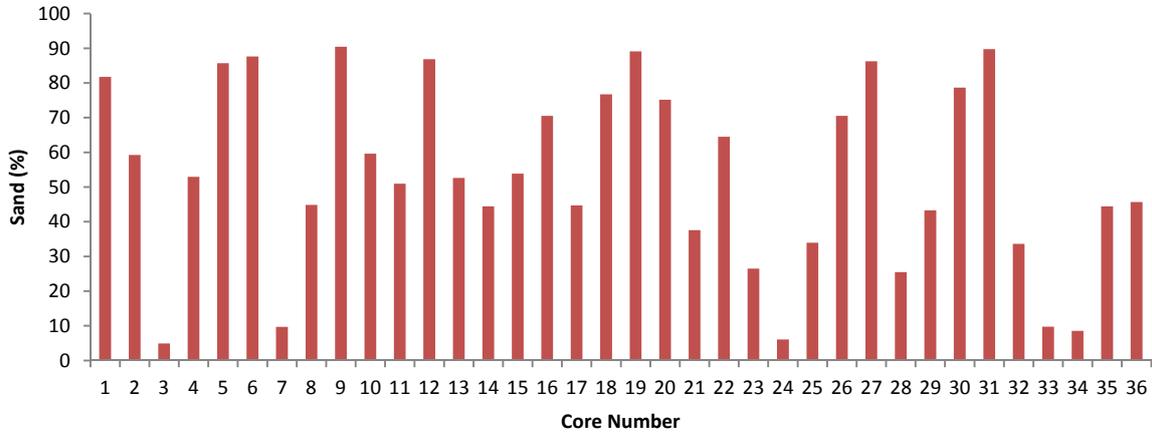
3.5 ORGANIC MATTER

Loss on ignition varied between 3.18 and 12.06 % in the homogenised cores taken from the six water bodies. Fig 13 shows that there was a general tendency for LOI to increase as distance from the head waters increased. This could be expected based on the assumption that because of slowing water currents the sediment may become slightly finer as more silt and clay settle, these being the particles that organic matter will preferentially bind to. However, the particle size distributions down the river channel previously described would suggest that no consistent fining of sediment particles was found downstream, and that particle size alone may not control organic matter concentration. This was confirmed by the lack of correlation between % clay and LOI (Figure 14a). Included in the clay size fraction will be a range of minerals such as (i) sub-micron oxides, (ii) sub-micron quartz and (iii) sub micron carbonate that do not contribute significant binding surfaces for organic matter. Rawlins (2011) found that surface area was a better predictor than particle size for organic matter in sediments and this is largely controlled by the type and amount of clay minerals present. Further investigation by plotting organic matter against aluminium, a major component of clay, shows a positive correlation with organic matter (Figure 14b) suggesting that organic matter in the sediments is likely linked to clay content. A reasonable correlation is also found with titanium (Figure 14c) that is also a significant component of clay sized material.

Figure 13: Changes in organic matter as determined by loss on ignition (%) for the homogenised cores collected from the six water bodies of the River Nene. Water body 1 (cores 1-6), water body 2 (Cores 7-12), water body 3 (cores 13-18), water body 4 (cores 19-24), water body 5 (cores 25-30) and water body 6 (cores 31-36).
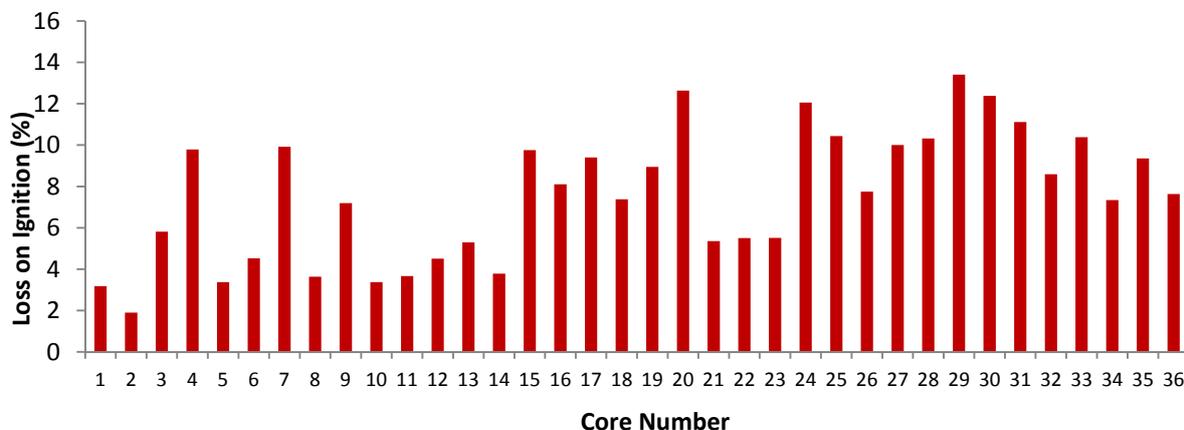
Figure 14: Relationship between organic matter content with (a) clay, (b) total Al and (c) total Ti
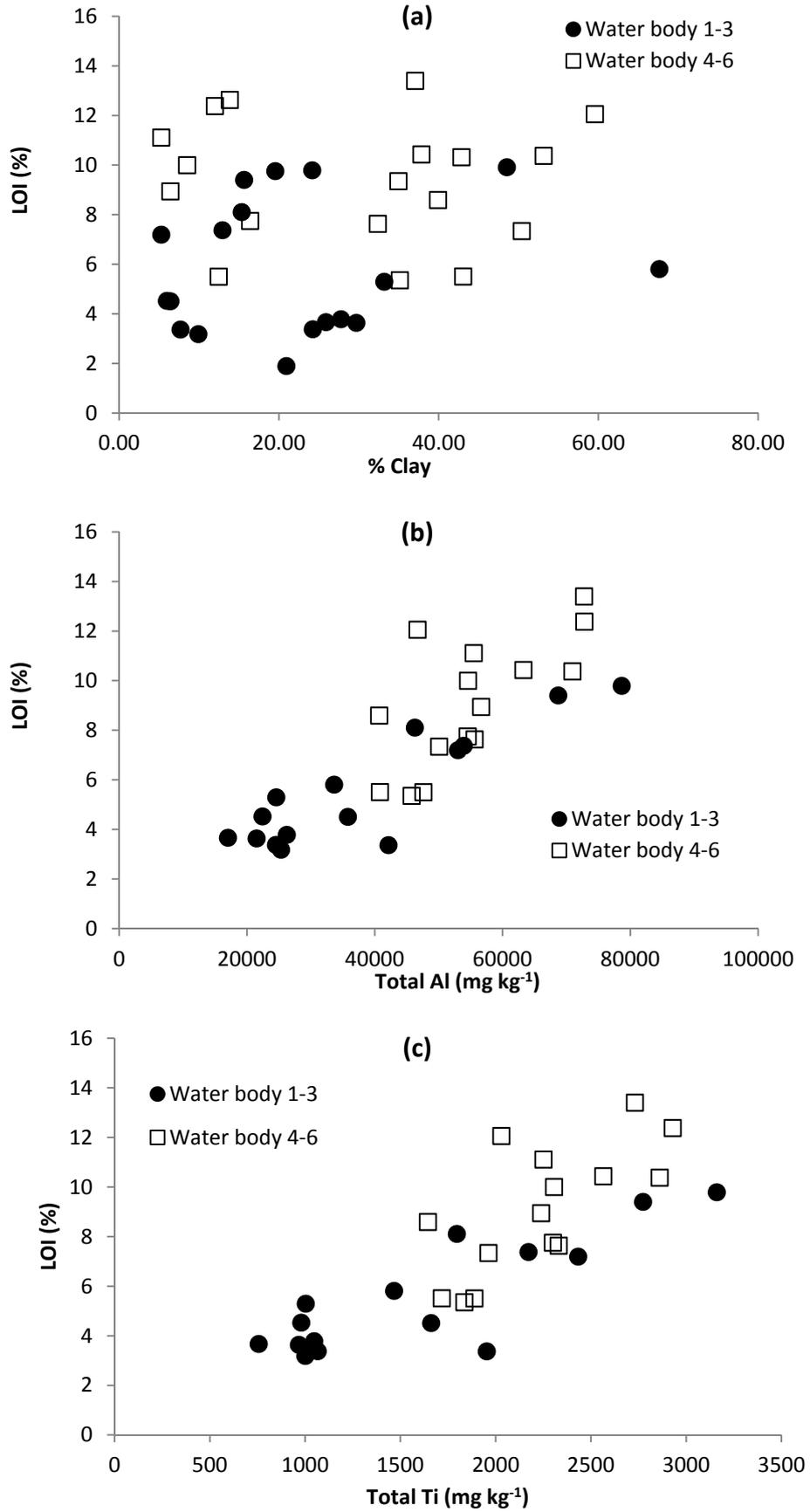
3.6   TP (TP) IN HOMOGENISED SEDIMENT CORES

TP (TP) was analysed in the homogenised sediment cores and results are shown in Figure 15. The source of TP can potentially be from numerous sources including (i) soil parent material (geological), (ii) fixation and occlusion of P in oxide minerals or the precipitation of P containing minerals where P is derived from agricultural fertilisers and (iii) similar processes as (ii) occurring in the river channel. It is evident that there was an increase in TP after core 18, the end of water body 3. This roughly coincides with the change of geology to the Whitby mudstone formation and suggests that from water body 4 onwards there may have been a different geological influence on TP concentrations in the eroding soil and river bed. We assessed TP along with particle size, organic matter and other major elements commonly associated with P minerals and sorption such as Ca, Mg, Fe and Mn. Initial correlation analysis suggested no strong relationships were present between TP and these parameters. Therefore, the TP dataset was divided into (i) water body 1-3 and (ii) water body 4-6 based on the TP results (Fig 15). Improved relationships (Figure 16) were found between TP and other elements (Fe & Mn), probably partly driven by the different soil parent materials found in different parts of the catchment. Van der Perk et al. (2007) found both soil parent material and its chemical properties to be major factors in controlling catchment scale spatial variation in TP concentrations in sediments. Both Fe and Mn oxides are known to sorb P and eventually become occluded or precipitating with these oxide minerals, so the relationships whereby P and Fe/Mn are positively correlated is expected. These minerals could be iron phosphate or combined Mn/Fe phosphate minerals such as vivianite ($Fe_3(PO_4)_2 \cdot 8H_2O$) for example. In particular, Mn appears to show a strong correlation with P in both water bodies 1-3 and 4-6. Kawasima et al. (1986) found that phosphate is sorbed by MnOx via the presence of divalent cations (Ba^{2+}, Ca^{2+}, Sr^{2+}, Mg^{2+}) or transition metals (Mn^{2+}, Co^{2+}, Ni^{2+}). For water body 4-6, a wide range of P concentrations were found sorbed to similar concentrations of Fe, possibly suggesting that the Fe oxides contained in the sediment have further capacity to sorb phosphate from the river waters. Many reports state that Phosphorus is often found associated with Ca in river sediments, probably as apatite which can precipitate as a mineral if water chemistry is suitable, but can also be found in the shells of aquatic molluscs. From these results it would appear that water bodies 1-3 have a positive correlation whilst in water bodies 4-6 there appeared to a slight negative correlation (Figure 16). It was obvious that mollusc shells were more plentiful in water bodies 1-3 and this may be the result why a positive correlation was observed.

Figure 15: Changes in concentrations of TP in cores taken from the six water bodies of the River Nene. Water body 1 (cores 1-6), water body 2 (Cores 7-12), water body 3 (cores 13-18), water body 4 (cores 19-24), water body 5 (cores 25-30) and water body 6 (cores 31-36). Missing values are where $Core_D$ samples were taken.
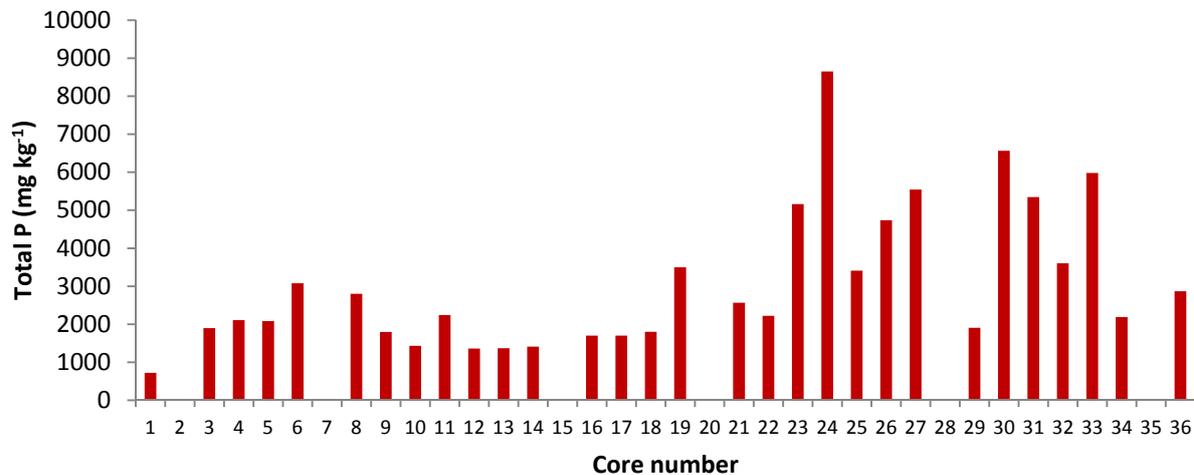
Figure 16: Relationships between TP and (a) Total Fe and (b) Total Mn (c) Total Ca in homogenised sediment cores taken from the six water bodies of the River Nene
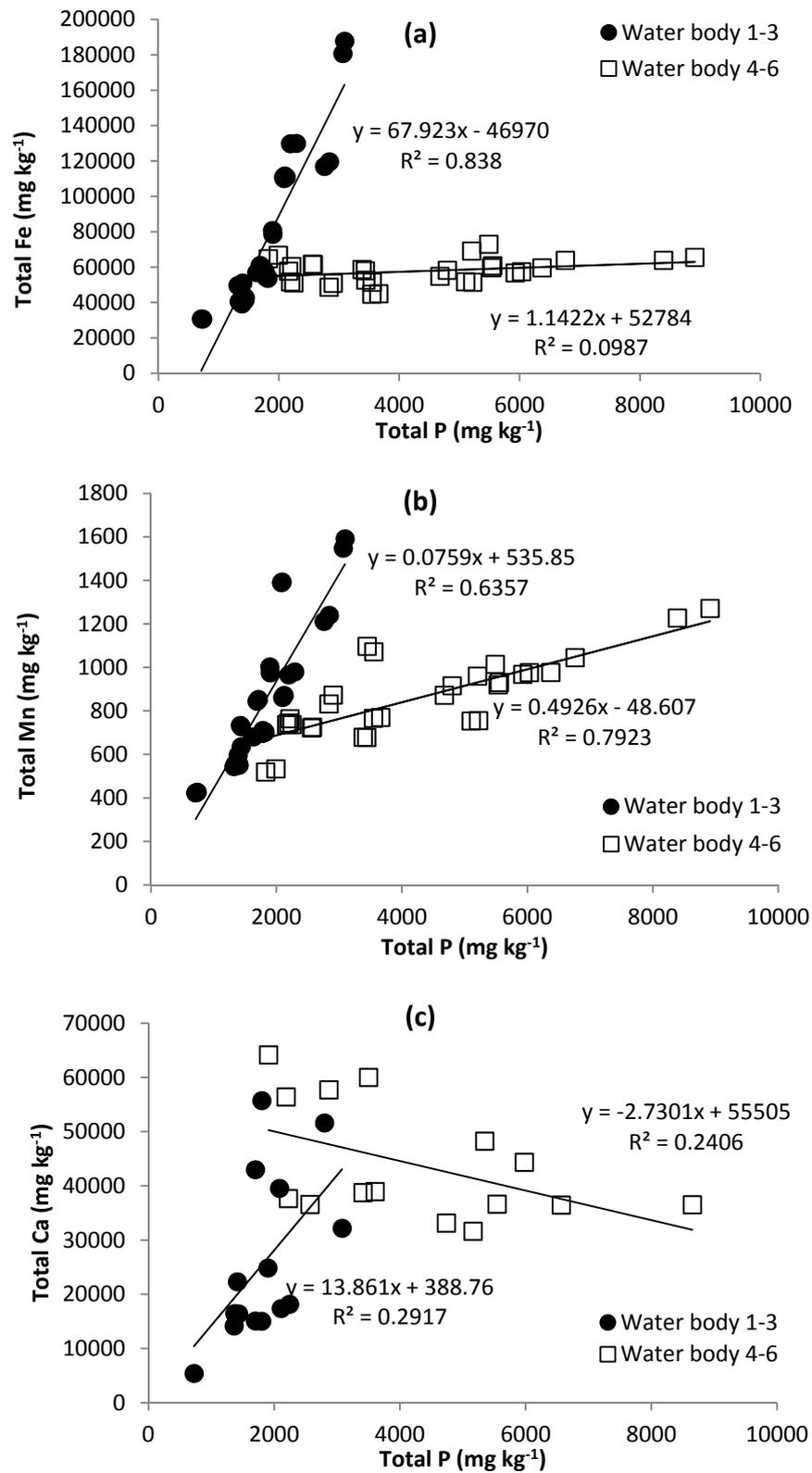
3.7   EXTRACTABLE P IN HOMOGENISED SEDIMENT CORES

Concentrations of Olsen extractable P (OEP) for the 5 homogenised cores taken from each water body are shown in Figure 17 and mean values for each water body are shown in Figure 18. Results show a trend of increasing OEP concentrations from water body 1 through to water body 6. This is likely for three reasons. Firstly, the sediment distribution was slightly coarser in the headwaters, suggesting that clay and silt-sized particles that enter the channel are washed downstream by the faster flowing waters. The greater surface area provided by fine sediments will provide a greater sorption capacity for SRP from the river water. Secondly, greater deposition of sediment is found lower down the river as the cumulative catchment size increases, water currents are slower and catchment erosion rates generally increase (Tables 15 & 16). Thirdly, the number of sources of SRP entering the river increase as the distance from the headwaters increase. This is demonstrated by the increase in SRP which appears to be associated with STW's within the catchment (Section 3.11). Concentrations of OEP vary between ~17 -100 mg kg^{-1}. There were no relationships between OEP and the typical sorption surfaces including LOI, Fe and Mn when analysing the whole dataset. However, splitting the data into water bodies 1-3 and 4-6 produced stronger linear regressions (Figure 19). No relationships were found in water bodies 1-3 between OEP and Fe, Mn and Ca. However, for water bodies 4-6, a positive linear regression with Mn and a weak negative linear regression with Ca were found. These results suggest that no specific sorption surface was dominant for OEP in water bodies 1-3, whereas in water bodies 4-6, Mn oxides appeared to assume a greater importance. It was found that OEP was < 5% of TP in all instances with most samples being < 2%. A positive correlation of r_s = 0.72 was found between TP and OEP. However, there is no mechanistic basis for this relationship and it is likely that it is a consequence of more TP containing minerals being found as there is a gradual fining of sediment which also carries a greater sorption capacity.

Figure 17: Changes in OEP concentration (mg kg^{-1}) in homogenised cores with distance going down the 6 water bodies sampled of the River Nene. Error bars show the standard deviation of the 3 replicates analysed for each core. Water body 1 (cores 1-6), water body 2 (cores 7-12), water body 3 (cores 13-18), water body 4 (cores 19-24), water body 5 (cores 25-30) and water body 6 (cores 31-36). Missing values are where Core$_D$ samples were taken.
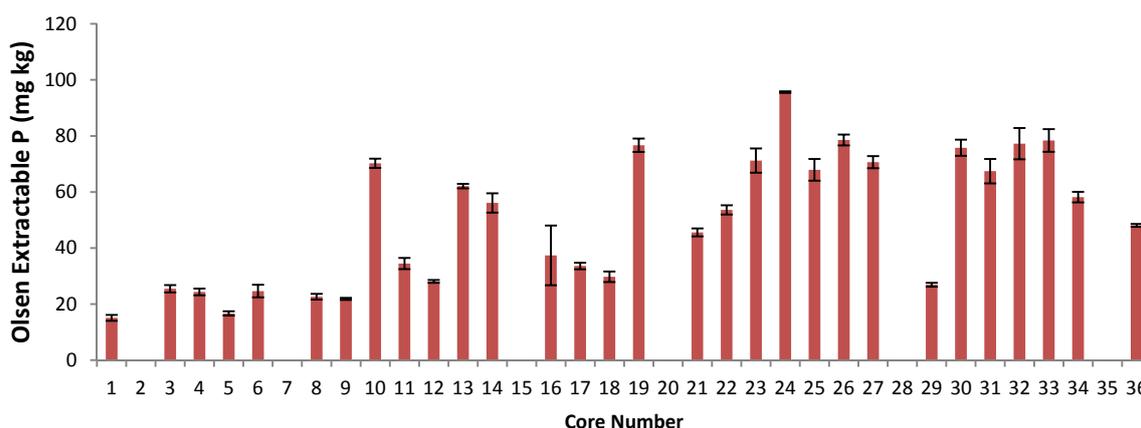
Figure 18: Mean Olsen Extractable P concentrations for each water body sampled from the River Nene. Error bars are ±1 standard deviation
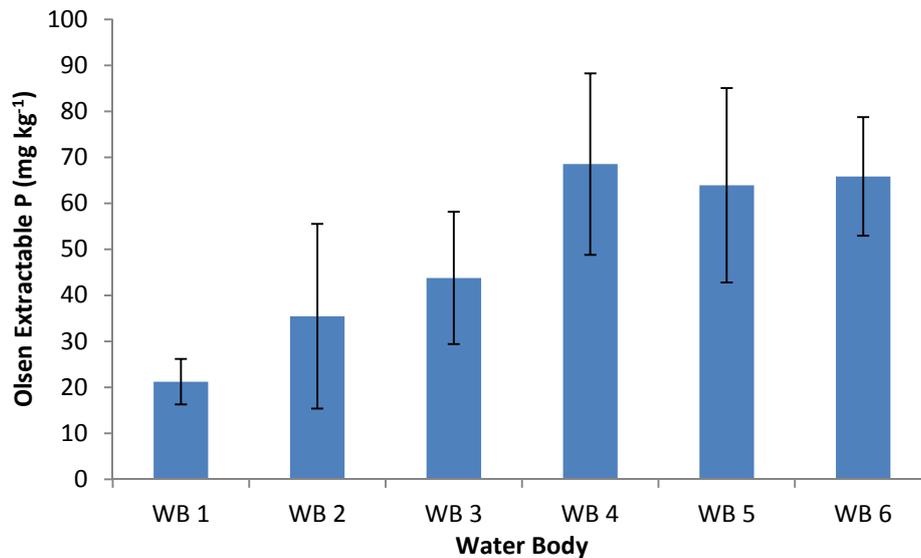
To place some context on the concentrations of OEP found in the sediments, it is possible to examine them compared to soil OEP values. This is generally undertaken by comparing soil Olsen P values on a 9 point scale based on mg P L^{-1} of soil (Table 5) produced by MAFF (2000). Litres are used because the roots of most agricultural crops were considered to grow in a litre of soil. Assuming soil bulk density is about 1.5 g cm-^{3}, the sediment OEP concentrations can be multiplied by ~0.66 to roughly fit this index. Therefore, sediment values from the Nene roughly coincide with Index categories 1-4, with most being in categories 3-4 in the later water bodies. It is suggested that no extra growth response is found in most crops above Index level 2 (MAFF, 2000). Thus, it can be seen the sediment samples collected from the Nene contain relatively high levels of OEP compared to those required for agriculture, and that substantial OEP would be available for macrophyte growth in river sediments.

Table 5: Phosphorus Availability Index (MAFF, 2000) based on Olsen P values

Index Value	Olsen P (mg L^{-1} Soil)
0	0-9
1	10-15
2	16-25
3	26-45
4	46-70
5	71-100
6	101-140
7	141-200
8	201-280
9	>280

Figure 19: : Relationships between OEP and (a) Total Fe and (b) Total Mn (c) Total Ca in homogenised sediment cores taken from the six water bodies of the River Nene.
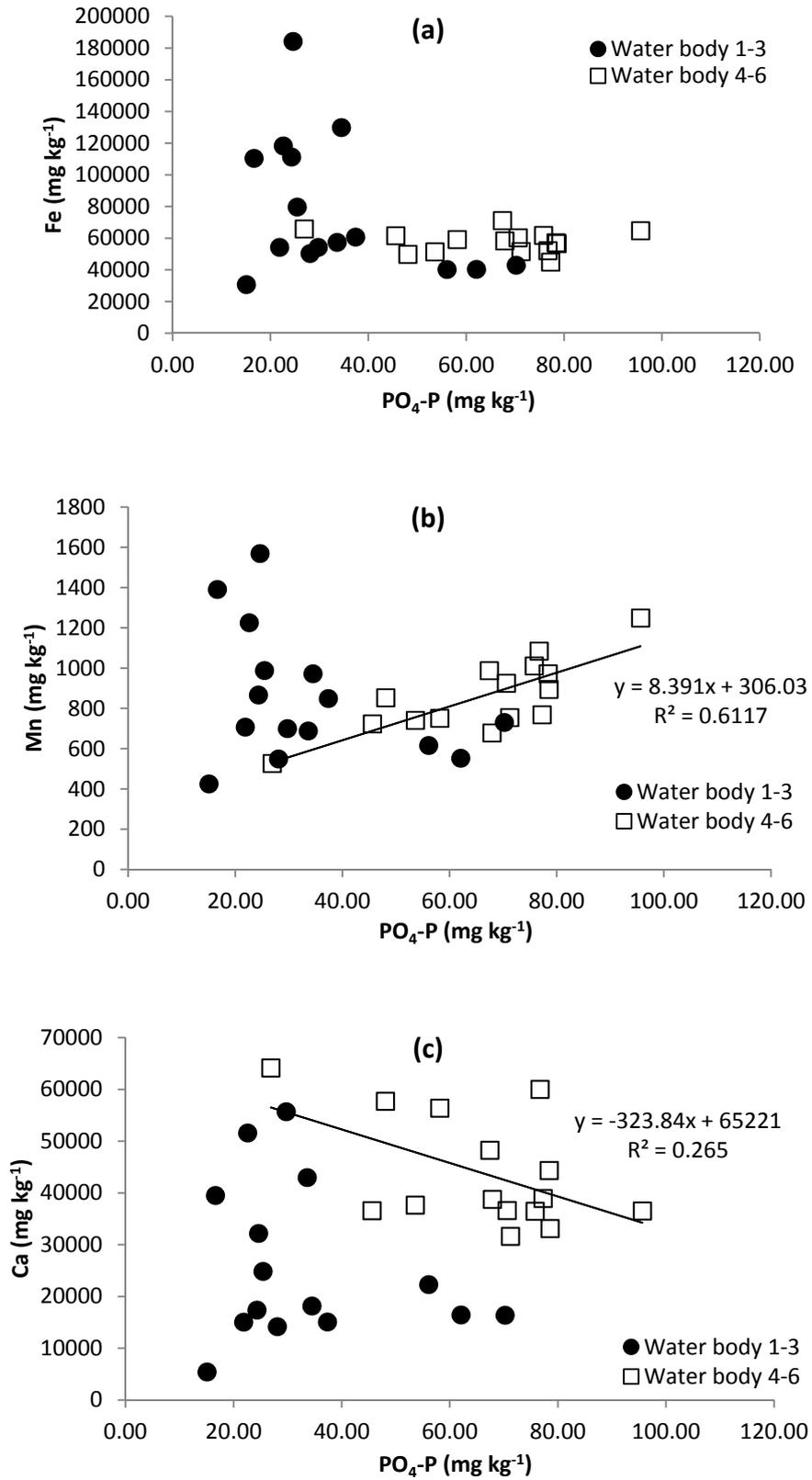
3.8   DEPTH PROFILES OF TP AND OEP IN SEDIMENT CORES

Core$_D$ from each of the six water bodies was used to examine the distribution of TP and PO$_4$-P with depth (Fig 20 & 21). Concentrations of TP (Figure 20) in the sediment showed a wide range of concentrations up to ~ 5000 mg kg^{-1}. Whilst individual cores demonstrated patterns of increase or decrease with depth, there was no systematic pattern across all the cores, suggesting that TP concentration with depth was a function of depositional environment, time and erosion. Similarly, Figure 21 shows the OEP concentrations with depth, with maximum concentrations being a little over 60 mg kg^{-1}. There was little evidence of a systematic pattern of OEP deposition in any of the six water bodies. Concentrations of OEP were in a similar range to those from the homogenised cores. Results suggest that deposition, particle size, river flow speed and plant uptake are the major factors determining OEP concentration with depth.

Figure 20: Concentrations of Total Phosphorus (TP) in sediment cores from each water Body of the River Nene.
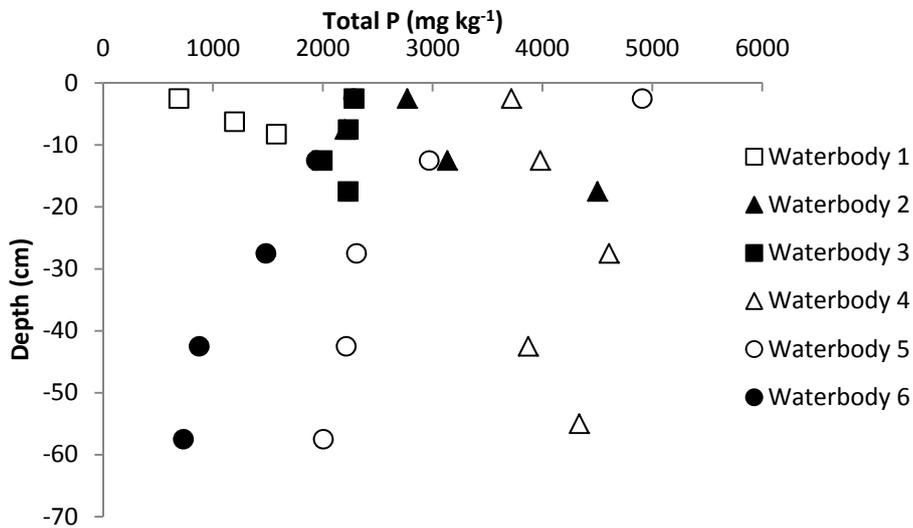
Figure 21: Concentrations of OEP in sediment cores from each water body of the River Nene.
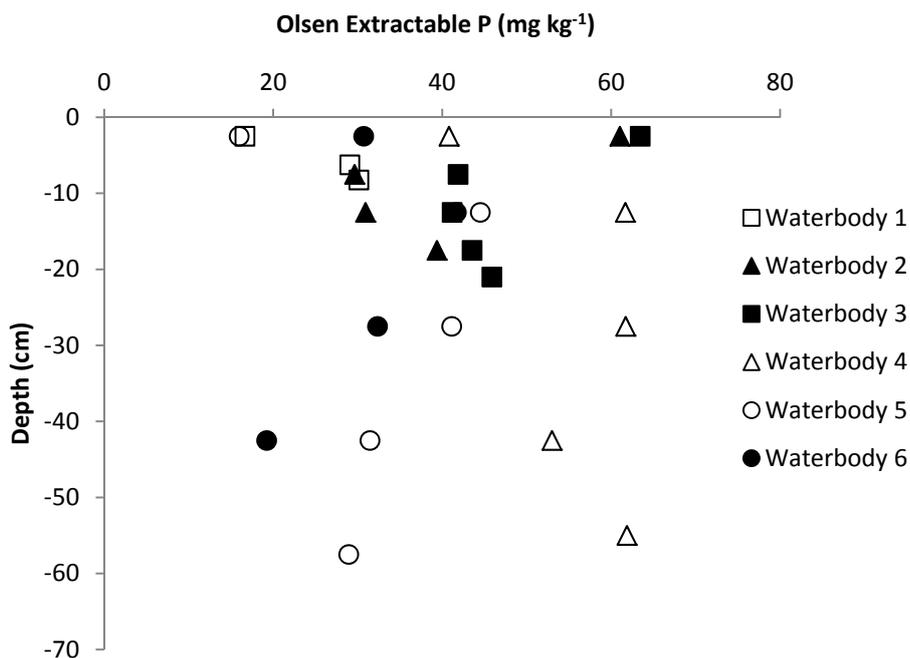
3.9 DETERMINING THE EFFECTIVE PHOSPHORUS CONCENTRATIONS (EPC$_0$) IN SEDIMENTS

Using the top 5cm taken from Core$_D$ from each water body, the 'Effective Phosphorus Concentration' (Section 2.6.7) was determined. This figure represents the equilibrium concentration of phosphate in solution where desorption is equal to adsorption. This figure will likely be a function of the sediment properties such as particle size distribution, iron and aluminium oxide concentrations, organic matter as well as water properties such as electrical conductivity (as a proxy for ionic strength) and pH. Thus the results presented are indicative of the composition of sediment sampled and are broadly representative for the water body.

Figure 22 reports the isotherm and best fit lines for each of the six water bodies. In each case, the value of the EPC$_0$ is determined where the isotherm crosses the X-axis. Comparison of the EPC$_0$ concentrations of P with the SRP concentration determined in the water sample taken at each site (Table 6) shows that only in water body 1 does the EPC$_0$ exceed the SRP in the water sample, thus suggesting that the sediment is a source of SRP. However, we believe that this is function of the high water flow causing dilution of SRP at the time of sampling, because the kinetic analysis (described in more detail in Section 2.6.8) did not indicate that desorption of SRP from this sediment occurred. For water bodies 1, 2 and 3 the EPC$_0$ is below 1μmol P L^{-1} whilst for water bodies 4, 5 and 6 the EPC$_0$ is between 1 and 2 μmol P L^{-1}. If the water SRP is greater than the EPC$_0$ it is likely that the sediment has the capacity to adsorb SRP from the water column. If the water concentration of SRP is less than the EPC$_0$ than desorption of phosphate may occur from the sediment to the water body.

Most studies from the UK suggest that most sediments have the potential for the adsorption of SRP (e.g. House & Denison, 1997; House & Denison, 1998). Jarvie *et al*. (2006) reported that >80 % of the river bed samples they tested had the potential for net SRP uptake from the water under stable low flow conditions. Potential for desorption may occur when water SRP concentrations fall below the EPC$_0$ (Jarvie *et al*. 2006). We can compare the EPC$_0$ and SRP measurements using an 'EPC0 percentage saturation' term (EPC$_{0sat}$) calculation, which describes the increase or decrease in SRP compared to the EPC$_0$. This is defined as

EPC$_{0Sat}$ (%) = 100*(EPC$_0$-SRP)/EPC$_0$)   **Equation 15**

Results from Table 6 suggest that there is considerable under saturation of the EPC$_0$ suggesting that the sediment has considerable capacity to absorb more SRP before there is leakage back into the water at the measured concentration of SRP in the waters.

Table 6: Parameters obtained from isotherm fitting analysis

Sample	F	k	RSS	EPC$_0$ (μm P L^{-1})	EPC$_{0Sat}$ (%)	k$_d$ L kg^{-1}	SRP (μm P L^{-1})
Water body 1	43.9	0.008	0.03	1.31	87.59	33	0.18
Water body 2	52.2	0.029	0.44	0.61	-180	249	1.65
Water body 3	176	0.048	2.33	0.85	-444	3743	4.63
Water body 4	413	0.027	2.78	1.19	-185	4286	3.40
Water body 5	403	0.055	9.56	1.67	-160	8445	4.35
Water body 6	296	0.023	1.50	1.69	-126	1555	3.83

Figure 22: Isotherms used to estimate the Effective Phosphate concentrations. The graph shows measured (♦) and predicted (■) values with the modelled line of best fit based on equation 2 from which the Freundlich constants are derived.
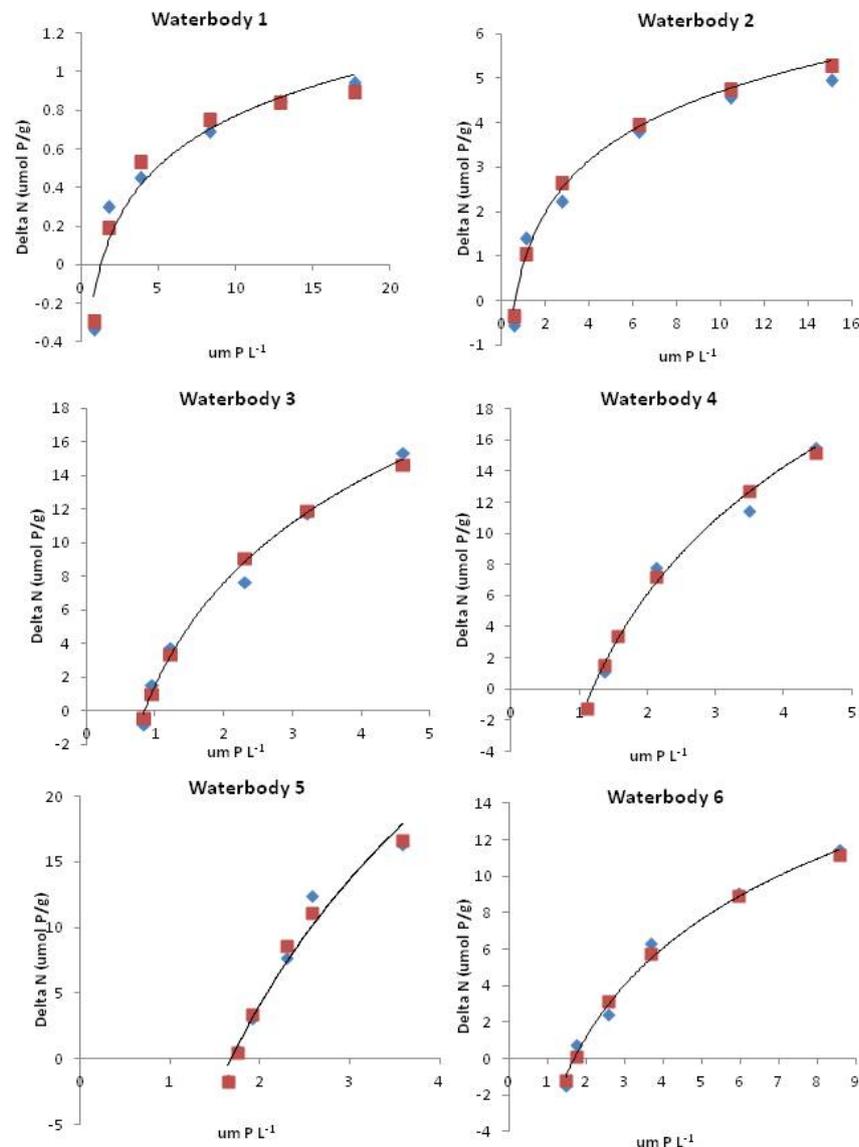
3.10   DETERMINING THE RATE OF P UPTAKE OR DESORPTION IN SEDIMENTS (KINETICS)

Rate constants were determined for the 0-5 cm segments of CoreD from each water body. As in the calculation of EPC_0, values obtained are a function of the sediment composition sampled in terms of particle size, oxide content and pH. All sediments tested showed a rapid absorption of SRP (Figure 23), with a pseudo-equilibrium generally being reached within one hour. For water body 1 & 2, a 2μM P solution was used and for the other 4 water bodies a 4μM P equilibrating solution was used, these concentrations being slightly greater than those measured in the river waters at the time of collection. This rapid absorption is typical and has been found by other researchers (Jarvie et al. 2005). However, in water bodies 3-6, a slight increase in SRP concentrations were found after about 6 hours. Although this was only a slight increase it appeared to be consistent. One possible explanation is that there is calcite present in the river sediment and its dissolution may have allowed PO_4^- ion exchange with HCO_3^- ions. However, it

appeared not to strongly influence the kinetic coefficients determined (Table 7). These coefficients will be used in determining the take up of SRP from river water.

Figure 23: Adsorption kinetic graphs for sediment in water bodies of the River Nene
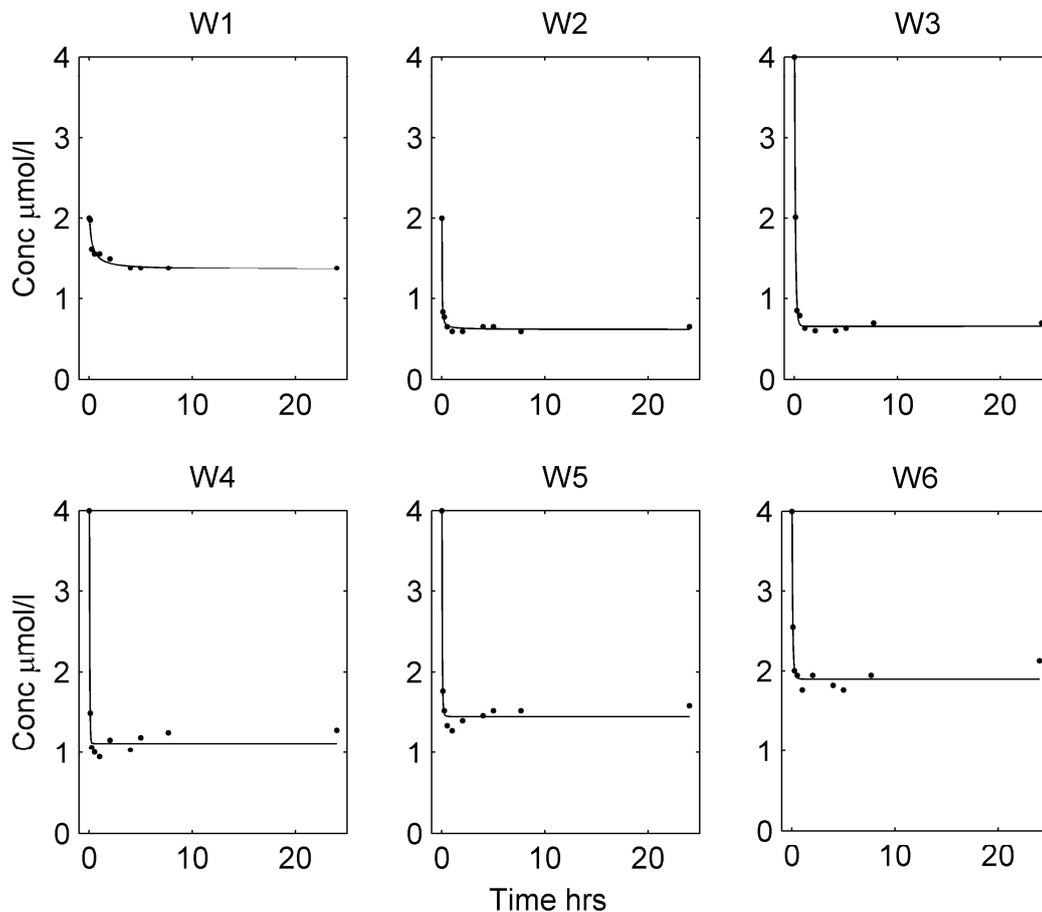
Table 7: Kinetic constants for water body samples

	K_r µmol l g h	C_o	N
Waterbody 1 Site 2	2.366	1.363	2.05
Waterbody 2 Site 1	51.714	0.623	2.16
Waterbody 3 Site 3	10.687	0.662	1.09
Waterbody 4 Site 2	25.477	1.117	1
Waterbody 5 Site 4	26.954	1.45	1.26
Waterbody 6 Site 5	14.113	1.89	2.29

3.11 RIVER NENE WATER CHEMISTRY

A water sample was collected and soluble reactive phosphorus (SRP) analysed at the same time as $Core_D$ from each water body as part of the methodology to determine EPC_0 and the kinetic rate constants. In addition, the complete hydrochemistry of this sample was analysed and is shown below (Table 8). Concentrations of TP and SRP were similar suggesting that most of the

P in the <0.45μm filtered sample was phosphate P. Different samples collected at the same sites as well as analytical error probably account for the fact that SRP is generally slightly greater than Total P determined by ICP-MS. The other element of particular note from this analysis is boron (B) whose background concentration is generally considered to be < 30 μg L^{-1} (Jarvie *et al.*, 2005). The major source of boron in river waters is predominantly sewage effluent derived as it is used as a whitener in washing powders. Thus it is commonly used a tracer to assess whether PO$_4$-P is sewage or agriculturally derived (Jarvie *et al.* 2006; Neal *et al.* 2010). In this study, despite the small number of sample points there was a positive correlation of r=0.80 (Figure 24) suggesting that the PO$_4$-P in the river water was linked to discharges from STW's. The increasing concentrations of PO$_4$-P and B with increasing distance from the headwaters are likely a result of increasing numbers of STW's feeding water into the river system. Figure 1 shows the STW's that feed directly into the Nene or via tributaries. Jarvie *et al.* (2006) report that typically SRP:B ratios in soil waters were between 36:1 and 53:1 for a range of arable and grassland soils, this being an order of magnitude higher than those found in river waters where the phosphate is derived from sewage treatment. In our samples we have PO$_4$-P:B ratios of between 0.15:1 to 2:1. A ratio of 9.5 is considered a mean value for PO$_4$-P:B for sewage effluent discharged without tertiary treatment (P treatment). The PO$_4$-P:B ratios found in Table 8 are between 1 and 2.6 (excluding site 1). Jarvie et al. (2006) suggest that when ratios are lower than 9.5, there are no major additional diffuse sources of SRP in relation to dominant point sources entering the water and that there may be losses of P to bed sediment or biota relative to B.

Figure 24: Scatterplot of the relationship between PO$_4$-P and B found in the 6 water bodies of the River Nene.
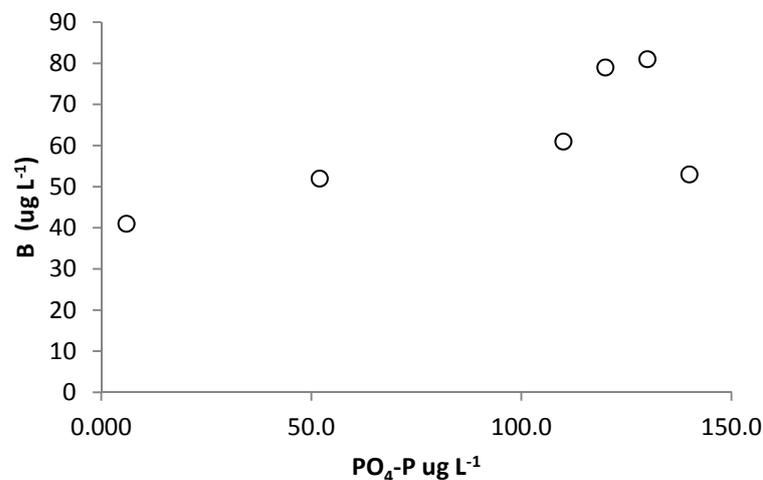
Table 8: Hydrochemistry of water (filtered <0.45 µm) samples collected at the same time as the collection of Core$_D$ samples from the six water bodies of the River Nene. These samples are snapshots of the river at the time of sampling.

	pH	NPOC	EC	Ca^{2+}	Mg^{2+}	Na^{2+}	K^+	Si	HCO_3^-	Cl^-	SO_4^{2-}	NO_3^-	SRP	TP	Total Fe	Total S	B	PO_4:B
		mg l^{-1}	µs s^{-1}	mg l^{-1}	mg l^{-1}	mg l^{-1}	mg l^{-1}	mg l^{-1}	mg l^{-1}	mg l^{-1}	mg l^{-1}	mg l^{-1}	mg l^{-1}	mg l^{-1}	µg l^{-1}	mg l^{-1}	µg l^{-1}	
Detection Limit		0.50		0.3	0.01	0.2	0.02	0.050	5.00	0.050	0.050	0.020		0.01	1.00	1.00	10	
Waterbody 1	8.20	1.86	630	106	6.59	9.1	3.07	5.04	285	23.1	60.9	25.6	0.006	0.01	2	19	41	0.15
Waterbody 2	8.24	2.71	640	102	7.19	13.3	3.93	5.13	252	29.2	63.1	27.2	0.052	0.05	7	22	52	1.0
Waterbody 3	8.14	2.99	808	96.9	6.93	21.9	4.51	4.59	243	47.4	71.4	40.3	0.14	0.11	11	22	53	2.6
Waterbody 4	8.14	3.04	892	99.6	7.16	23.1	4.67	4.28	233	48.7	74.8	41.7	0.11	0.10	10	23	61	1.8
Waterbody 5	8.16	3.90	990	114	8.37	37.2	6.98	4.17	262	65.8	102	49.2	0.13	0.12	15	34	81	1.6
Waterbody 6	8.20	4.21	893	123	9.03	37.2	6.58	4.09	277	63.9	117	46.8	0.12	0.11	15	39	79	1.5

3.12 SEDIMENT DYNAMICS

The aims of work package 2 were associated with sediment, its volume, erosion, deposition and transport within the upper six water bodies of the river Nene. Understanding the sediment characteristics is essential to compiling the first-order estimates of TP and OEP masses and transport through the river system.

3.12.1 Probing sediment volumes and masses in water bodies

Estimates of contemporary volumes of sediment stored in the river channel were made by probing sediment at the time of sampling. Following on from section 3.1 and 3.2, estimates of sediment volume were calculated and converted to masses using the Bulk Density (Section 3.3) calculated from the cores. Results can be found in Table 9.

Table 9: First Order Estimates of the volume and mass of sediments calculated by probing of the sediments in the River Nene and using the justifications outlined in Table 4. As a result of the variation of sediment architecture present in the river, a mean value of all the Bulk density (equation 1) values calculated was used.

Water body	Sediment Volume (m^3)	Sediment (kg)	Bulk Density ($g\,cm^{-3}$)
1	584	291829	0.5
2	512	255755	0.5
3	851	425728	0.5
4	1381	690439	0.5
5	1654	826924	0.5
6	3911	1955294	0.5

3.13 ASSESSING SEDIMENT TRANSPORT DYNAMICS THROUGH WATER BODIES USING THE CDP MODEL

Sediment flux rates are presented for each water body catchment and for the whole catchment upstream of Peterborough from model predictions. Cumulative sediment discharge from each of these sub-catchments represents the total input of all upstream catchments through time. The percentage of these total sediment discharge rates transported as suspended sediment is also provided.

3.13.1 Two model runs

During the modelling phase of the study, there was an unforeseen interruption to the simulation, resulting in the 40 year modelling period being separated into two 20 year periods. Although the hydrology is re-initialised at steady state, the distribution of sediment uses the same initial homogeneous distribution, resulting in a spin-up requirement at the beginning of each period as the grain size distribution adjusts to hydrological conditions. The 'spin-up' is the period where the model is allowed to reach a

'steady state' and accounts for initial conditions that are not correct (i.e. no water in the system and heterogeneous sediment distribution). Sediment flux rates during the spin-up periods are not representative of the catchment and therefore are neglected in the assessment of the simulated results and in the projections forwards and backwards in time. The spin-up time, required for each period was 10 years, since beyond this, sediment flux rates are approximately linear when averaged over time. We use the average of the two model runs to estimate sediment transport in the intervening period.

3.13.2   Modelled sediment flux rates

The sediment flux rates for each of the sub-catchment outlets are given in Table 10 (1972-81) and Table 11 (1992-01). The total upstream sediment loss and annual flux rates includes sediment input from all upstream tributary catchments. The net volume change in sediment is equivalent to the change in volume for that particular water body stream reach (i.e. the amount of sediment entering the water body at its furthest upstream extent, minus the amount evacuated downstream to the next water body). The simulated annual average amount of sediment lost from the entire catchment is 864m^3 for the earlier simulation and 869 m^3 for the later simulation.

Sediment flux in the upper sub-catchments (water bodies 1 and 2) is very low, averaging less than 26 m^3 y^{-1}. All of the water bodies show either a near even ($\pm$5 m^3 y^{-1}) net volume change or net loss of sediment over the simulated periods, with the exception of water body 6. Modelling predicts that water body 6 is accumulating on average 587 m^3 y^{-1} during 1972-81 and 1533 m^3 y^{-1} during 1992-01. This is likely a result of changes in precipitation and ground water conditions leading to a higher sediment yield in the second period and reflects changes in the climate data.

Table 10: Volumetric sediment transport rates 1972 - 1981. Total volume change over the 10 year modelled period, the mean annual rate and the annual net volume change of each sub-catchment. The annual net volume change is equivalent to the sub-catchment volume change (i.e. The flux delivered from upstream of the water body minus the sediment flux evacuated at the water body outlet).

Water Body Outlet	Total Upstream Volume Loss (m³) 1972-81	Mean Annual Flux Rate (m³) 1972-81	Annual Net Volume Change (m³) 1972-81
1	11	1	-1
2	0	0	1
3	1336	134	-134
4	1313	131	3
5	14507	1451	-1320
6	8638	864	587

Table 11: Volumetric sediment transport rates 1992 - 2001. Total volume change over the 10 year modelled period, the mean annual rate and the annual net volume change of each sub-catchment. The annual net volume change is equivalent to the sub-catchment volume change (i.e. the flux delivered from upstream of the water body minus the sediment flux evacuated at the water body outlet). *Rates for water body 6 are projected back to 1992, as steady state sediment transport was not achieved in the model in this sub-catchment until 1995.

Water Body Outlet	Total Upstream Volume Loss (m3) 1992-01	Mean Annual Flux Rate (m3) 1992-01	Annual Net Volume Change (m3) 1992-01
1	11	1	-1
2	258	26	-25
3	227	23	3
4	1532	153	-130
5	24016	2402	-2248
6*	8628	869	1533

3.13.3 Distributed Sediment Flux Rates

The distributed net changes in sediment volume during the two modelling phases are presented in Figure 25 and Figure 26. In both cases the upper reaches of the catchment show less than 500 m^3 change per model node over the 10 year period. The majority of net sediment changes occur in the lower reaches of the main river channel. The pattern of erosion and accumulation is similar in both scenarios and exhibits little change through time. Along the lower reaches of the river channel, sediment is eroded over long stretches and deposited at several intervals. Following the deposition of sediment, there is a down-river region of zero net volume change (i.e. no erosion or deposition). The reach where the most accretion occurs is water body 6, c. 10 km from the end of the catchment, where over 44,000 m^3 of material was deposited in a single node over the 10 year period 1972-82. The regions of greatest deposition occur in conjunction with a widening of the river channel in the Digital Elevation Model (DEM) and reduction in channel slope.

Figure 25: Distributed net change in sediment volume (m^3) 1972 - 1981
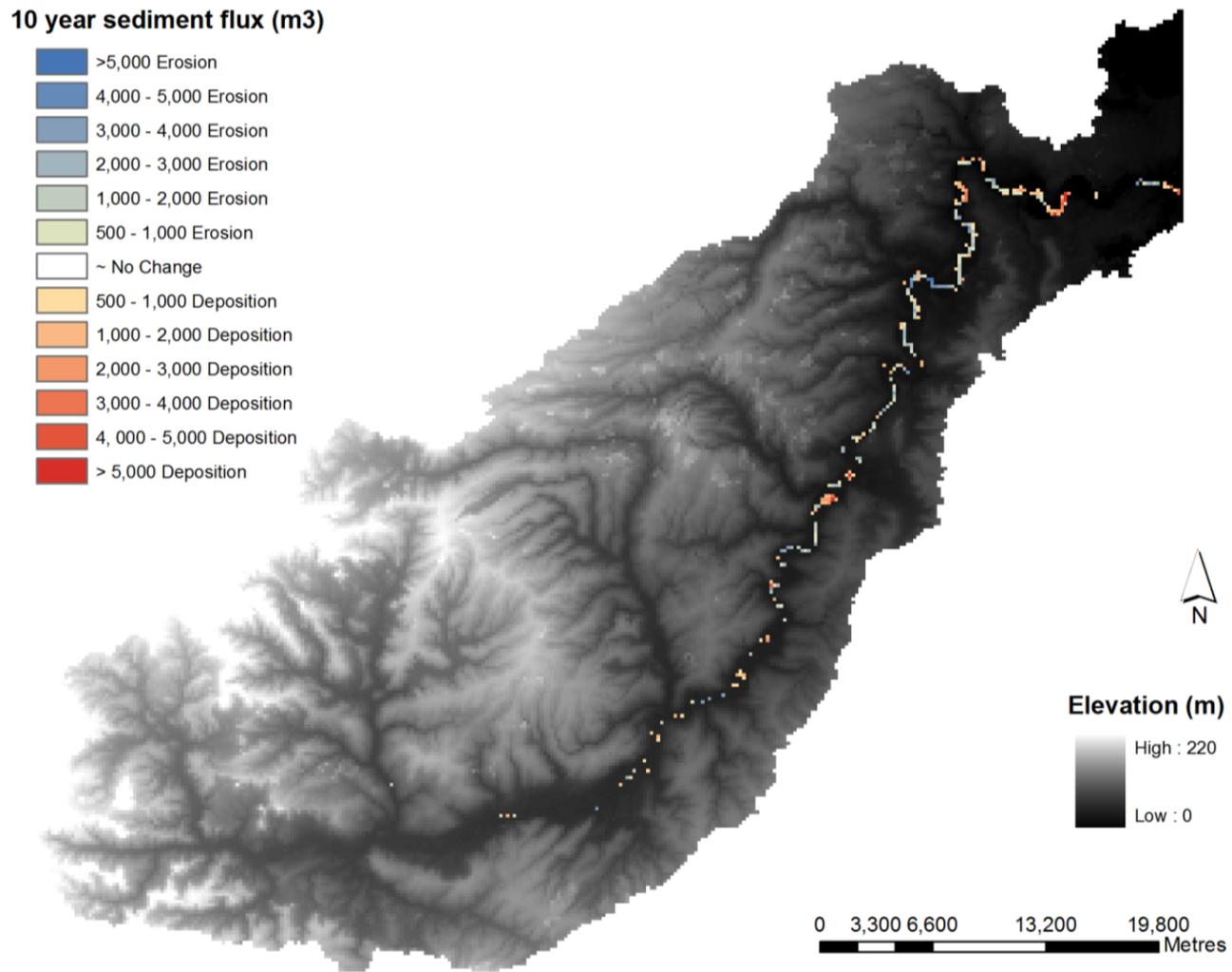
Figure 26: Distributed net change in sediment volume (m³) 1992 – 2001
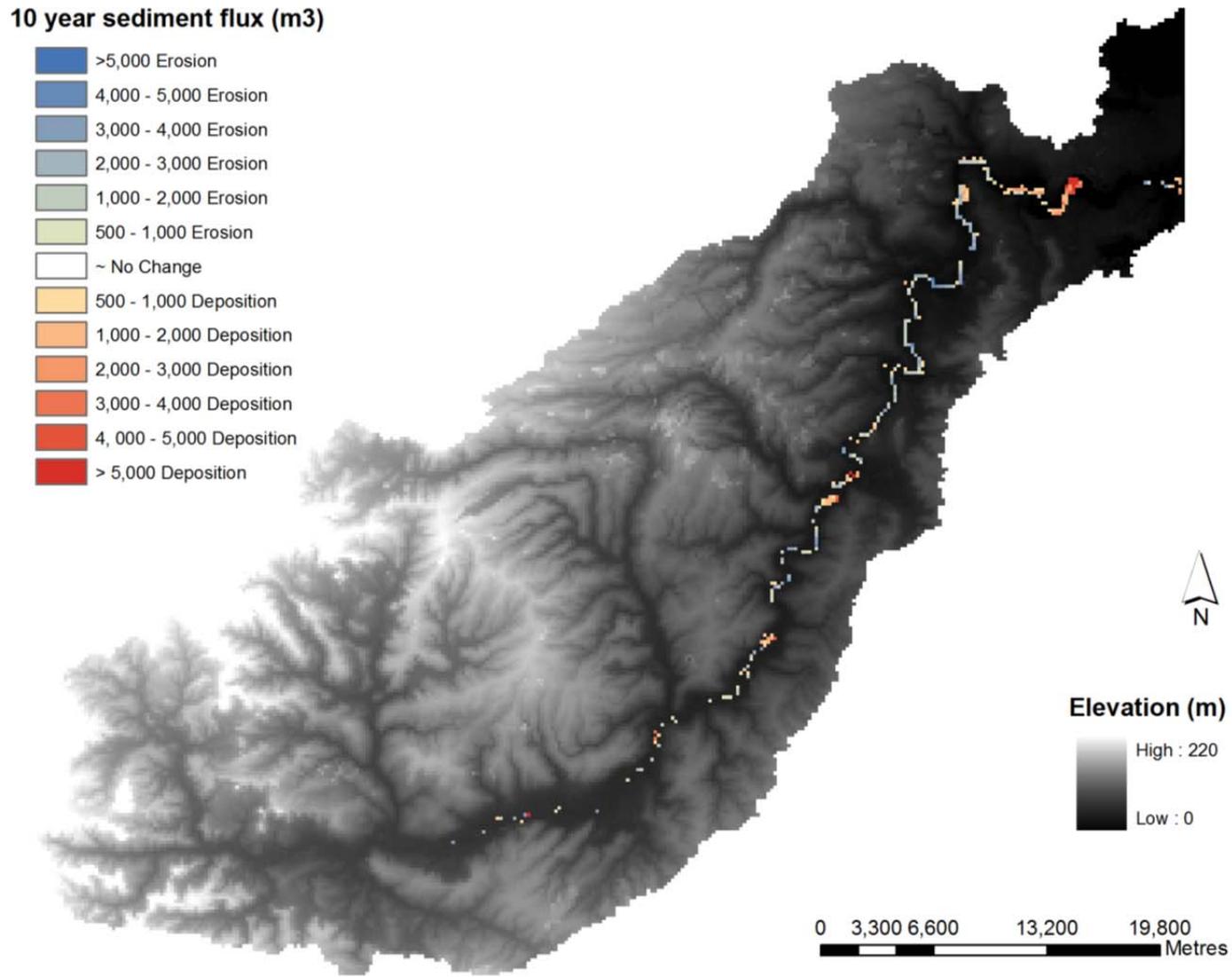
3.13.4 Cumulative twentieth Century sediment flux rates

The cumulative twentieth century sediment fluxes simulated by the model are presented in Figure 27. The two red lines in each of the water body plots represent the cumulative rate from the two modelled periods that have attained an approximately linear steady-state relationship. For the period prior to 1972, the mean flux rates from the 1972-1982 simulations were assumed appropriate and projected backward to assess sediment flux over 1910 to 1972. Similarly, beyond 2002, the mean flux rates from the 1992-2002 model run were used to project cumulative sediment flux forward to 2010. For the interim period 1982-1992, the average mean flux rates from the two simulated periods were used to predict sediment flux.

The cumulative flux rates are arbitrarily set to zero at 1910. The unknown influence of the 1947 snow melt floods on sediment erosion and deposition rates suggest greater uncertainty on the earlier sections of the plots (finer dashing). Water bodies in the upper reaches of the river (1, 2, and 3) show a varied response over the modelled periods. Water body one has a near perfect linear response, while water body 2 has differing responses when the two periods are compared, creating a non-linear overall appearance, with a more rapid rate of sediment loss observed in the 1992-2001 period of the simulation. Water body 3 has a tendency for sediment flux rates to tail-off towards the end of the simulation. The water bodies in the lower reaches of the river catchment (4, 5, and 6) exhibit a more uniform near-linear trend in sediment flux rates.

The percentage of sediment flux transported as bed load and suspended load is captured in Table 12. These proportions were determined by the simulation and were derived using a mean of the two steady-state modelling periods. However, for water body 1, these proportions could not be determined as there was insufficient flux of sediment leaving the water body during both modelling runs. For water body 2, bedload and suspended sediment percentages could only be determined from the second simulation period, again due to the low sediment flux in the first simulation. The water bodies with the highest proportion of suspended sediment are 2 and 4, with lowest being water body 5, which only averaged 8% suspended load over the steady-state simulation periods. This likely reflects greater bedload transport as a function of deeper flowing water in the model resulting in highest erosion rates (see Table 11 & Figure 26).

Figure 27: Projected cumulative sediment discharge plots for the six sub-catchments. The simulated rates are given as red lines and projected rates as dashed line. The fainter dashed line represents a projection back beyond the 1947 flood event.

Waterbody 4: Projected Cumulative Sediment Flux (m^3)

Waterbody 5: Projected Cumulative Sediment Flux (m^3)

Waterbody 6: Projected Cumulative Sediment Flux (m^3)
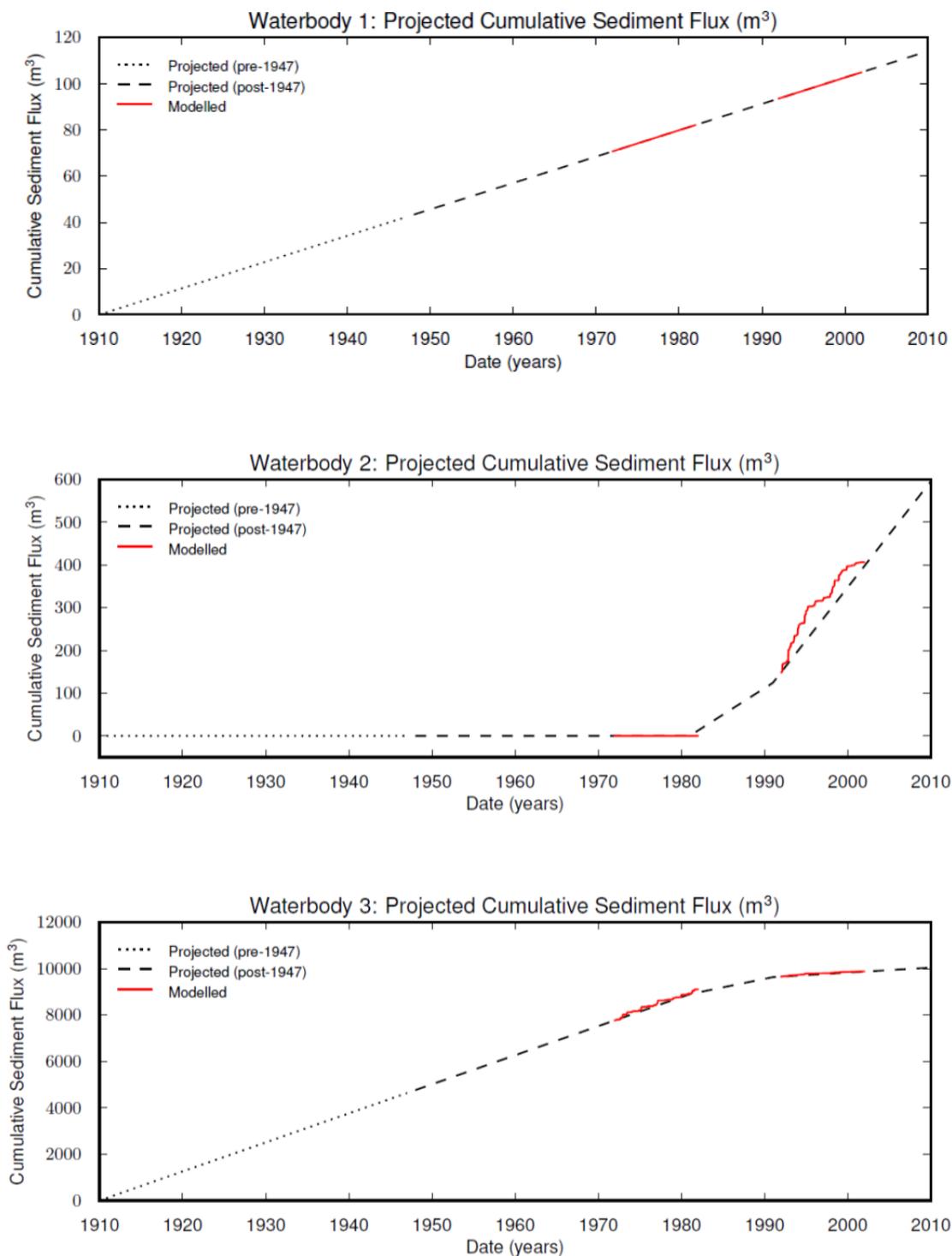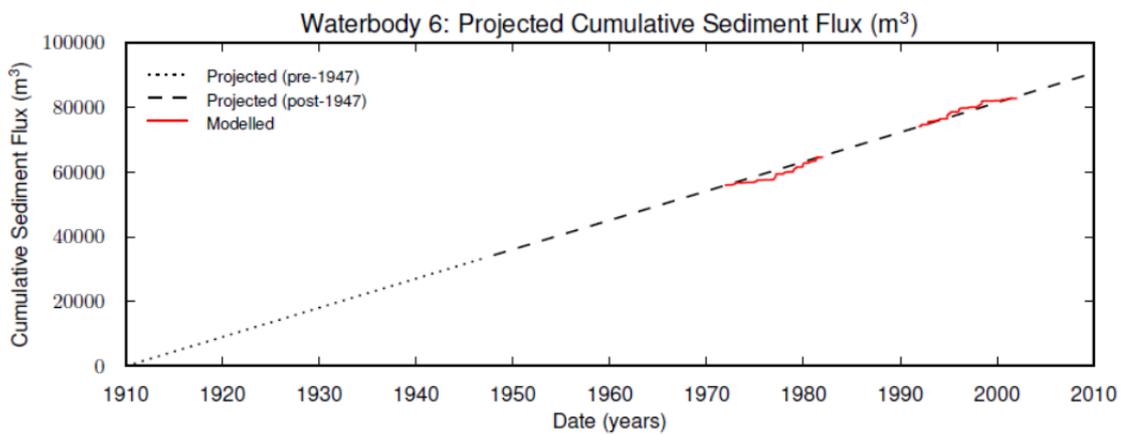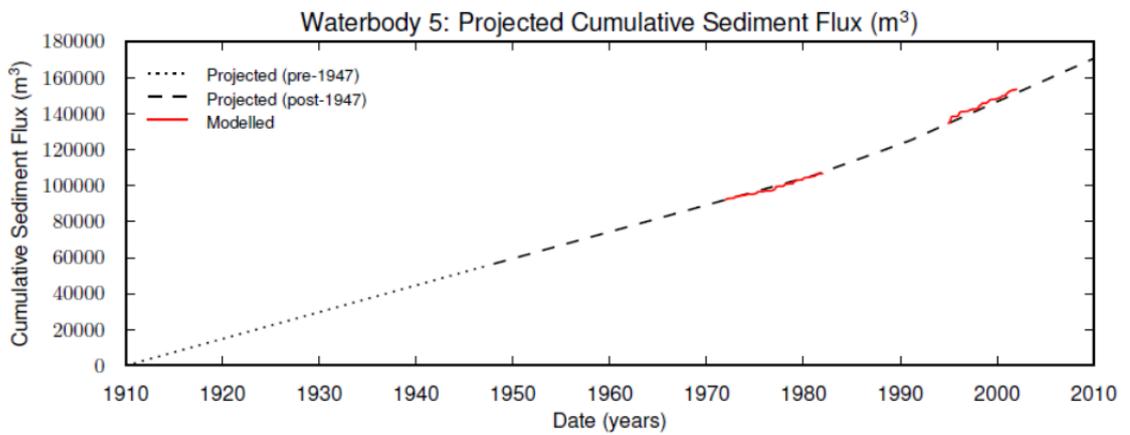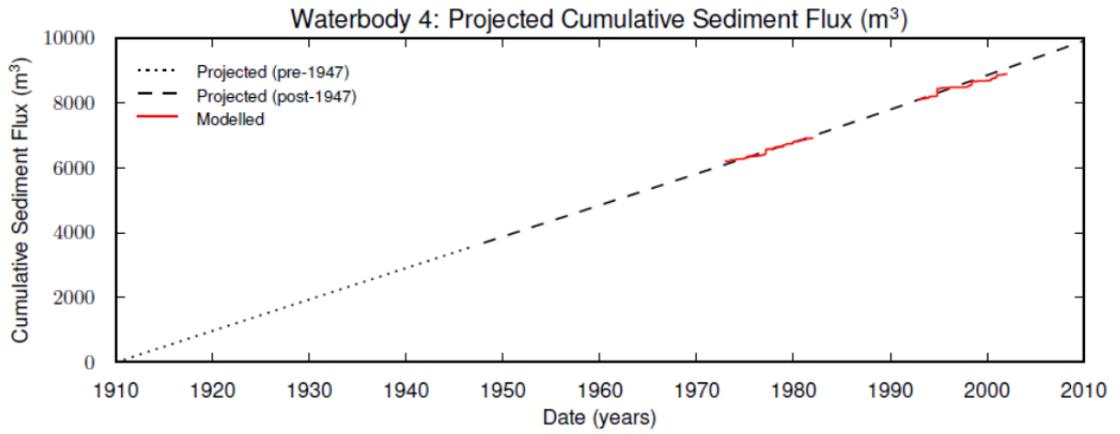
Table 12: Percentage components of sediment flux for each of the water body outlets. For water body 1 there was insufficient sediment flux during either of the modelling periods to determine the percentages of suspended and bedload sediment transport. *For the 2nd water body outlet the percentage could only be compiled from the later simulation because there was zero volume change in the modelled first period.

Water Body Outlet	Percentage Bedload	Percentage Suspended
1	NA	NA
2	80*	20*
3	85	15
4	79	21
5	92	8
6	86	14

3.13.5 Catchment River Discharge and Sediment discharge events

To assess the relationship between river flows and sediment flux events, the two are plotted independently in Figure 28. Whilst some high flow events are accompanied by high sediment flux rates, particularly at the start of winter there are also high discharge events which result in little sediment transport. In Figure 29, modelled sediment transport from water bodies 6 and 3 are plotted directly against observed discharge at their two nearest gauging stations in the Nene Catchment (Orton and Upton respectively). Regression analysis reveals that there is no statistically significant relationship between catchment flow rates and sediment discharge events, preventing river gauging data from providing an alternative method to project modelled flux rates back through time.

Figure 28: River flow data from the Orton gauging station, and modelled sediment transport events plotted for water body 6 for the two modelling periods (1972-1982 and 1992-2002). The blue line is gauging station discharge and black discs are modelled sediment fluxes. River gauging data was only available from 1995-1997 in the second modelling period.
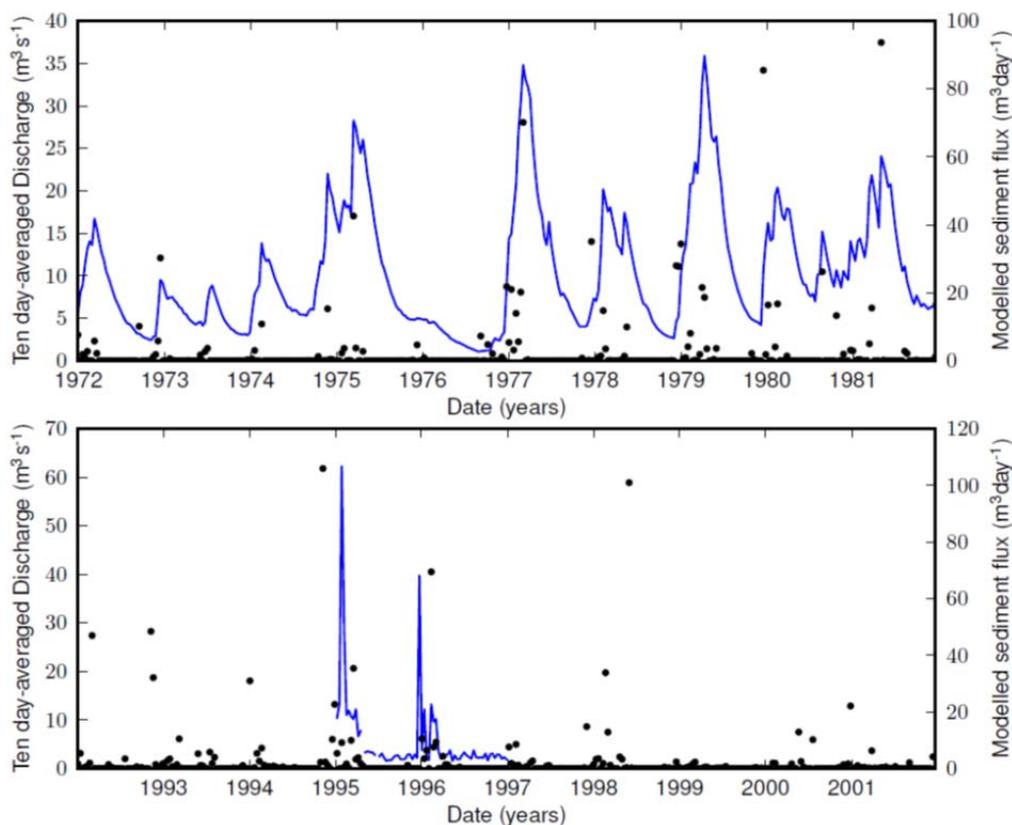
Figure 29: Plots of ten-day averaged water discharge from the Orton gauging station versus modelled sediment flux for the two modelled periods (1972-1982 and 1992-2002 respectively).
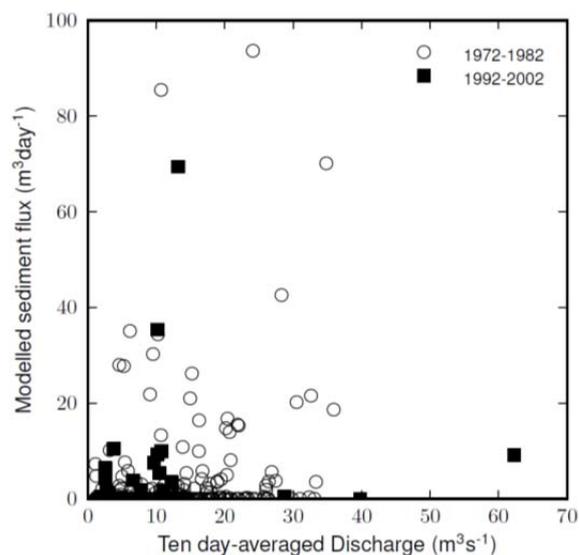
3.13.6 Analysis and Discussion of CDP Model results

The patterns of erosion and deposition are similar in both scenarios, suggesting catchment morphology is the dominant influence on the distribution of sediment transport in the Nene catchment. Water body 2 and 3 experienced markedly different rates of sediment flux between the two modelled periods. Water body 2 experienced more rapid rates in 1992-2002 than 1972-1982 whilst water body 3 saw a reduction in rates between the two periods (Figure 27). This is not a reflection of differing climate conditions but rather a reflection of the dynamic nature of sediment transport predicted by the CDP model.

The majority of erosion and deposition occurs along the main stem of the River Nene with deposition occurring in reaches where the channel gradient is lowest resulting in a wider channel and low modelled flow velocities. These reaches tend to coincide with areas that have been exploited for gravel extraction adjacent to the River Nene. In these locations the actual river course has often been fixed, however at the spatial resolution utilised for simulation this management of the water course cannot be taken into consideration. Hence, in the simulations the river naturally finds a course through these standing water bodies.

Water bodies 1 and 2 have the smallest relative catchment areas and therefore, may respond to small scale rainfall events not captured in the other water bodies. Also, due their elevation, they have low baseflow inputs from groundwater and the highest average precipitation values. These factors are likely to influence the sediment flux rates in these areas when compared to the other water bodies in the catchment and may explain why the sediment flux rates for water body 2 are inconsistent with the other areas.

Water body 6 has the largest suspended sediment transport volume and the most deposition. Both are attributable to the large bodies of standing water near Orton, where low channel gradient and low modelled flow velocities lead to deposition. The point of greatest deposition migrates down the river as sediment accumulates at the upstream end of this low gradient reach.

We were unable to find a direct relationship between modelled sediment flux and observed river gauging data for either of the gauging station sites, despite good agreement between gauging data and simulated water discharge. The lack of linear relationship represents both the distributed nature of the initialising and forcing datasets and the time lagging effects introduced by the groundwater component. This lack of a clear linear relationship prevented us using the gauging data to predict sediment flux rates for the periods where the model did not provide usable data (i.e. prior to 1972). Positive discharge excursions are not necessarily expected to link linearly to sediment discharge since there will be grain-size controlled thresholds in sediment transport such that a discharge event of a certain size will be required to achieve significant sediment transport for a particular grain-size fraction. Additionally, sediment transport will be dependent on sediment availability, such that when two events occur closely together there may be less sediment readily available for transport in the second event since a large amount of sediment has been transported in the first event. This phenomenon may explain why better agreement between gauging data and sediment flux was qualitatively observed for high flow events at the onset of winter.

The data extension pre-1947 has a large amount of associated uncertainty. It is likely that the 1947 flooding event flushed the channel system of sediment and this could be taken as a baseline from which sediment could be stored. It could also have placed sediment on the floodplains, where slack water reduced the ability to transport sediment. Although a relatively smaller event, the winter 2012 flooding in the Nene appeared to have scoured much of the sediment from the river bed (as noted in Section 2.5.1).

Several potential caveats are apparent in using the proposed modelling technique for derivation of sediment volumes. In modelling the hydrology that drives sediment transport we only have detailed observations for the past 50 years. Estimations of sediment transport for the past century will therefore have to be made by extrapolating erosional/depositional rate changes into the past. This assumes that current hydrology is analogous to the past. A detailed analysis of uncertainty in the second phase of modelling will be difficult to quantify without undertaking a suite of simulations. This was not possible given the timeframe or funding levels for this study.

Differences between water discharge and sediment flux rates are expected, due to the influence of groundwater and the complex interactions with surface hydrology on the spatial distribution of river flow.

3.14 A COMPARISON OF THE CDP MODEL AND REPORTED LITERATURE VALUES OF SEDIMENT YIELD IN THE NENE CATCHMENT

Catchment-averaged erosion rates ($t\ km^2\ yr^{-1}$) were calculated from the CDP model output based on estimates of sediment leaving the catchment at the end of water body 6 (Table 13) assuming a sediment density of $1.3\ g\ cm^3$ to convert volume to mass. A search of the scientific literature found other estimates of erosion for the catchment of the river Nene and these are given in Table 13 for comparison. The literature values are mostly suspended sediment values, with those of Wilmot and Collins (1981) being collected close to the Dog-in-Doublet lock, this being the end of water body 6. These values were converted to a catchment erosion rate ($t\ km^2\ yr^{-1}$) of inorganic sediment, using the 34 % organic matter value that Wilmot & Collins (1981) cited.

Table 13: Comparison of CDP model and reported literature values of erosion in the River Nene Catchment.

Study	Method	Total estimated sediment passing through water body 6	Type of sediment	Organic matter % LOI From Wilmot & Collins 1981	Corrected Total Sediment for LOI	Total upstream Catchment size	Erosion rate Inorganic
		T yr⁻¹			T yr⁻¹	Km²	T km² yr⁻¹
CDP Model	Landscape evolution model	676	Inorganic			1590	0.42
Plater et al. 1994	Uranium series dating		Inorganic			2274	0.19 (summer) 0.91 (winter)
[a]Wilmot & Collins (1981)	Suspended sediment	19500	Inorganic + organic	34	12870	1590	8.09
[b]Wilmot & Collins (1981)	Total load based on depth integrated sampling a restricted sections	24000	Inorganic + organic	34	15840	1590	9.96
[c]Wilmot & Collins (1981)	Total load based on prediction of suspended sediment + 20% bed load	16400	Inorganic + organic	34	10824	1590	6.81
[d]Wilmot & Collins (1981)	Overall Rating curve	8400	Inorganic		8400	1590	5.28

Notes

[a] Suspended sediment determined based on a prediction equation relating catchment size to sediment load based on British Catchments.

[b] Depth integrated sampling at sluices to estimate 'Total Load'. An average sediment concentration of 60ppm derived from this sampling program was used and combined with monthly and annual mean daily water discharges to provide estimates of average annual loads.

[c] Short term suspended sediment data (bucket sampling) and mean daily discharges used to construct ratings curves between concentration and discharge. Annual suspended sediment loads were derived by combining the sediment concentration rating curves with the flow duration curve covering the same period. This was done by (i) dividing the discharge into 41 equally spaced logarithmic divisions, (ii) using the rating curve to predict sediment concentration corresponding to each discharge division and (iii) multiplying this concentration by the average discharge within the divison and the corresponding frequency of the occasion of flows.

[d] Analysis of longer term suspended sediment and water discharge data using annual, seasonal and overall rating curves. Reported annual suspended load values derived from an overall rating curve combined with a long term (overall) flow duration curve.

Comparison of the literature and the CDP modelled rates of catchment erosion (Table 13) measured in the River Nene provide a range of erosion rates. The CDP model and Uranium dating series estimates of Plater et al. (1994) suggest erosion rates of < 1 t km^2 yr^{-1}, these being an order of magnitude lower than the erosion rates calculated by the various different methodologies used by Wilmot and Collins (1981) whose maximum catchment erosion rates were estimated at nearly 10 t km^2 yr^{-1}. The way in which rating curves are used can lead to significant over-estimation of the amount of sediment load (Walling, 1977). Thus, Wilmot and Collins (1981) considered that estimates of erosion produced by using methods (c) and (d) (see Table 13 footnotes) of ~5 - 6 t km^2 yr^{-1} were the most reliable. The suspended sediment yields reported for the river Nene in Table 13 are generally quite low compared to the median suspended sediment in UK rivers of ~50 t km^2 yr^{-1} (Walling & Webb, 1987). Wilmot and Collins (1981) suggest that sediment concentration in the rivers of the Wash basin (Nene, Welland, Great Ouse) is controlled by sediment availability rather than the transporting capacity of the rivers, this being a result of the wide, flat catchments, typical of the Nene.

We consider that the differences in the catchment erosion rates (Table 13) are largely a function of anthropogenic influences in the catchment which are included in the higher estimated rates of Wilmot & Collins (1981). Estimates provided by the CDP model are natural erosion rates based on landscape evolution and as such do not include anthropogenic factors such as under-land drainage and urban runoff. Similarly, the measurements based on uranium dating are described as being based on a time scale commensurate with the half-lives of ^{230}Th and ^{234}U, providing estimates of sediment yield integrated over the late Quaternary (Plater *et al.* 1988). Thus, both these methods provide a baseline or 'steady-state' estimate of erosion. However, the results published by Wilmot and Collins (1981) are suspended sediment concentrations and represent a snapshot of catchment erosion rates during sampling, and will include anthropogenic influences that affect erosion and transport to the river system such as land drainage and urban development.

It is unknown to what extent the Catchment Sensitive Farming Initiative (Collins et al. 2007) in the Nene Catchment that runs until 2014 has reduced soil erosion with associated P input into the river but most arable fields bordering the river in the study area appeared to have buffer strips. However, it is evident that within the Nene catchment, where the soils are poorly draining, a significant proportion of contemporary catchment erosion is anthropogenically influenced with soil erosion to the river via land drains a major contributor (Worsfold, 2006). For example, Foster *et al.* (2003) suggested that >50 % of the total catchment suspended sediment yield over a 2 year period originated from land drains in the Rosemaud experimental catchment in Herefordshire. In their study, annual erosion from just one land drain amounted to 964 and 978 kg ha^{-1}yr^{-1}. With the inclusion of buffer strips along most arable fields as an aid to nutrient filtering and soil erosion management to protect river waters, the land drainage pathway is probably of greater importance.

In the current study it is evident that anthropogenic influences increase the catchment erosion by approximately 10 – 12 times from 0.5 t km^2 yr^{-1} to 5-6 t km^2 yr^{-1}. The difference in erosion process (natural erosion or largely anthropogenically mediated events), also produces a difference in the bed load:suspended sediment ratio in the river channel. The CDP model calculates that without anthropogenic mediation, between 80-90% of sediment is moved as bed load (Table 5) (though the use of a single grain-size distribution in model initiation may influence these values). However, Wilmot & Collins (1981) suggest that the influence of land drains, urban areas and sewage works results in

suspended sediment and bed load making up 80 and 20% of the total sediment yield respectively. In the next section these ratios are used to calculate channel transport of sediment based on CDP model outputs and literature catchment erosion rates.

3.14.1 Obtaining first order estimations of catchment erosion and sediment transport

When compared to literature results the CDP model predictions were found to be order of magnitude lower than published values as a result of the CDP model not being able to account for more anthropogenically mediated erosion processes. Thus, we scale the modelled sediment discharges for the entire catchment, and for each water body, to approximate anthropogenic sediment inputs in the simulated data.

The modern value of catchment suspended sediment discharged from water body 6 was obtained from the combined rating curve estimate of 8,400 t yr^{-1} as defined by Wilmot & Collins (1981). Using the catchment area (1,590 km^2), the catchment averaged erosion rate is 5.28 t km^2 yr^{-1}. Wilmot & Collins (1981) cite a ratio of 80:20 suspended sediment to bed load. To take into account the bed load the total catchment sediment discharge is increased according to this ratio (6.6 t km^2 yr^{-1} or 10,500 t yr^{-1}). For direct comparison of the catchment sediment discharge, the average model simulated discharge (866.5 m^3 yr^{-1}) is converted into an average sediment discharge rate (1,126 t yr^{-1}) using a sediment density of 1.3 g cm^{-3}. This rate can be divided into bed load and suspended load discharge rates based on the water body 6 ratio defined in Table 12.. The total catchment sediment discharge scaling ratio (Table 14), which we use to approximate the anthropogenic influence on the simulated naturalised rates for each water body, is derived as the ratio of simulated to published sediment discharge values.

To calculate the additional influence of anthropogenic sediment fluxes on the modelled results, the sediment discharge scaling ratio is applied to the simulated sediment discharge rates for each water body for each period (1972-81 (Table 15) and 1992-01 (Table 16). To maintain uniformity with published results, we also convert the calculated sediment discharge rates into water body erosion rates based on the water body area. These values were used to calculate phosphorus and phosphate transport through the river body (Section 3.15.2).

Table 14: Model and literature values used to obtain scaling ratios which were then applied to erosion from each water body based on the catchment erosion rate of 6.24 t km^2 yr^{-1}.

	Sediment passing WB6 (T yr^{-1})	Bedload (T yr^{-1})	Suspended Load (T yr^{-1})
Model	1126	969	158
Wilmot & Collins, 1981	10500	2100	8400
Scaling Ratio		**0.46**	**0.019**
CDP model : Wilmot & Collins 1981.			

A comparison of results between the naturalised (or baseline) CDP model predictions and those assuming a greater anthropogenic influence are shown in Table 15 and 16 and Figures 30 and 31. These results are likely to give the range of first order approximation of sediment movement between water bodies for the River Nene under typical annual

weather scenarios. It is considered unlikely that they will provide accurate data for extreme years such as 1947 or 2012.

Table 15: Comparison of CDP model (background) v anthropogenically mediated (Wilmot & Collins, 1981) estimates of bedload and suspended sediment leaving each waterbody for the six water bodies of the River Nene based on model parameters produced for the period 1972-1981.

	Model Total sediment (T yr^{-1})	Model Bed load (T yr^{-1})	Model Suspended Sediment (T yr^{-1})	Literature Bed load (T yr^{-1})	Literature Suspended sediment (T yr^{-1})	Literature Total sediment (T yr^{-1})	Catchment area (km^2)	Cumulative Catchment area (km^2)	Model Catchment Erosion rate (T km^2 yr^{-1})	Literature Catchment Erosion rate T km^2 yr^{-1}
Water Body 1	1.43	0.286	1.14	0	1.144	0.286	38.32	38.2	0.037	0.007
Water Body 2	0	0	0	0	0	0	108.72	146.92	0	0
Water Body 3	173.68	147.62	26.05	320.837	1391.19	1712.03	391.68	538.6	0.322	3.178
Water Body 4	170.69	134.84	35.84	293.05	1914.14	2207.19	395.84	934.44	0.182	2.362
Water Body 5	1885.91	1735.0	150.87	3770.725	8056.70	11827.43	233.36	1167.8	1.614	10.12
Water Body 6	1122.94	965.72	157.21	2098.8	8395.2	10494.0	422.68	1590.48	0.706	6.59

Table 16: Comparison of CDP Model v literature (Wilmot & Collins, 1981) estimates of bed load and suspended sediment leaving each water body for the six water bodies of the River Nene based on model parameters produced for the period 1992-2001.

	Model Total sediment (T/yr^{-1})	Model Bedload (T/yr^{-1})	Model Suspended Sediment (T/yr^{-1})	Literature Bedload (T yr^{-1})	Literature Suspended sediment (T yr^{-1})	Literature Total sediment (T yr^{-1})	Catchment area (km^2)	Cumulative Catchment area (km^2)	Model Catchment Erosion rate T km^2 yr^{-1}	Literature Catchment Erosion rate T km^2 yr^{-1}
Water Body 1	1.43	0	0	0	0	0	38.32	38.2	0.037	0.00
Water Body 2	33.54	26.832	6.708	58.38	358.62	417.00	108.72	146.92	0.228	2.83
Water Body 3	29.51	25.0835	4.4265	54.57	236.65	291.22	391.68	538.6	0.054	0.54
Water Body 4	199.16	157.3364	41.8236	342.33	2235.99	2578.32	395.84	934.44	0.213	2.75
Water Body 5	3122.08	2872.314	249.7664	6249.58	13353.14	19602.73	233.36	1167.8	2.673	16.78
Water Body 6	1121.64	964.6104	157.0296	2098.8	8395.2	10494	422.68	1590.48	0.705	6.59

Figure 30: Estimates of annual cumulative sediment export from the upper six water bodies of the River Nene. The values are comparisons determined using the CDP model and the catchment erosion estimate of Wilmot & Collins (1981) of 6.24 t km^2 yr^{-1} and are based on model outputs for the periods 1972-1981 and 1992-2001.
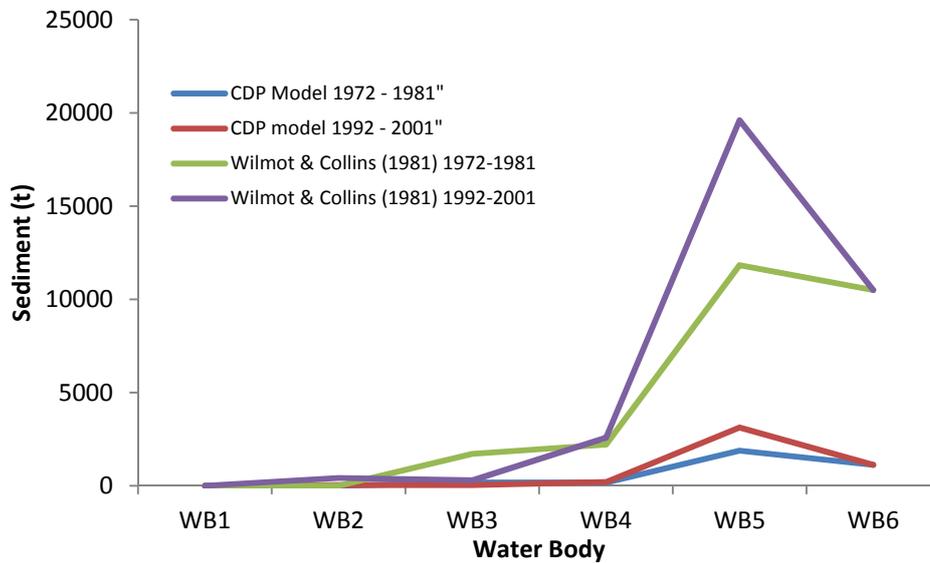
Figure 31: Estimates of annual net erosion for the upper six water bodies of the River Nene. The values are comparisons determined using the CDP model and the catchment erosion estimate of Wilmot & Collins (1981) of 6.24 t km^2 yr^{-1} and are based on model outputs for the periods 1972-1981 and 1992-2001. Net erosion occurs where results are positive and net deposition occurs where values are negative.
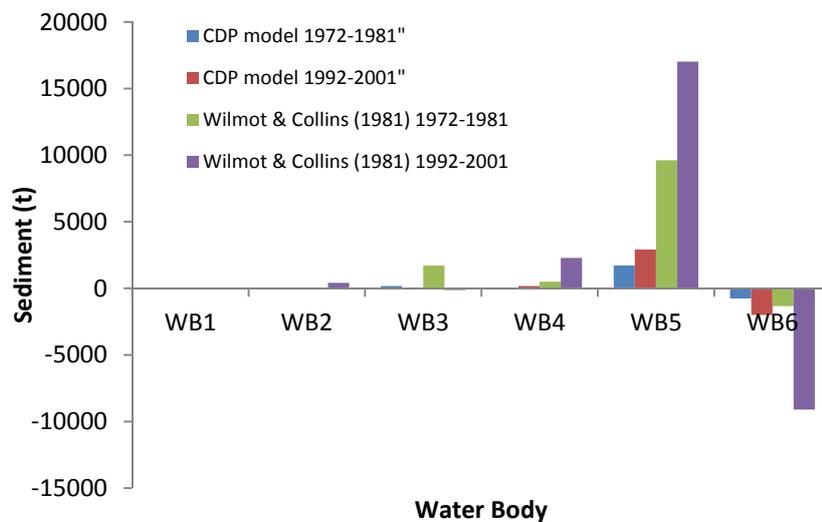
3.15 CALCULATING P LOADS IN THE SEDIMENTS AND WATERS OF THE RIVER NENE

3.15.1 Masses of Phosphorous and extractable phosphate in river sediment

Probed sediment volumes, sediment bulk density (Db), TP and OEP results were combined to determine first order estimates of the quantities of P in the sediments of each of the six water bodies (Table 17). Estimates of sediment volume were based on the river channel conditions outlined in Table 4.

Table 17: First Order Estimates of TP and extractable P in sediments of the River Nene

Water body	Sediment Vol (M^3)	Sediment (kg)	Bulk Density ($g\ cm^{-3}$)	Mean TP ($mg\ kg^{-1}$)	TP (Tonnes)	Mean PO_4-P ($mg\ kg^{-1}$)	PO_4-P (Tonnes)
1	584	291829	0.5	1978	577	21.22	6.19
2	512	255755	0.5	1927	493	35.45	9.07
3	851	425728	0.5	1597	680	43.78	18.64
4	1381	690439	0.5	4420	3052	68.55	47.33
5	1654	826924	0.5	4433	3666	63.94	52.87
6	3911	1955294	0.5	3997	7815	65.85	128.76

3.15.2 Masses of sediment associated TP and OEP moving between water bodies – CDP & Wilmot & Collins (1981)

Based on the two scenarios discussed in Section 3.14.1 and shown in Tables 15 & 16 the movement of sediment associated TP and OEP is estimated between the different water bodies. These were calculated by combining sediment movement with concentrations of sediment TP and OEP (Tables 18-21). As would be expected the amount of sediment associated P that moves between water bodies will be largely a function of total sediment transport and concentration (Figure 32). For both TP and OEP, export of P from water bodies is reasonably low as sediment movement (Tables 15 & 16) is low. After water body 4 erosion input and transport of sediment increases, thus increasing the movement of TP and OEP (Tables 15 & 16).

Table 18: Comparison of the movement of sediment TP between water bodies using values obtained from the CDP model and based on the catchment erosion rate of 6.60 t km^2 yr^{-1} derived from Wilmot & Collins (1981) using data from the period 1972-1981. Sediment volume is converted to mass using a sediment density of 1.3 g cm^3.

	CDP Model				**Literature value = 6.60 t km^2 yr^{-1}**			
Water body	Sediment volume leaving water body (M^3)	Sediment leaving water body (t)	Mean TP (mg kg^{-1})	TP lost from water body (kg)	Sediment volume leaving water body (M^3)	Sediment leaving water body (t)	Mean TP (mg kg^{-1})	TP lost from water body (kg)
1	1	1.3	1978	2.57	-	0.286	1978	0.57
2	0	0	1927	0	-	0	1927	0.00
3	134	173.7	1597	277	-	1712	1597	2734
4	131	170.7	4420	754	-	2207	4420	9755
5	1451	1885	4433	8360	-	11827	4433	52431
6	864	1122	3997	4487	-	10494	3997	41944

Table 19: Comparison of the movement of sediment Phosphate-P between water bodies using values obtained from the CDP model and based on the catchment erosion rate of 6.60 t km^2 yr^{-1} derived from Wilmot & Collins (1981) using data from the period 1972-1981. Sediment volume is converted to mass using a sediment density of 1.3 g cm^3.

Water body	Model				Literature value = 6.60 t km^2 yr^{-1}			
	Sediment volume leaving water body (M^3)	Sediment leaving water body (t)	Mean OEP (mg kg^{-1})	OEP lost from water body (kg)	Sediment volume leaving water body (M^3)	Sediment leaving water body (t)	Mean OEP (mg kg^{-1})	OEP lost from water body (kg)
1	1	1.3	21.2	0.03	-	0.286	21.2	0.01
2	0	0	35.4	0	-	0	35.4	0.00
3	134	173	43.7	7.59	-	1712	43.7	74.8
4	131	170	68.5	11.69	-	2207	68.5	151
5	1451	1885	63.8	120.3	-	11827	63.8	754
6	864	1122	65.8	73.89	-	10494	65.8	690
Total								

Table 20: Comparison of the movement of sediment OEP between water bodies using values obtained from the CDP model and based on the catchment erosion rate of 6.60 t km^2 yr^{-1} derived from Wilmot & Collins (1981) using data from the period 1992-2001. Sediment volume is converted to mass using a sediment density of 1.3 g cm^3.

	Model				**Literature value = 6.60 t km^2 yr^{-1}**			
Water body	Sediment volume leaving water body (M^3)	Sediment leaving water body (t)	Mean TP (mg kg^{-1})	TP lost from water body (kg)	Sediment volume leaving water body (M^3)	Sediment leaving water body (t)	Mean TP (mg kg^{-1})	TP lost from water body (kg)
1	1	1.3	1978	2.57	-	0	1978	0
2	26	33.8	1927	65.1	-	417	1927	803
3	23	29.9	1597	47.7	-	291	1597	465
4	153	199	4420	879	-	2578	4420	11396
5	2402	3122	4433	13842	-	19602	4433	86898
6	869	1130	3997	4516	-	10494	3997	41944
Total								

Table 21: Comparison of the movement of sediment OEP between water bodies using values obtained from the CDP model and based on the catchment erosion rate of 6.60 t km^2 yr^{-1} derived from Wilmot & Collins (1981) using data from the period 1992-2001. Sediment volume is converted to mass using a sediment density of 1.3 g cm^3.

	Model				Literature value = 6.60 t km^2 yr^{-1}			
Water body	Sediment volume leaving water body (M^3)	Sediment leaving water body (t)	Mean OEP (mg kg^{-1})	OEP lost from water body (kg)	Sediment volume leaving water body (M^3)	Sediment leaving water body (t)	Mean OEP (mg kg^{-1})	OEP lost from water body (kg)
1	1	1. 3	21.2	0.03	-	0	21.2	0.00
2	26	33.8	35.4	1.19	-	417	35.4	14.7
3	23	29.9	43.7	1.31	-	291	43.7	12.7
4	153	199	68.5	13.64	-	2578	68.5	176
5	2402	3122	63.8	199.2	-	19602	63.8	1250
6	869	1129	65.8	74.3	-	10494	65.8	690

Figure 32: Estimates of annual exports of (a) TP and (b) OEP leaving the upper six water bodies of the River Nene. The values are comparisons based on sediment exports determined using the CDP model and the catchment erosion estimate of Wilmot & Collins (1981) of 6.60 t km^2 yr^{-1} and are based on model outputs for the periods 1972-1981 and 1992-2001.
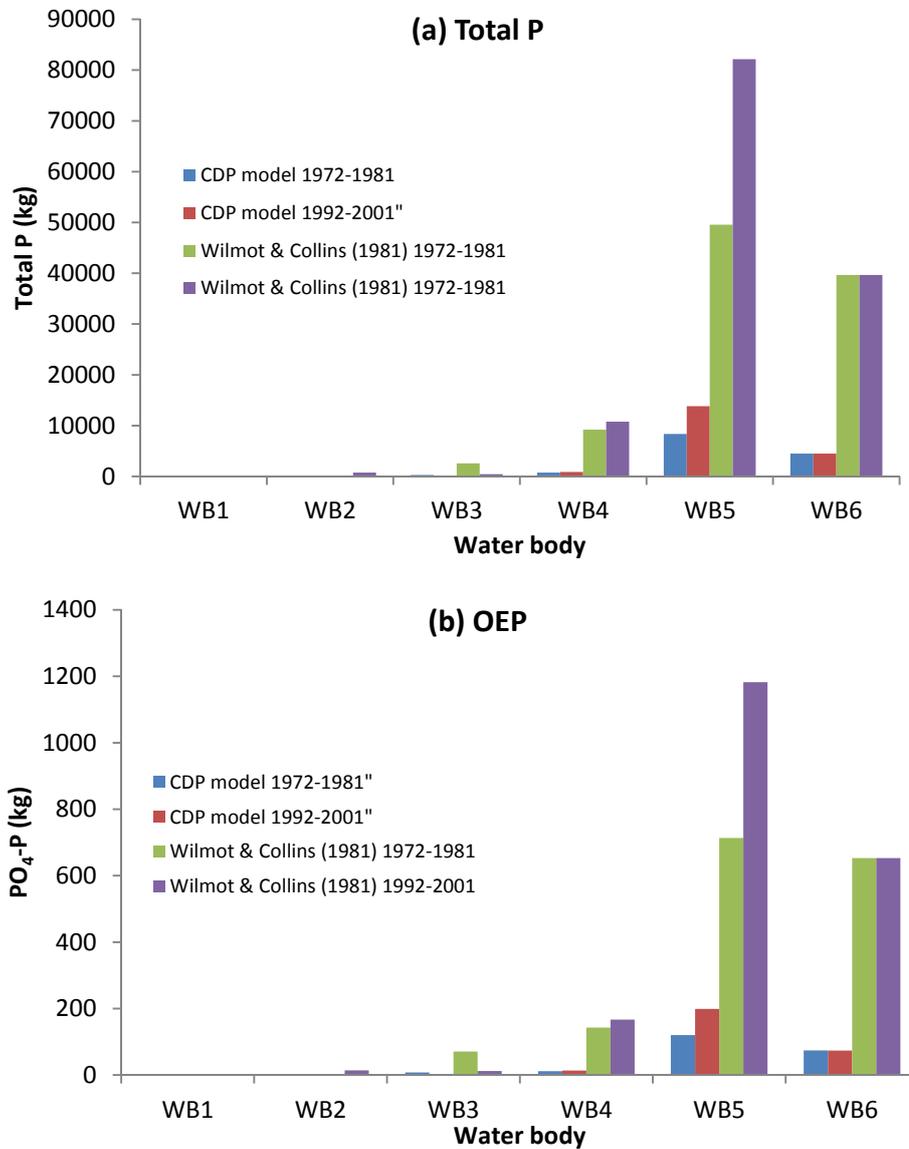
3.15.3 Uptake of SRP from river water in each water body

By combining results from the kinetic experiments (section 3.10) with river speed (m s^{-1}) we can determine first order estimates of the quantity of SRP that is potentially absorbed by the sediment. Calculations were based on an active sediment layer (0-5cm), corresponding to the 0-5 cm fraction analysed and a water depth of 10 cm above the sediment. Sediment volumes from the probing analysis were used to provide the amount of sediment that would interact with it (Table 4) and these values were used in calculating T_{res} (Equations 4 & 5). Water speed in River Bodies 1, 2 and 3 were measured whilst we use mean flow (9.3 cumecs) data obtained from Orton, converting from cumecs to m sec^{-1} for use in equation 4 & 5 for Water Bodies 4-6. This gave water speeds of ~1100 m hr^{-1} for the headwaters and for Water Bodies 4-6 a mean value 440 m hr^{-1} was used.

Table 22 reports the characteristics used in equations 4 & 5 to determine the quantity of SRP sorbed by the sediment per km of water body. In Table 23 we report this figure as a percentage of the total SRP that was found in the water at the time of sampling. Results suggest that potentially the highest SRP sorption occurred in water body 5 where up to 40 g P could be sorbed per km. This amounts to about 10 % of the SRP that is contained in the water in the 10 cm layer that interacts with the 5cm of sediment.

Table 22: SRP sorbed (g) from 1 km stretch of water body.

Waterbody	Kr	n	Ct	EPc0	S (g)	µmol P	g P	T_{res}	g P Sorbed
Waterbody 1	2.36	2.05	0.18	1.36	93000000	NC	NC	0.11	NC
Waterbody 2	51.7	2.16	1.65	0.62	183000000	10024238223	310490	0.21	0.045
Waterbody 3	10.6	1.09	4.63	0.66	180000000	8641147685	267650	2.63	6.89
Waterbody 4	25.4	1	3.4	1.12	180000000	10469518380	324282	5.45	29.7
Waterbody 5	26.9	1.26	4.35	1.45	180000000	18557403313	574797	6.36	40.5
Waterbody 6	14.1	2.29	3.83	1.89	180000000	11586647861	358884	4.55	20.7

NC = Not calculated because of dilution of the measured PO_4-P concentration meant it was below EPC_0.

Sediment however was an absorbing sediment and not a desorbing one.

Table 23: Percentage of river water SRP sorbed in a km

	Width of channel	Depth of water	length channel	volume of water	L of water	µmol P L^{-1}	µmol P in channel	g P in channel water	g P sorbed	%
Waterbody 1	1.55	0.1	1000	155	155000	0.18	27900	0.86	-	-
Waterbody 2	3.05	0.1	1000	305	305000	1.65	503250	15.58	0.044	0.28
Waterbody 3	11.55	0.1	1000	1155	1155000	4.63	5347650	165.63	6.89	4.16
Waterbody 4	24	0.1	1000	2400	2400000	3.4	8160000	252.74	29.75	11.77
Waterbody 5	28	0.1	1000	2800	2800000	4.35	12180000	377.26	40.49	10.73
Waterbody 6	20	0.1	1000	2000	2000000	3.83	7660000	237.26	20.66	8.70

4 General Discussion and Conclusions

4.1   SEDIMENT PHOSPHORUS CHEMISTRY

The results of the sediment TP and OEP chemistry and its dynamics conform to previous research in similar fluvial settings. However, the expectation that sediment texture in the sampled cores would become finer as distance from the headwaters was not met, as it was obvious that spatial and temporal influences as well as the depositional environment were large determinants on sediment texture. Organic matter content of the sediment was generally found to increase with distance from the headwaters, and results suggested that this was strongly dependent on clay content and not particle size. Bedrock geology appeared to be the biggest influence on TP concentration, with the depositional environment in which the various rocks were laid down controlling the associations of P containing minerals. This was demonstrated by the strong correlations to Mn and Fe. However, there were few geochemical associations between OEP and the measured reactive surfaces that are generally considered to be important for sorption, thus suggesting that OEP concentration in the sediment was more a function of the local depositional environment. OEP was also found to be a small proportion of TP, typically being < 5%. The importance of depositional environment was demonstrated by the analysis with depth (core$_D$) from each water body. No consistent pattern being found throughout the length of the river analysed. Pinay *et al*. (2002) and Fisher *et al*. (2004) both emphasise the importance of flooding in particular for resetting the sediment structure and texture both within the channel and floodplain.

Concentrations of OEP in the sediment were found to be as high as 100 mg kg^{-1} and these levels of phosphate P will obviously have the potential to increase macrophyte growth. Rooted aquatic plants have the potential to derive almost all their P requirements from bio-available sediment P reserves (Mainstone & Parr, 2002), although Pelton et al. (1998) suggested that the relative contribution of root uptake to macrophyte P demand varied on the SRP concentration in the overlying water. The increased growth of aquatic plants where there are high levels of bio-available P can lead to other problems. Along with greater plant growth trapping more sediment, Mainstone & Parr (2002) suggest that extra P (i) increases re-growth after plant management, (ii) the species community structure can be altered, favouring species with high growth rates and (iii) root depth is reduced, potentially increasing the plants susceptibility to being ripped out at high river flows and associated sediment remobilization.

As the amount of OEP is higher in the sediments than is recommended for most agricultural soils, this may suggest that the sediments have sorbed additional phosphate from non-agricultural sources, once in the channel. Indeed, results from Table 6 examining the potential for further sorption of SRP using EPC$_{0Sat}$ suggest that the sediments have the potential to adsorb significantly more SRP. Sediments with such high potentially bio-available phosphate may pose problems in the future with issues associated with climate and river management. In particular, the management of phosphates associated with Sewage and Waste Water may present challenges. The limited analysis of PO$_4$-P:B ratios in the river waters suggests that the PO$_4$-P present is largely associated with the output of sewage and wastewater treatment. The benefit of examining the 'Effective Phosphorus Concentration' is that it has demonstrated that the sediment is likely to absorb, rather than desorb P. However, this depends largely on the concentration of PO$_4$-P in the river water and consideration that the EPC$_0$ is a function of sediment and water chemistry and therefore can be expected to vary slightly as river conditions change and sediment properties change with time (Stutter & Lunsdon, 2008). Whilst water PO$_4$-P concentrations were always greater than the EPC$_0$ when we sampled, examination of data supplied by the EA for PO$_4$ concentrations at Oundle give a range of between 0.05 and 0.6 mg L^{-1}. Dividing these values by three to obtain PO$_4$-P concentrations, suggest that on occasion the water PO$_4$-P concentrations may be lower than the EPC$_0$

calculated for water body 6 (0.05 mg L^{-1}). Thus although these events don't appear to last long it may be possible that at some points in the yearly cycle, the sediments may desorb PO_4-P. However, generally water PO_4 concentrations are around 0.2 mg L^{-1} PO_4-P which means they are greater than the EPC_0 and sediments will favour the sorption of PO_4-P. Calculations suggest that the sediment can take up about 10 % of the PO_4-P that occurs in the 10 cm water depth above the sediment over the distance of a kilometre.

It would appear that a major decrease in PO_4 water concentration was achieved for the River Nene in 1998, where values were reduced from 2-3 mg L^{-1} to 0.1-0.2 mg L^{-1}. Thus, if further improvements were to be made to the STW output, the concentration of SRP in the water could become lower than the EPC_0 more often leading to desorption of PO_4-P. Evidence from the EPC_0 calculations suggest that initially water bodies 5 and 6 would be most vulnerable to decreasing PO_4-P concentrations in river water as these have the highest EPC_0 values.

Climate forecasts for future decades suggest that dryer conditions are more likely to occur in the summer in eastern England (Murphy et al. 2009). This could produce low flow conditions in the Nene. However, assuming that the water PO_4-P is largely derived from sewage waters, it is likely that concentrations would increase as sewage waters may constitute a greater proportion of the river causing less dilution of P (Neal et al. 2010). Jarvie et al (2006) also suggests also that as a guide, where river water SRP concentration exceeds $EPC_0,$ release of SRP from the sediment to the water column during periods of low flow (i.e. times of greatest eutrophication risk) is low. With respect to flooding conditions, it would generally be considered that dilution of PO_4-P may occur which could lower river PO_4-P concentrations to below those of the EPC_0. However the survey of Nene waters carried out in this research showed concentrations of PO_4-P still greater than EPC_0 values, even after a prolonged period of high stream flow. Neal *et al.* (2010) suggest that river SRP concentrations could be maintained during flooding periods due to overflow of sewage facilities such as septic tanks.

4.2   SEDIMENT DYNAMICS WITHIN THE RIVER SYSTEM

As large quantities of phosphate within the river channel is primarily attached to sediment, the erosion, deposition and transport of the sediment within the channel has been shown to be of great importance to where phosphate accumulates, and then its potential interactions with the river water. The CPD model has demonstrated that there is low sediment input into the Nene, largely due to the catchment topography. Thus, the dynamics of sediment input and transport can be seen as being largely driven by both low sediment supply as well as precipitation.

The survey of the sediment during the sampling program demonstrated that the sediment observed was largely based in little inlets of the main river channel, in backwaters and around locks, these being areas where water currents are slowest. The striking outcome of this survey was how little sediment was found. Sampling was carried out after a long period of sustained high water flow. It is recognised that high flow can act to scour sediment from the channel. In addition the removal of plants, which normally act as sediment traps (Cotton *et al.* 2006) will probably allow greater erosion of existing sediment deposits during the high flow periods. This was observed particularly around Water body 4 (Willy Watt Marina) but also in Water bodies 5 and 6. Brierley *et al.* (1989) report a similar occurrence of large scale plant removal through scouring after abnormally high flows during the winter of 1976/77.

Without previous knowledge of sediment conditions before the wet autumn and winter of 2012/13 it is impossible to assess the extent of this sediment scouring in the river channel of the Nene. However, there is a strong indication, based on the survey undertaken, that these large and prolonged flooding events can largely reset the sediment system by flushing. Trimmer *et al.* (2012) suggest that major flooding events can change the sediment structure and distribution in the river channel and this can have major impacts on the residence times of

nutrients within the catchment by (i) depositing sediment back on the floodplains and (ii) washing sediment out towards the coast.

If extensive sediment flushing of the river channel is linked to periods of extended high water flow (e.g. one in 50 year events), then calculations for the accumulation of sediment in the river channel can be started at the end of these events. The CDP model and literature calculations give a potential range of sediment erosion/accumulation for each water body covering baseline to typical catchment erosion rates under typical yearly weather patterns. Thus, depending on the weather in any one year somewhere between $1000 - 10000$ t yr^{-1} of sediment could be expected to depart water body 6. The CDP model suggests, based on morphology of the catchment that sediment erosion is greatest in water body 5 followed by significant deposition in water body 6. With phosphate being attached to the sediment, phosphate deposition and erosion in the channel will typically follow sediment transport patterns.

4.3   IMPLICATIONS OF RESULTS FOR RIVER MANAGEMENT

The results of this work demonstrate that the gradual, long-term reduction of SRP concentrations in the River Nene will only be achieved by balancing a range of management strategies. The central points from this work to be considered when developing these strategies are:

- After the recent floods (Sept 2012 to Jan 2013) only a small quantity of sediment remained in the main channel of the Nene.
- Undertaking major de-silting operations would seem inappropriate at the present time (summer 2013) because there is insufficient silt for this to have any substantive impact. Targeted de-silting could disrupt the remaining aquatic plants which require silt for growth. Our analyses showed that whilst there are large concentrations of OEP in river sediment, this sediment still acts as an SRP sink, and will continue to take up SRP from the river water.
- The remaining silt is the substrate for macrophyte growth and these plants will also absorb some of the SRP from river water, in addition to bio-available OEP in the river sediment. Harvesting these plants would remove some of the phosphate (contained within the biomass) but also may have detrimental effects on biodiversity (described in Sections 4.1 & 4.2).
- There was a correlation between dissolved SRP and boron in the water bodies of the Nene which suggests that sewage treatment works have an influence on river SRP concentrations.
- Any further decrease of SRP from sewage works will need to be undertaken in recognition of the EPC$_0$ of sediments. To a large degree the EPC$_0$ is related to the geochemical properties of the sediment as determined by geology (e.g. clay type, oxides concentration) and sediment architecture as defined by depositional environment and is likely to be in similar to those determined in this work. Decreasing river water SRP concentrations below the EPC$_0$ by STW treatment will potentially allow SRP to desorb from the sediment initially, so there may be a potential time-lag before the benefits of STW treatment are seen as the system moves towards a new equilibrium.

4.4   FURTHER WORK

There are a number of aspects where further understanding of the interactions between sediment and SRP in the River Nene may require further research to improve the evidence-base where management interventions aim to improve ecological status. These are as follows:

- Now that river conditions have returned to more typical flow conditions (June 2013), it would be helpful to quantify the importance of STW source in contributing to SRP in river and sediment. It may be possible to do so using the strong relationship between SRP and boron concentrations given that data from surveys by the British Geological Survey show that across the wider catchment there are few bedrock sources of boron. Confirming the dominant source of SRP (is it STW derived) would be a major stepping stone to developing management plans to deliver improved 'Ecological Status'.

- The major flushing of sediment that appears to occur during periods of flooding and could be a fundamental process that removes sediment associated P from the upper six water bodies of the Nene. An improved understanding of both the long-term (decadal) and seasonally-related annual cycle of erosion, deposition, storage and transport of sediment within the river channel would provide fundamental knowledge related to the outcomes of management interventions. In particular understanding the frequency of high river flow conditions required for these natural flushing events to occur would be beneficial.

- The extent to which the results of this study are representative of the long term state of the river Nene system following the recent wet winter remains unclear. Future modelling efforts could focus on simulating sediment transport for the period leading up to and including the recent wet winter of 2012/2013 for comparison to the existing modelled periods to identify whether the recent winter was likely to have resulted in exceptional levels of sediment transport, or whether the model would predict that the hypothesised 'flushing events' occur regularly/frequently.

- The efficiency of bedload and suspended load sediment transport are governed by typical values from the literature. Sediment transport estimations are also highly sensitive to the imposed grain size distribution. Better parameterisation of sediment transport in the river Nene could be achieved through monitoring the distribution of turbidity and water discharge at stations along the catchment (e.g. water body outlets) in order to quantify the spatio-temporal distribution of suspended sediment load which could be used to calibrate the model.

- The small, natural erosion rates across the catchment (as determined by the CPD model) suggest that we require a better understanding of the magnitude of human-influenced point sources of sediment input (e.g. land drains). In addition, understanding the proportion of sediment derived from point sources that are subsequently stored in the channel or lost (transported) from the system could improve river silt management. Comprehensive measurements on P speciation (particulate, dissolved) and fluxes of these drainage inputs would be of great value in understanding their importance for P dynamics (EPC_0) of this sediment which subsequently enters the main channel, with implications for SRP concentrations in the main channel.

- The Representative Soil Sampling Scheme (RSSS) of England and Wales (Baxter et al. 2006) showed that since 1971, a broad decrease in total P in agricultural soils has taken place, especially in the east of England. This would suggest that in future soil eroded into the river will probably contain less total P than in recent decades. However, identification of the volume and P dynamics of possible legacy P sources could be important. Although this study encompassed the main channel of the Nene, it

did examine sediment depths and P dynamics in the headwaters/backwaters, where boat navigation was not practicable. In a complex, bifurcating river system such as the Nene, backwater areas are substantial, typically with slower water flows and longer sediment residence times.   Phosphorus stored in sediment in drainage ditches throughout the catchment may also provide potential legacy issues. The influence of buffer strips may also need to be investigated to assess whether greater SRP is generated in these and later lost to the rivers through drains (Roberts et al. 2012; Stutter et al. 2009).

- Any further changes in the management of PO_4-P from STW should be monitored in relation to the EPC_0 so that sediment does not become a source of PO_4-P to the water in the future.

- Resolving many of these issues could be achieved by undertaking a more detailed study of sediment input, transport and SRP interactions in a representative sub-catchment or water body where significant STW inputs occur.

Appendix 1: Bulk Density values for cores. Missing values are where grab samples were taken or are Core_D samples.

Core	Easting	Northing	Bulk Density g cm^{-3}
1	454668	259939	0.26
2	455686	259547	
3	456805	259310	
4	458594	259162	
5	460344	259190	0.00
6	461267	259351	
7	461866	259468	
8	462407	259408	
9	463437	259533	0.91
10	463878	259581	
11	464266	259241	
12	464410	259499	0.33
13	465508	259520	
14	465954	259209	
15	467658	258658	
16	469086	259417	
17	472527	258899	0.62
18	473116	259827	0.40
19	478072	259818	
20	478939	260444	
21	479560	460603	0.52
22	483040	261292	0.51
23	484972	261894	0.44
24	485819	262062	0.25
25	496111	271705	0.21
26	497006	272577	0.43
27	496724	274635	0.35
28	497095	275067	
29	497019	276613	
30	497702	276988	0.30
31	500721	280009	0.19
32	500498	280090	0.54
33	503930	286096	0.35
34	504785	287055	0.38
35	508022	297311	
36	507695	299399	0.42

Appendix 2: Data collected for homogenised cores collected from the River Nene

Core	Easting	Northing	Clay	Silt	Sand	LOI	Tot P	OEP	OEP of TP	Tot Fe	Tot Mn	Tot Ca	Tot Al
			%	%	%		mg kg^{-1}	mg kg^{-1}	%	mg kg^{-1}	mg kg^{-1}	mg kg^{-1}	mg kg^{-1}
1	454668	259939	5.33	12.92	81.75	3.18	723	15.06	2.08	30684	425	5414	25317
2	455686	259547	10.27	30.47	59.26	1.90							
3	456805	259310	35.52	59.57	4.91	5.81	1898	25.44	1.34	79619	988	24840	33633
4	458594	259162	13.29	33.77	52.94	9.79	2110	24.31	1.15	111222	866	17365	78640
5	460344	259190	4.35	9.93	85.72	3.37	2083	16.64	0.80	110363	1391	39540	42139
6	461267	259351	3.21	9.14	87.65	4.53	3078	24.62	0.80	184187	1569	32196	22415
7	461866	259468	20.14	70.18	9.69	9.92							
8	462407	259408	15.23	39.91	44.86	3.64	2799	22.60	0.81	118227	1225	51592	21510
9	463437	259533	3.10	6.46	90.44	7.19	1799	21.86	1.21	54161	707	15038	53031
10	463878	259581	11.86	28.54	59.61	3.38	1433	70.22	4.90	42904	730	16392	24534
11	464266	259241	13.07	35.98	50.95	3.67	2243	34.48	1.54	129848	972	18165	17010
12	464410	259499	3.35	9.81	86.85	4.51	1361	28.08	2.06	50311	548	14166	35787
13	465508	259520	19.05	28.32	52.63	5.29	1371	62.08	4.53	40308	552	16449	24572
14	465954	259209	11.91	43.65	44.44	3.78	1413	56.09	3.97	40248	616	22300	26228
15	467658	258658	8.74	37.39	53.87	9.76							
16	469086	259417	6.70	22.76	70.54	8.11	1700	37.37	2.20	60708	848	15076	46279
17	472527	258899	7.50	47.78	44.72	9.40	1700	33.60	1.98	57306	688	42975	68708
18	473116	259827	6.25	17.02	76.73	7.38	1802	29.73	1.65	54237	700	55709	53916
19	478072	259818	3.07	7.81	89.12	8.94	3499	76.69	2.19	52032	1084	60011	56642
20	478939	260444	6.06	18.76	75.18	12.63							
21	479560	460603	15.52	46.88	37.59	5.36	2567	45.59	1.78	61527	723	36571	45761
22	483040	261292	6.03	29.49	64.48	5.50	2223	53.61	2.41	51321	740	37657	47605
23	484972	261894	19.71	53.81	26.48	5.51	5162	71.21	1.38	51555	754	31637	40801
24	485819	262062	28.60	65.35	6.04	12.06	8650	95.65	1.11	64645	1249	36525	46685

25	496111	271705	16.76	49.29	33.96	10.43	3410	67.88	1.99	58251	678	38751	63256
26	497006	272577	7.27	22.22	70.51	7.75	4738	78.53	1.66	56520	894	33135	54531
27	496724	274635	3.87	9.88	86.25	10.00	5543	70.61	1.27	60169	925	36616	54613
28	497095	275067	18.71	55.83	25.46	10.32							
29	497019	276613	18.18	38.54	43.27	13.40	1909	26.89	1.41	65745	526	64148	72758
30	497702	276988	5.98	15.35	78.67	12.38	6565	75.79	1.15	61714	1010	36476	72799
31	500721	280009	2.76	7.47	89.77	11.11	5346	67.41	1.26	71002	987	48244	55479
32	500498	280090	17.56	48.84	33.60	8.59	3603	77.25	2.14	44806	768	38937	40691
33	503930	286096	23.59	66.69	9.72	10.38	5978	78.37	1.31	57063	972	44353	70944
34	504785	287055	21.63	69.82	8.54	7.34	2188	58.15	2.66	59084	750	56393	50070
35	508022	297311	15.08	40.49	44.43	9.35							
36	507695	299399	15.61	38.73	45.66	7.63	2869	48.08	1.68	49709	852	57705	55615

Appendix 3: Data collected for Core$_D$ samples collected from River Nene

Core	Depth	LOI	Tot P	OEP	Tot Fe	Tot Mn	Tot Ca	Tot Al
	cm	%		mg kg^{-1}	mg kg^{-1}	mg kg^{-1}	mg kg^{-1}	mg kg^{-1}
2	0-5	1.90	689	16.65	29975	335	7386	18805
2	5-7.5		1195	29.06	52680	610	15884	34711
2	7.5-10		1576	30.12	69906	837	21947	37904
7	0-5	9.92	2769	61.04	102323	1217	31381	48028
7	5-10		2203	29.63	101223	1169	41237	48274
7	10-15		3134	30.93	147362	1678	50001	29537
7	15-20		4501	39.39	166460	2125	59920	38204
15	0-5	9.76	2284	63.44	69433	1171	16891	58835
15	5-10		2232	41.88	71990	1055	14338	62491
15	10-15		1993	41.18	74118	737	9040	67952
15	15-20		2230	43.55	67807	547	11011	68275
15	20-22		18832	45.87	70492	489	7410	18832
20	0-5	12.63	3716	40.81	68394	805	30018	72943
20	5-20		3980	61.68	70701	851	30266	76442
20	20-35		4605	61.72	74420	1054	32879	88985
20	35-50		3870	53.00	65039	809	34766	70537
20	50-60		4335	61.88	70592	893	37213	83156
28	0-5	13.40	4907	15.96	56362	1122	45359	57434
28	5-20		2968	44.51	57852	906	84863	63774
28	20-35		2306	41.11	55420	679	88748	71064
28	35-50		2212	31.45	69608	862	90720	68195
28	50-65		2004	28.93	61399	667	85933	64267
35	0-5	9.35	2279	30.71	43856	605	67485	43498
35	5-20		1941	41.67	47999	525	75669	49351
35	20-35		1482	32.33	46992	447	106535	55349
35	35-50		874	19.22	46630	357	130641	48992
35	50-65		730		44543	304	158774	42860

References

British Geological Survey holds most of the references listed below, and copies may be obtained via the library service subject to copyright legislation (contact libuser@bgs.ac.uk for details). The library catalogue is available at: http://geolib.bgs.ac.uk.

Allen, R., Pereira, L.A., Raes, D., and Smith, M., 1998. Crop evapotranspiration: guidelines for computing crop water requirements. FAO, Irrigation and Drainage Paper No. 56. FAO, Rome, Italy.

Barkwith, A., Wang, L., Jackson, C.R., and Ellis, M. 2012. Towards understanding the dynamics of environmental sensitivity to climate change: introducing the DESC model. EGU General Assembly, Vienna, 2012, 1.

Bates, P.D., Horritt, M.S., and Fewtrell, T.J., 2010. A simple inertial formulation of the shallow water equations for efficient two-dimensional flood inundation modelling. J. Hydrol., 387, 33–45.

Bilotta, G.S., Brazier, R.E., Haygarth, P.M., Macleod, C.J.A., Butler, P., Granger, S., Krueger, T., Freer, J. & Quinton, J.N.2008.Rethinking the contribution of drained and undrained grasslands to sediment-related water quality problems. Journal of Environmental Quality, 37, 906-914.

Bilotta, G.S., Krueger, Brazier, R.E., Butler, P., Freer, J., Hawkins, J.M.B., Haygarth, P.M., Macleod, C.J.A. & Quinton, J.N. 2010. Assessing catchment-scale erosion and yields of suspended solids from improved temperate grassland. Journal of Environmental Monitoring, 12, 731-739.

Brierley, S.J., Harper, D.M. & Barham, P.J. 1989. Factors affecting the distribution and abundance of aquatic plants in a navigable lowland river; The River Nene, England. Regulated Rivers: Reaserach & Managemnt, 4, 263-274.

Brown, A.G., Keough, M.K., Rice, R.J. 1994. Floodplain evolution in the east-midlands, United Kingdom – The late glacial and Flandrian alluvial record from the Soar and Nene valleys. Philosophical Transactions of the Royal Society A – Mathematical and Engineering Sciences, 348(1687), 261-293.

Collins, A.L., Strömqvist, J., Davison, P.S. & Lord, E.I. 2007. Appraisal of phosphorus and sediment transfer in three pilot areas indentified for the catchment sensitive farming initiative in England: application of the protype PSYCHIC mode. Soil Use and Management, 23(S1), 117-132.

Cotton, J.A., Wharton, G., Bass, J.A.B., Heppell, C.M. & Wotton. 2006. The effects of seasonal changes to in-stream vegetation cover on patterns of flow and accumulation of sediment. Geomorphology, 77, 320-334.

Coulthard, T.J. & Van de Wiel, M.J. A cellular model of river meandering. Earth Surface Processes and Landforms, 31, 123-132.

Cox, B M, Sumbler, M G and Ivimey-Cook, H C. 1999. A formational framework for the Lower Jurassic of England and Wales (onshore area) British Geological Survey Research Report, RR/99/01

EC. 2000. Directive 2000/60/EC of the European Parliament and of the Council establishing a framework for the Community action in the field of water policy. Official Journal L 327, p.0001-0073 (22/12/2000)

Fisher, S.G., Sponsellar, R.A. & Heffernan, J.B. 2004. Horizons in stream biogeochemistry: Flowpaths to progress. Ecology, 85(9), 2369-2379.

Fortune, S., Lu, J., Addiscott, T.M. & Brookes, P.C. 2005. Assessment of phosphorus leaching losses from arable land. Plant & Soil, 269, 99-108.

Foster, I.D.L., Lees, J.A., Jones, A.R., Chapman, A.S. & Turner, S.E. 2002. The possible role of agricultural land drains in sediment delivery to a small reservoir, Worcestershire, U.K.

Foster, I.D.L., Chapman, A.S., Hodgkinson, R.M., Jones, A.R., Lees, J.A., Turner, S.E. & Scott, M. 2003. Changing suspended sediment and particulate phosphorus loads and pathways in underdrained lowland agricultural catchments; Herefordshiore and Worcestershire, U.K. Hydrobiologia, 494, 119-126.

Griffiths, J., Keller, V., Morris, D., Young, A.R., 2008. Continuous Estimation of River Flows (CERF). Environment Agency Science Report SC030240, Bristol.

Haygarth, P.M., Hepworth, L. & Jarvis, S.C. 1998. Forms of phosphorus transfer in hydrological pathways from soil under grazed grassland. European Journal of Soil Science, 49(1), 65-72.

Haygarth, P.M., Bilotta, G.S., Bol, R., Brazier, R.E., Butler, P.J., Freer, J., Gimbert, L.J., Granger, S.J., Krueger, T., Macleod, C.J.A., Naden, P., Old, G., Quinton, J.N., Smith, B & Worsfield, P. 2006. Processes affecting transfer of sediment and colloids, with associated phosphorus, from intensively farmed grasslands: an overview of key issues. Hydrological Processes, 20, 4407-4413.

House, W.A., Denison, F.H. & Armitage, P.D. 1995. Comparison of the uptake of inorganic phosphorus to a suspended and stream bed-sediment. Water Research, 29, 767-779.

House, W.A. & Warwick, M.S. 1999. Interactions of phosphorus with sediments in the River Swale, Yorkshire, UK. Hydrological Processes, 13, 1103-1115.

House, W.A. & Denison, F.H. 1997. Nutrient dynamics in a lowland stream impacted by sewage effluent: Great Ouse, England. Science of the Total Environment, 205, 25-49.

House, W.A. & Denison, F.H. 1998. Phosphorus dynamics in a lowland river. Water Research, 32(6), 1819-1830.

Jarvie, H.P., Withers P.J.A. & Neal, C. 2002. Review of robust measurement of phosphorus in river water: sampling, storage, fractionation and sensitivity. Hydrology and Earth System Sciences, 91), 113-132.

Jarvie, H.P., Jürgens, M.D., Williams, R.J., Neal, C., Davies, J.J.L., Barrett, C. & White, J. 2005. Role of river bed sediments as sources and sinks of phosphorus across two major eutrophic UK river basins: the Hampshire Avon and Herefordshire Wye. Journal of Hydrology, 304, 51-74.

Jarvie, H.P., Neal C. & Withers, P.J.A. 2006. Sewage-effluent phosphorus: a greater risk to river eutrophication than agricultural phosphorus? Science of the Total Environment, 360, 246-253.

Johnes, P.J., Foy, R., Butterfield, D. & Haygarth, P.M. 2007. Land use scenarios for England and Wales: evaluation of management optyions to support 'good ecological status' in surface waters. Soil Use and Management, 23 (suppl. 1), 176-194.

Kawashima, M., Tainaka, Y., Hori, T., Koyama, M. & Takamatsu, T. 1986. Phosphate adsorption onto hydrous manganese (IV) oxide in the presence of divalent cations. Water Research, 20(4), 471-475.

Lagarias, J.C., J. A. Reeds, M. H. Wright, and P. E. Wright, "Convergence Properties of the Nelder-Mead Simplex Method in Low Dimensions," SIAM Journal of Optimization, Vol. 9 Number 1, pp. 112-147, 1998.

Liang, D., Falconer, R.A., and Lin, B., 2006. Improved numerical modelling of estuarine flows. Proceedings of the ICE - Maritime Engineering, 159(1), 25–35.

MAFF. 2000. Fertiliser recommendations for agricultural and horticultural crops (RB209). The Stationary Office, London, UK.

Mainstone, C.P. & Parr, W. 2002. Phosphorus in rivers – ecology and management. Science of the Total Environment, 282-283, 25-47.

McDowell, R., Sharpley, A. & Folmar, G. 2001. Phosphorus export from an agricultural watershed: Linking source and transport mechanisms. Journal of environmental Quality, 30, 1587-1595.

McDowell, R.W., Sharpley, A.N. & Folmar, G. 2003. Modification of phosphorus export from an eastern USA catchment by fluvial sediment and phosphorus inputs. Agriculture, Ecosystems, and Environment, 99, 187-199.

Meadows, I. 2007. Hydrology. In Synthetic Survey of the Environmental Archaeological and Hydrological record for the River Nene from its source to Peterborough. eds. Allen, P, WA Boismier, AG Brown, A Chapman and I Meadows. Northamptonshire Archaeology, Report PNUM 3453

Murphy, J & Riley, J.P. 1962. A modified single solution method for the determination of phosphate in natural waters. Anal. Chim. Acta, 27, 31-36.

Murphy, J. M., Sexton, D. M. H., Jenkins, G. J., Boorman, P. M., Booth, B. B. B., Brown, C. C. *et al.* 2009. UK Climate Projections Science Report: Climate change projections. Met Office Hadley Centre, Exeter.

Neal, C., Jarvie, H.P., Withers, P.J.A., Whitton, B.A. & Neal, M. 2010. The strategic significance of wastewater sources to pollutant phosphorus levels in English rivers and to environmental management for rural, agricultural and urban catchments. Science of the Total Environment, 408, 1485-1500.

Pelton, D.K., Levine, S.N. & Braner, M. 1998. Measurements of phosphorus uptake by macrophytes and epiphytes from the LaPlatte River (VT) using 32P in stream microcosms. Freshwater Biology, 39, 285-299.

Pinay, G., Clément, J.C., & Naiman, R.J. 2002. Basic principles and ecological consequences of changing water regimes on nitrogen cycling in fluvial systems. Environmental Management, 30, 481-491.

Plater, A.J., Dugdale, R.E. & Ivanovich, M. 1994. Sediment yield determination using uranium-series radionuclides: the case of The Wash and Fenland drainage, eastern England. Geomorphology, 11, 41-56.

Plater, A.J., Dugdale, R.E. & Ivanovich, M. 1988. The application of Uranium series Disequilibrium concepts to sediment yield determinations. Earth Surface Processes and Landforms, 13, 171-182.

Quinton, J.N., Govers, G., van Oost, K. & Bardgett, R.D. 2010. The impact of agricultural soil erosion on biogeochemical cycling. Nature Geoscience, 3, 311-314.

Ravazzani, G., Rametta, D., and Mancini, M., 2011. Macroscopic cellular automata for groundwater modelling: A first approach. Environ. Modell. Softw., 26 (5), 634–643.

Rawlins, B.G. 2011. Controls on the phosphorus content of fine stream bed sediments in agricultural headwater catchments at the loandscape-scale. Agriculture, Ecosystems and Environment, 144, 352-363.

Reid, D.K., Ball, B, Zhang, T.Q. 2012. Accounting for the risks of phosphorus losses through tile drains in a phosphorus Index. Journal of Environmental Quality, 41(6), 1720-1729.

Roberts, W.M., Stutter, M.I. & Haygarth, P.M. 2012. Phosphorus retention and remobilization in vegetated buffer strips: A review. Journal of Environmental Quality, 41(2), 389-399.

Rothman, D.H., 1988. Cellular-automaton fluids: A model for flow in porous media. Geophys., 53(4), 509–518.

Rushton, K.R., 2003. Groundwater hydrology: conceptual and computational models. John Wiley and Sons Ltd, West Sussex, England.

Stutter, M.I., Langan, S.J. & Lumsdon, D.G. 2009. Vegetated buffer strips can lead to increased release of phosphorus to waters. Environmental Science and Technology, 43(6), 1858-1863.

Stutter, M.I. & Lumsdon, D.G. 2008. Interactions of land use and dynamic river conditions on sorption equilibria between benthic sediments and river soluble reactive phosphorus concentrations. Water Research, 42, 4249-4260.

Trimmer, M., Grey, J., Heppell, C.M., Hildrew, A.G., Lansdown, K., Stahl, H. & Yvon-Durocher, G. 2012. River bed carbon and nitrogen cycling: State of play and some new directions. Science of the Total Environment, 434, 143-158.

Van der Knijff, J.M., Younis, J., and De Roo, A.P.J., 2010. LISFLOOD: a GIS-based distributed model for river-basin scale water balance and flood simulation. Int. J. Geogr. Inf. Sci., 24(2), 189-212.

Van der Perk, M., Owens, P.N., Deeks, L.K., Rawlins, B.G., Haygarth, P.M. & Bevan, K.J. 2007. Controls on catchment-scale patterns of Phosphorus in soil, streambed sediment and stream water. Journal of Environmental Quality, 36, 694-708.

Van De Wiel, M.J., Coulthard, T.J., Macklin, M.G., and Lewin, J., 2007. Embedding reach-scale fluvial dynamics within the CAESAR cellular automaton landscape evolution model. Geomorphology, 90, 283–301.

Walling, D.E. 1977. Limitations of the rating curve technique for estimating suspended sediment loads, with particular reference to British rivers: Erosion and solid matter transport in inland waters. IAHS Publication, Wallingford, 122, 34-48.

Walling, D.E. & Webb, B.W. 1987. Suspended load in gravel-bed rivers: UK experience. In: C.R. Thorne, J.C. Bathurst, & R.D. Hey, eds. *Sediment transport in gravel-bed rivers*, 691-723. Chichester: Wiley.

Wang, L., Barkwith, A., Jackson, C.R., and Ellis, M.A., 2012. SLiM: an improved soil moisture balance method to simulate runoff and potential groundwater recharge processes using spatio-temporal weather and catchment characteristics. 12th UK CARE Annual General Meeting, UK Chinese Association of Resources and Environment, Bristol, UK, 8 Sept 2012.

Wilcock, P., and Crowe, J., 2003. Surface-based transport modelling for mixed-size sediment. J. Hydraul. Eng., 129(2), 120–128.

Williams, J.J.R. & Fawthrop, N.P. 1988. A mathematical hydraulic model of the river Nene – a canalized and heavily controlled river. Regulated Rivers: Research and Management, 2, 517-533.

Wilmot, R.D. & Collins, M.B. 1981. Contemporary fluvial sediment supply to the Wash. Special Publication International Association of Sedimentologists, 5, 99-110.

Withers, P.J.A. & Haygarth, P.M. 2007. Agriculture, phosphorus and eutrophication: a European Perspective. Soil Use and Management, 23(suppl. 1), 1-4.

Worsfold, P. 2006. Processes affecting transfer of sediment and colloids, with associated phosphorus, from intensively farmed grasslands: an overview of key issues, Hydrological Processes, 20, 4407-4413.

Young, A.R., Grew, R., Keller, V., Stannett, J., Allen, S., 2008. Estimation of river flow timeseries to support water resources management: the CERF model. Sustainable Hydrology for the 21st Century, Proc. 10th BHS National Hydrology Symposium, Exeter, 100–106.